Metabolic Bioactivity of *Athrixia phylicoides*

Charity Mandisa Masilela

Student number: 201068320

A thesis submitted in fulfilment of the requirements for the degree of Masters in Biochemistry in the Department of Biochemistry and Microbiology, Faculty of Science and Agriculture, University of Zululand

Supervisors: Dr. Sylvia Riedel-van Heerden and Dr. Abidemi Paul Kappo

Co-supervisor: Prof. Christro J.F. Muller

December 2016

Declaration

I, **Charity Mandisa Masilela** (student number 201068320), hereby declare that the work on which this thesis is based is my original work (except where acknowledgements indicate otherwise), and that neither the whole work or part of it has been, is being, or is to be submitted for another degree in this or any other university.

I empower the University of Zululand to reproduce for the purpose of research either the whole or any portion of the contents in any manner whatsoever.

Signature: …….. Date: …..13 December 2016

ABSTRACT

BACKGROUND: Insulin resistance is a major risk factor for the development of type 2 diabetes (T2D). It is characterized by insufficient response to secreted insulin in target tissues. *In vitro* studies demonstrated the ability of an aqueous extract of *Athrixia phylicoides* to increase glucose uptake and utilization in myocytes, adipocytes and in Chang cells. It is therefore likely that this extract could also modulate glucose metabolism in insulin-resistant cells. This study investigated the effect of an aqueous *A. phylicoides* extract on glucose metabolism in differentiated, insulin-resistant C2C12 myocytes, C3A liver cells, 3T3-L1 adipocytes and in diabetic *db/db* mice.

METHODS: Insulin resistance was induced *in vitro* using palmitic acid (750µM) for 16 hours followed by treatment with two concentrations (10 and 100 µg/ml) of the extract, in the presence and absence of insulin, for 3 hours. Glucose uptake was assessed by 2-deoxy-[^{3}H]-D-glucose uptake. Western blot analysis of proteins involved in insulin dependent (AKT) and insulin independent (AMPK) glucose uptake were investigated. The inhibitory effect of *A. phylicoides* on PTP1B enzyme activity was also assessed. Six-week old obese C57BLKS *db/db* mice were treated with *A. phylicoides* extract (20 and 200 mg/kg body weight) in the diet for 30 days. Body weights, fasting blood glucose levels, food and water intake were monitored weekly followed by an oral glucose tolerance test and serum lipids assessment. The degree of steatosis was assessed in liver sections.

RESULTS: Results suggested that *A. phylicoides* increased glucose uptake as well as AMPK phosphorylation in insulin-resistant C2C12 myocytes but had no effect on insulin resistance in C3A liver cells and 3T3-L1 adipocytes. In *db/db* mice, the *A. phylicoides* extract had no effect on body weight, fasting blood glucose or oral glucose tolerance. However, serum triglyceride content was markedly reduced with the lowest dose while the high dose markedly reduced the steatosis score in the liver sections.

CONCLUSION: *A. phylicoides* extract was able to improve insulin stimulated glucose uptake in insulin-resistant C2C12 myocytes through AMPK dependent pathways. The extract is a potential inhibitor of PTP1B enzyme. While *A. phylicoides* had no effect on hyperglycemia and insulin resistance under the current experimental conditions, the effect on lipid metabolism should be further investigated.

ACKNOWLEDGEMENTS

I would like to acknowledge the following people:

- My supervisor Dr S Riedel for her guidance, dedication and for helping me grow as a scientist. Thank you, I wouldn't have made it this far without your assistance.
- My co-supervisors Dr C.J.F Muller and Dr A.M.P Kappo for believing in me and encouraging me to always do my best.
- Prof Andy Opoku who saw something in me that I never thought I had. Thank you so much for believing in me.
- My sincere gratitude goes to Dr S Mazibuko, Dr N Chellan and Dr R Johnson for all the support that they have provided throughout this journey.
- Dr Babalwa Jack, Dr Phiwayinkosi Dludla and Dr Kwazikwakhe Gabuza for always being there for my endless questions. You guys have been amazing.
- My friends Nokulunga Hlengwa, Yonela Ntamo and Dr Israel Olonade for making this journey much easier than it should have been. The amount of support that you have provided throughout this journey means the world to me. Thank you for being in my corner at all times.
- My lab mates Amsha Viraragavan and Namani Ngema, none of this would have been possible without your assistance. Thank you ladies.
- Mr Desmond Linden and Ms Charna Chapman for assisting with the *in vivo* experiments. Thank you.
- SAMRC for providing financial support and Prof Johan Louw for providing me with the opportunity to work at the Biomedical Research and Innovation Platform.
- My family for their encouragement, prayers and for always making sure that I don't feel the distance between us. Special thanks goes to my mom and dad for allowing me to chase my dreams. Ngiyabonga boVungandze, boMsekelave, boMvundlane lencane umkhemetelwane, khemekheme linile. Sengatsi ningachubeka ningisekela.

Dedication

I dedicate this work to my late grandmother "Zanny Ngwenya" who lived most of her life with type 2 diabetes. Siyakukhumbula Mzilikazi.

Table of Contents

List of Figures

List of Tables

ABBREVIATIONS

β-cells	Pancreatic beta cells
β-actin	Beta actin
ACC	Acetyl-CoA
ADP	Adenosine-5-diphosphate
AICAR	5-Aminoimidazole-4-carboxamide-1-β-D-ribofuranoside
AKT	Threonine kinase B
AMP	Activated protein kinase
AMPK	Adenosine monophosphate-activated protein kinase
ANOVA	Analysis of variance
ATCC	American type culture collection
ATGL	Adipose triglyceride lipase
ATP	Adenosine-5-triphosphate
BSA	Bovine serum albumin
CD36/FAT	Fatty acid translocase
CO_2	Carbon dioxide
CPM	Counts per minute
CPTI	Carnitine palmitoyltransferase 1
CVD	Cardiovascular disease
DAG	Diacylglycerol
DMEM	Dulbecco's modified eagle's medium
DMSO	Dimethyl sulfoxide
DPBS	Dulbecco's phosphate buffered saline
DPM	Disintegrations per minute
ECRA	Ethical consumer research association
EFFAs	Essential free fatty acids
ELISA	Enzyme-linked immunosorbant assay
EMEM	Eagle's minimum essential medium
F6P	Fructose-6-phosphate
FABP	Fatty acid binding protein
FATP1	Fatty acid transporter one
FBS	Fetal bovine serum
NCS	New born calf serum

FFA	Free fatty acid
FOXO1	Forkhead box protein O1
G3PDH	Glyceraldehyde 3-phosphate dehydrogenase
G6P	Glucose-6-phosphate
G6Pase	Glucose-6-phosphatase
GAPDH	Glyceraldehyde-3-phosphate dehydrogenase
GLUT	Glucose transporter
GLUT1, 2, 3 and 4	Glucose transporter one, two, three and four
GSK3	Glycogen synthase kinase three
H	Hour
HDL	High density lipoprotein
HOMA-IR	Homeostasis model assessment-estimated insulin resistance
HPLC-DAD	High-performance liquid chromatography with diode-array detection
HS	Horse serum
IBMX	3-Isobutyl-1-methylxanthine
IR	Insulin receptor
IRS	Insulin receptor substrate
IRS-1 and 2	Insulin receptor substrate one and two
JNK	c-Jun N-terminal kinases
LCFA	Long chain fatty acids
LKB 1	Liver kinase B1
MAPK	Mitogen-activated protein kinase
mRNA	Messenger ribonucleic acid
miRNA	Micro RNA
MTT	3-(4,5-dimethylthiazol-2-yl)-2,5-diphenyltetrazolium bromide
NADH	Nicotinamide adenine dinucleotide
$NaHCO_3$	Sodium bicarbonate
NaOH	Sodium hydroxide
NF-κB	Nuclear factor kappa beta
OGTT	Oral glucose tolerance test
PEP	Phosphoenolpyruvate
PEPCK	Phosphoenolpyruvate carboxykinase
PFK	Phosphofructokinase

PI3K	Phosphatidylinositol 3-kinase
PIP_3	Phosphatidylinositol (3, 4, 5)-triphosphate
PKC	Protein kinase C
PKCθ	Protein kinase C theta
PKCε	Protein kinase C epilson
PKCζ	Protein kinase C zeta
PMSF	Phenylmethylsulfonyl fluoride
PPARs	Peroxisome proliferator-activated receptors
PVDF	Polyvinylidene difluoride
SDS	Sodium dodecyl sulfate
SDS-Page	Sodium dodecyl sulfate poly-acrylamide gel electrophoresis
SH2	Src homology 2 domain
SOCS3	Suppressor of cytokine signaling 3
STZ	Streptozotocin
T2D	Type 2 diabetes
TBST	Tris-buffered saline and Tween 20
TC	Tissue culture
TCA	Tricarboxylic citric acid
TG	Triglycerides
TNF-α	Tumor necrosis factor alpha
VLDL	Very low density lipoproteins
WHO	World health organis
ORO	Oil Red O

Chapter 1

1. Literature review

1.1. Introduction to the present study

Non-communicable diseases are a leading cause of death worldwide, with an increasing number of these deaths occurring in developing countries (WHO, 2013). The prevalence of T2D in South Africa has increased significantly over the past 20 years, more especially in black African urban-dwelling populations (Peer *et al*., 2012). Insulin resistance is a major pre-disposing factor for developing T2D and cardiovascular disease. The effect of insulin resistance in muscle and pancreatic islets is worsened by dyslipidemia, which is prevalent in insulin-resistant and diabetic patients (Kahn, 2003; Kahn *et al*., 2006). Recent research appears to be more focused on polyphenols for their biological activities, such as anti-diabetic properties, in order to find new ways to treat T2D, insulin resistance and associated metabolic complications (Pandey and Rizvi, 2009). Polyphenols are part of a healthy diet since they are components of plant-based foods such as vegetables, fruits, herbs and cereal grains (Pandey and Rizvi, 2009). The interest in phenolic compounds is mainly due to anecdotal evidence, but epidemiological studies are also showing a correlation between fruit and vegetable intake and health effects (D'Archivio *et al*., 2010).

The potential health promoting properties of polyphenols include anti-hyperglycemic, anti-inflammatory and anti-oxidant effects (Babu *et al*., 2013; Bahadoran *et al*., 2013). Bush tea (*Athrixia phylicoides*) has been a refreshment drink for decades and scientists have taken an interest in investigating its effect on metabolism because of its polyphenol content. A toxicological study showed that the aqueous extract of *A. phylicoides* has no toxic effect *in vivo* (Chellan *et al*., 2008). The aqueous extracts were shown to possess antioxidant properties, which may be due to the high content of phenolic acids and polyphenols. *In vitro* studies further demonstrated their ability to increase glucose uptake and utilization in myocytes, adipocytes and in Chang cells (Chellan *et al*., 2012). It is, therefore, likely that extracts of *A. phylicoides* can also modulate glucose metabolism in insulin-resistant cells.

1.2. Diabetes mellitus

Diabetes mellitus (DM) is a group of complex metabolic abnormalities characterized by increased levels of glucose in the blood, which may be a result of impaired insulin secretion, insulin action or both (ADA, 2010; Babu *et al*., 2013). Diabetes mellitus is classified into 2 major types: type 1 and type 2 diabetes. Type 1 diabetes, which is also known as insulin-dependent diabetes mellitus (IDDM), juvenile or childhood onset, is the result of autoimmune destruction of β-cells of the pancreas, which has been associated with a complex interaction between genetics and environmental factors (ADA, 2010; Bhattacharya *et al*., 2007). Type 1 diabetes has also been associated with damage, dysfunction and failure of various organs including the heart, kidneys, eyes and nerves. Classical clinical manifestations include frequent urination, feeling very thirsty and hungry, feeling very tired, blurry vision, sores that heal slowly, weight loss together with foot ulcers (ADA, 2010).

The prevalence of diabetes mellitus is increasing at an alarming rate and imposing a burden on the economy worldwide (IDF, 2014). About 11 % of the world's heath expenses are dedicated to treating diabetes. Currently, 387 million people in the world are living with diabetes and the number is expected to rise to 592 million by the year 2035. About 55 % of cases are expected to be of type 2 diabetes (IDF, 2014) (Figure 1.1). Type 2 diabetes is the leading cause of cardiovascular diseases, disabilities and premature death (Liu *et al*., 2010; WHO, 2016). In the year 2015, 321,100 deaths were attributed to diabetes according to the International Federation of Diabetes (IDF) estimated. Current treatment has been associated with the risk of hypoglycemia, lactic acidosis and weight. Therefore, there is a great need to find alternative drugs that can be used to treat type 2 diabetes.

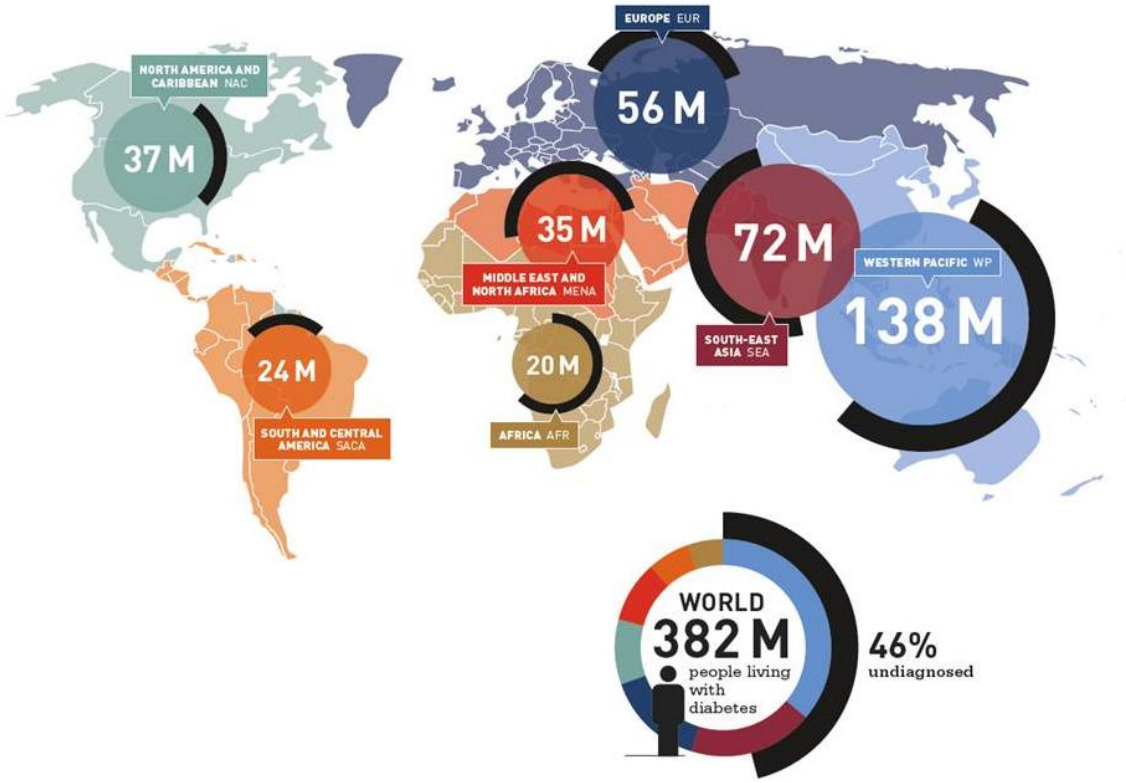

Figure 1.1 Statistical diagrammatic illustrating global occurrence of diabetes.
According to IDF 2016, the statistics shows that most prominent cases of diabetes are observed in the western pacific. Figure taken from Sixth edition, 2013 online version of IDF Diabetes Atlas: **www.idf.org/diabetesatlas6th**.

Type 2 diabetes, also referred to as insulin independent diabetes, is a progressive disease that is characterized by obesity, impaired insulin action, insulin secretory dysfunction and increased endogenous glucose output (ADA, 2010; Babu *et al*., 2013; Bhattacharya *et al*., 2007). Type 2 diabetes is preceded by a number of complex metabolic abnormalities such as oxidative stress, endoplasmic reticulum stress, dyslipidemia, hyperinsulinemia and subclinical inflammation, which eventually leads to insulin resistance and moderate to complete β-cell failure (Esposito and Giugliano, 2004; Esser *et al*., 2014; Fonseca, 2009; Monteiro and Azevedo, 2010). All of these metabolic diseases are collectively known as the metabolic syndrome or syndrome X (Jiamsripong *et al*., 2008). Type 2 diabetes is often accompanied by other clinical conditions, such as hypertension and hyperlipidemia. However, the pathogenesis of T2D is not completely understood (Kahn, 2003; Zierath *et al*., 2000).

1.2.1. Glucose metabolism

Glucose is a simple sugar and is an important source of fuel across most life forms (Garrett and Grisham, 2008). Glucose is utilized to yield adenosine triphosphate (ATP), which drives essential metabolic processes within a living cell (Garrett and Grisham, 2008). Glucose also regulates insulin secretion by the pancreatic β-cells (Donath *et al*., 2005). Abnormally high glucose level in the circulatory system is termed hyperglycemia. Continuous exposure of skeletal muscle cells, hepatocytes, adipocytes and the pancreatic β-cells to high levels of glucose have been associated with loss of insulin sensitivity and impaired insulin secretion by the β-cells, via the generation of reactive oxygen species (ROS) (Cerf, 2013; Kawanaka *et al*., 2001; Nelson *et al*., 2000; Yano *et al*., 2004; Yu *et al*., 2011). Loss of insulin sensitivity and impaired insulin secretions are characteristics of type T2D (Abdul-Ghani and DeFronzo, 2010; Cerf, 2013; Inzucchi *et al*., 2012).

1.2.2. Glucose transport

The entry of glucose into cells is accomplished by glucose transporter proteins. Glucose transporters (GLUT) also facilitate the transport of other sugars across membranes through facilitative diffusion (Kahn, 1992; Wood and Trayhurn, 2003). Glucose transporters demonstrate different substrate specificity, kinetic properties and tissue expression profiles (Wood and Trayhurn, 2003) and are expressed in all mammals with about 12 encoded in the human genome (Huang and Czech, 2007; Mueckler, 1994).

1.2.3. Glucose transporter 2 (GLUT 2)

Glucose transporter 2 is expressed in the liver, kidney, intestinal epithelium and pancreatic beta cells (Cohen *et al*., 2014; Koranyi *et al*., 1990; Tal *et al*., 1992; Thorens and Mueckler, 2010; Wood and Trayhurn, 2003). Unlike other glucose transporters, GLUT 2 is usually found on the cell surface. Glucose transporter 2-mediated glucose transport is proportional to the amount of glucose circulating in the circulatory system allowing an appropriate response by the liver and the pancreas. Knockout of the GLUT 2 gene in mice resulted in glucose intolerance, hyperglycemia and hyperinsulinemia (Guillam *et al*., 1997; Leturque *et al*., 2005; Seyer *et al*., 2013). As a result, the mice die shortly after birth. This demonstrates that GLUT 2 is essential for viability and for maintaining a stable level of glucose in the blood (Gorovits and Charron 2003).

1.2.4. Glucose transporter 4 (GLUT 4)

Glucose transporter 4 (GLUT 4) is an insulin-stimulated glucose transporter that is predominantly expressed in insulin-sensitive tissues such as skeletal muscle and adipose tissue (Nikzamir *et al*., 2014; Huang and Czech, 2007 Gorovits and Charron 2003). Glucose transporter 4 resides intracellularly in vesicles in the perinuclear region of adipocytes and skeletal muscle cells. In response to insulin stimulation, GLUT 4 translocates to the cell membrane through exocytosis (Ikemoto *et al*., 1995; Kahn, 1992). The latter is facilitated through a microtubule network and actin filaments (microfilaments), which direct the movement of GLUT 4, allowing glucose to be transported into the cell (Chang *et al*., 2004). The rate at which glucose enters the cell is controlled by the concentration of GLUT 4 transporters on the cell membrane and the duration in which the protein remains on the surface of the membrane (Mueckler, 1994)

1.2.5. Other glucose transporters

Glucose transporter 1 (GLUT 1) is a universally expressed protein that is responsible for basal glucose uptake (Wood and Trayhurn, 2003). Glucose transporter 1 was the first glucose transporter to be isolated and characterized (Kahn, 1992; Khan and Pessin, 2002; Wood and Trayhurn, 2003). In the brain, GLUT 1 serves as the main transporter of glucose across the blood-brain barrier. This protein is also abundantly expressed in erythrocytes, adipose, liver and skeletal muscle tissue (Guo *et al*., 2005; Wood and Trayhurn, 2003).

Glucose transporter 3 is highly expressed in tissues with a greater demand for glucose such as the brain, neurons and the embryo (Fladeby *et al*., 2003; Mueckler, 1994).

1.3. Insulin

Insulin is a hormone that is composed of 51 amino acids, secreted by the pancreatic beta cells. The hormone consist of two peptides (A and B) joined together by disulfide bonds (Weiss *et al*., 2000). Insulin plays a central role in carbohydrate, lipid and protein metabolism. In response to increased levels of glucose in the blood, insulin binds the insulin receptor located on the membrane of insulin sensitive tissues (skeletal muscle, liver and adipose) and initiates glucose uptake, utilization and storage (Bhattacharya *et al*., 2007; Chang *et al*., 2004; DeFronzo and Ferrannini, 1991; Saltiel and Kahn,

2001; Snel *et al*., 2012). In adipose tissue, the hormone is responsible for the suppression of lipolysis thus promoting fat storage. This antilipolytic effect of insulin is mediated through the inhibition of hormone sensitive lipase (Meijssen *et al*., 2001). In the liver, insulin promotes lipogenesis, i.e. the conversion of excess glucose to fatty acids and triglycerides for storage (Beckman, 2000; Cohen, 1999), while in the muscle it promotes glucose storage in the form of glycogen (Dimitriadis *et al*., 2011; Drury, 1940). Insulin is also responsible for decreasing the rate of glycogen breakdown in both the skeletal muscle and the liver (Saltiel and Kahn, 2001; Zierath *et al*., 2000).

1.3.1. Molecular mechanism of insulin signaling

Insulin receptors (IR) possess intrinsic tyrosine kinase activity (Chang *et al.,* 2004) and contain two extracellular α-subunits and two transmembrane β-subunits that are connected together by disulfide bonds, forming a $\alpha_2\beta_2$ heterotetrameric complex (Gual *et al*., 2005; Pessin and Saltiel, 2000). Insulin binds to the extracellular α-subunit and promote autophosphorylation of the β-subunits on tyrosine residues, thereby creating a recognition motif for the binding domain in insulin receptor substrate protein (IRS-1/2/3/4) (Chang *et al*., 2004; Pessin and Saltiel, 2000). Insulin receptors bind insulin receptor substrate proteins (IRS) and are activated through phosphorylation of specific tyrosine residues, which leads to recruitment of other proteins containing proto-oncogene tyrosine-protein kinase (Src) homology 2-domains, such as growth factor receptor-bound protein 2 (Grb2), non-catalytic region of tyrosine kinase adaptor protein (Nck) and most prominently phosphoinositide 3-kinase (PI3-K) (Chang *et al*., 2004; Cheatham and Kahn, 1995; Li and Zhang, 2000; Pessin and Saltiel, 2000) (Figure 1.2).

Phosphoinositide 3-kinase catalyzes the transfer of a phosphate group to phosphoinositol lipids, in particular phosphatidylinositol-4,5-bisphosphate (PIP2) forming phosphatidylinositol -3,4,5- triphosphate (PIP3). An increase in PIP3 results in activation of a number of proteins containing pleckstrin homology (PH) domain, which includes 3-phosphoinositide-dependent kinase (PDK) (Boura-Halfon and Zick, 2009; Li and Zhang, 2000; Pessin and Saltiel, 2000). The protein PDK phosphorylates and activates mammalian target of rapamycin (mTOR), p70 S6 kinase (S6K1) and, most importantly, protein kinase B (PKB)/AKT, and protein kinase C isoforms (PKCζ/λ) (Boura-Halfon and Zick, 2009; Chang *et al*., 2004). Activation of AKT promotes the

translocation of glucose transporter proteins to the plasma membrane, particularly GLUT 4 (Chang *et al*., 2004; Kahn, 1992; Khan and Pessin, 2002; Pessin and Saltiel, 2000; Saltiel and Kahn, 2001).

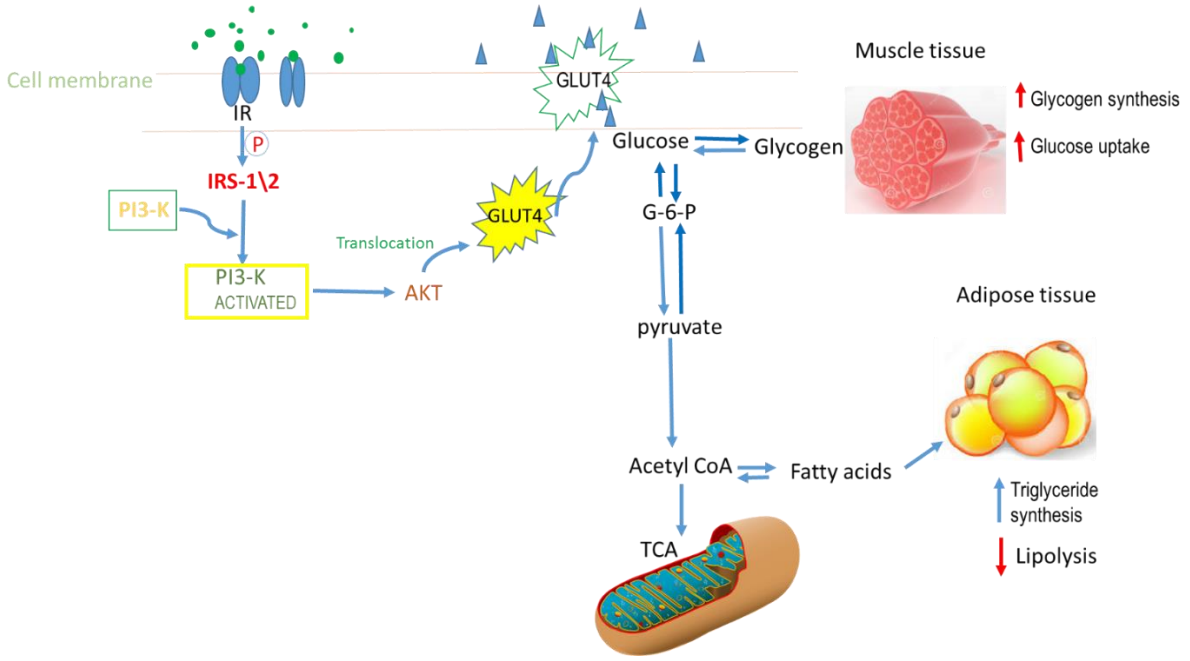

Figure 1.2 Illustrates how glucose is transported to the cells via the glucose transporter 4. Insulin-mediated GLUT4 translocation, glucose uptake into cells and the response of insulin-sensitive tissues. Phosphorylation of IRS-1/2 on serine/threonine residues can either enhance or diminish insulin sensitivity, leading to insulin -resistance. Figure adapted from Yu and Chai (2015).

1.3.2. Changes in insulin signaling to suit different metabolic needs

The body has the ability to switch to different signaling pathways according to its metabolic needs. For instance, in a state of low energy or glucose deprivation, the multifunctional enzyme Adenosine monophosphate-activated kinase (AMPK) is activated to facilitate signaling pathways that restore cellular ATP levels such as fatty acid oxidation and glucose uptake, while inhibiting ATP consuming biosynthetic pathways such as gluconeogenesis, lipid and protein synthesis (Hardie and Pan, 2002; Kahn *et al*., 2005; Towler and Hardie, 2007; Viollet *et al*., 2010). Once activated, AMPK inactivates acetyl-coenzyme A carboxylase 2 (ACC-2) by phosphorylation on its serine residues (Ser-77, Ser-1200 and Ser-1215). Acetyl-coenzyme A carboxylase 2 is a biotin-dependent enzyme that catalyzes the carboxylation of acetyl-CoA to malonyl-CoA. Therefore, inactivation of ACC-2 inhibits the production of malonyl-CoA allowing the activation of carnitine palmitoyl-CoA transferase-1 (CPT1), which

promotes the entry of fatty acids into the mitochondria for β-oxidation (Foster, 2012; Wakil and Abu-Elheiga, 2009). It is possible that the inhibition of malonyl-coA could be due to activation of malonyl-CoA decarboxylase by AMPK (Saha and Ruderman, 2003; Saha *et al*., 2000). Consequences of such events are increased β-oxidation and cellular energy restoration (Hopkins *et al*., 2003; Jeon, 2016; Kahn *et al*., 2005; Munday, 2002; Saha and Ruderman, 2003; Viollet *et al*., 2010; Witters and Kemp, 1992). Adenosine monophosphate-activated protein kinase can also stimulate glucose uptake by phosphorylating and inhibiting the activity of TBC1 domain 1 family member 1 (TBC1D1) and AKT substrate of 160 kDa (AS160), thereby increasing the activity of Rab family G protein and inducing the fusion of GLUT4 vesicle with the plasma membrane. The fate of glucose after entering the cell is glycolysis, which helps restore cellular ATP levels (Jeon, 2016; Sakamoto and Holman, 2008; Srivastava *et al*., 2012).

In a high-energy state, insulin aids the entry of glucose into cells while inhibiting catabolic processes such as β-oxidation and promoting anabolic processes such as glycogen synthesis. Insulin directly downregulates the activity of AMPK by inducing its phosphorylation on ser485 by AKT, blocking upstream kinases from accessing and phosphorylating tyrosine residue 172 (Hawley *et al*., 2014; Jeon, 2016). This allows an increased activity of ACC-2, which stimulates the production of malonyl-CoA in the mitochondria. Malonyl-CoA blocks the activity of CPT1 leading to the inhibition of fatty acids from entering the mitochondria and a subsequent decrease in β-oxidation (Hardie and Pan, 2002; Jeon, 2016).

Insulin can also stimulate glycogen synthesis through the activation of protein phosphatase-1 (PP1), which facilitates the activity of glycogen synthase through dephosphorylation of its C-terminus serine residues (Ser641, Ser645, Ser549 and Ser653) thereby initiating glycogen synthesis (Adeva-Andany *et al*., 2016; Rayasam *et al*., 2009). In the muscle, insulin stimulates the dephosphorylation of glycogen synthase kinases 3 (3α and 3β) (GSK3α and GSK3β) through the activation of AKT. Protein kinase B (AKT) phosphorylates the GSK3 isoforms on serine residues located on their N-terminus, thus inhibiting their interaction with the priming phosphate and rendering the protein inactive (Cross *et al*., 1995, 1997; Rayasam *et al*., 2009). This decreases the rate of phosphorylation of glycogen synthase, thereby increasing glycogen synthesis and maintaining a stable level of glucose in the blood. Under basal conditions, glucose transporters return to the cytoplasm, where they are recycled and

retained in the GLUT vesicles (Chang *et al*., 2004; Rayasam *et al*., 2009; Sakamoto and Holman, 2008).

1.4. Insulin resistance

Insulin resistance (IR) is a precursor to T2D, which can be detected long before a patient is diagnosed with the disease. Insulin resistance is defined as the impairment of insulin from achieving its physiological effects, including the stimulation of glucose uptake and inhibition of hepatic glucose output, leading to hyperglycemia (Gual *et al*., 2005; Kahn *et al*., 2006). Insulin resistance is often observed in pre-diabetic patients with impaired glucose tolerance and obesity (Kahn *et al*., 2006; Reaven, 1988; Saltiel and Kahn, 2001). At an early stage, β-cells increase insulin release sufficiently to overcome insulin resistance, maintaining normal blood glucose levels. Insulin resistance progresses to T2D when β-cells fail to compensate for the insulin impairment (Bollheimer *et al*., 1998; Gual *et al*., 2005; Kahn *et al*., 2006; Muoio and Newgard, 2008). Insulin-sensitivity of tissues is influenced by a variety of factors, which include: age, genetics, fat distribution, physical fitness, sedentary lifestyle and diet, with the latter being the main contributing factors (Kahn, 2003; Kahn *et al*., 1990; Stumvoll *et al*., 2005).

Adipose tissue and mitochondrial dysfunction, oxidative stress and inflammation are listed as major causes of insulin resistance and they have been connected to increased intracellular fat accumulation and chronic elevation of blood glucose levels (de Ferranti and Mozaffarian, 2008; Kaneto *et al*., 2007; Lowell and Shulman, 2004; Petersen and Shulman, 2002; Savage *et al*., 2007). Continuous exposure of β-cells to high levels of glucose and fat metabolites leads to β-cell failure (Bollheimer *et al*., 1998). Beta-cell destruction, together with decreased insulin sensitivity of the three target tissues, ultimately leads to T2D (Kahn, 2003; Kahn *et al*., 1990, 2006; Saltiel and Kahn, 2001).

1.4.1. Effect of lipid mediators on insulin signaling

Enlarged adipocytes are a characteristic of adipose tissue dysfunction and they are often observed in obese patients (Blüher, 2013). Adipocyte expansion could be a result of over-nutrition or other factors, such as hypoxia (Kim *et al*., 2015; Sun *et al*., 2013). Enlarged adipocytes often release signals that cause endoplasmic reticulum (ER) stress leading to an unfolded protein response (Boden, 2009; Kaneto *et al*.,

2006). Unfolded proteins upregulate genes that are involved in post-translational modification, degradation of proteins and also alleviation of ER stress (Bravo *et al*., 2013; Hotamisligil, 2010; Salvadó *et al*., 2015). Endoplasmic reticulum stress triggers other stress signals, such as the production and release of inflammatory cytokines and adipokines, which can disrupt adipocyte differentiation, insulin signaling and also induce a state of chronic inflammation in the adipose tissue (Bailey *et al.,* 2011; Hasnain *et al*., 2012; Kawasaki *et al*., 2012; Zhang and Kaufman, 2008). Endoplasmic reticulum stress can also induce lipolysis through activation of protein kinase A (PKA), which phosphorylates perilipin 1 and thereby initiating lipolysis (Duncan *et al*., 2007; Greenberg *et al*., 2011). Excess free fatty acids released into the circulatory system may lead to lipotoxicity, which eventually induces insulin resistance (Duncan *et al*., 2007; Kaneto *et al*., 2006; Rutkowski *et al*., 2015).

In the muscle tissue, free fatty acids (FFA) metabolites such as long-chain Acyl-CoA (LC-CoA), diacylglycerol (DAG), and ceramides induce the activation of serine/threonine kinases (Powell *et al*., 2004; Schmitz-Peiffer, 2010; Turban and Hajduch, 2011). Serine/threonine kinases include proteins such as protein kinase C (PKC) isoforms i.e.: PKC-θ, lKB-kinase-β and Jun N-terminal kinase, which phosphorylate insulin receptor substrates (IRS) on serine residues, rendering them poor substrates for insulin receptors (Consitt *et al*., 2009; Hage Hassan *et al*., 2014; Jornayvaz *et al*., 2011; Shulman, 2000; Yu *et al*., 2002). Insulin receptor substrate proteins (e.g. IRS-1) that are phosphorylated on serine residues, specifically ser307, cannot bind and activate PI3K, resulting in insufficient activation of AKT. Protein kinase B is directly involved in the translocation of glucose transporter proteins i.e. GLUT 4, therefore, failure to activate this protein leads to reduced GLUT 4 translocation and glucose transport into the cell (Aguirre *et al*., 2002; Huang *et al*., 2005; Jornayvaz and Shulman, 2012).

In the liver, elevated levels of DAG due to intracellular lipid accumulation impairs insulin signaling by activating PKC isoforms i.e. PKCε (Powell *et al*., 2004; Schmitz-Peiffer, 2013; Turban and Hajduch, 2011). Once activated, PKC targets and phosphorylates serine residues of IRS-2 leading to decreased insulin receptor kinase activity (Park *et al*., 2013). This lowers insulin-stimulated IRS-2 tyrosine phosphorylation and IRS-2-associated PI3K-activity leading to reduced AKT activity. Reduced AKT activity leads to decreases insulin stimulated glucose uptake and the

ability of insulin to suppress hepatic glucose production (Bugianesi *et al*., 2005; Samuel *et al*., 2004). Reduced AKT also leads to a decrease in phosphorylation of the forkhead box O (FOXO) transcription factor. Forkhead box O are proteins that are universally expressed in all mammalian tissues whose activity is inhibited by the PI3K/AKT pathway (Nakae *et al*., 2008; Nandi *et al*., 2004; White, 2003). Inhibition of AKT leads to the upregulation of FOXO, which in turn increases the translation rate of key enzymes involved in gluconeogenesis (glucose-6-phosphatase) and glycogenolysis (pyruvate carboxylase and phosphoenolpyruvate carboxykinase) (Galbo *et al*., 2013; Guo, 2014). Activation of the key enzymes of gluconeogenesis and glycogenolysis leads to an increase in hepatic glucose production and decrease hepatic glucose uptake, which both contribute to hyperglycemia (Guo, 2014; Oh *et al*., 2013; Perry *et al*., 2014; Puigserver *et al*., 2003; Qu *et al*., 2006).

The effect of pro-inflammatory proteins on insulin signaling inflammatory cytokines, such as tumor necrosis factor alpha (TNF-α) and Interleukin 6 (IL-6), impair adipocyte differentiation, reduce lipid accumulation, induce inflammation and increase adipocyte lipolysis, leading to accumulation of FFAs in the blood (Hoene and Weigert, 2008; de Luca and Olefsky, 2008; Wieser *et al*., 2013). Tumor necrosis factor alpha induces its inhibitory effect on glucose transport through phosphorylating serine/threonine residues of IRS-1/2 (ser 307), leading to a decrease in insulin stimulated glucose uptake in the liver and the skeletal muscle tissue, while enhancing lipolysis in the adipose tissue and increasing glucose output by the liver (Bulló-Bonet *et al*., 1999; Hotamisligil *et al*., 1995; Lang *et al*., 1992; Valverde *et al*., 1998; Van der Poll *et al*., 1991). It is believed that IL-6 induces its inhibitory effect on insulin stimulated glucose uptake by downregulating the expression of IRS-1 and GLUT 4 (Rotter *et al*., 2003). Interleukin 6 can also induce insulin resistance through the activation of the suppressor of cytokine, SOCS-3, a protein that inhibits the auto-phosphorylation of the IR proteins, leading to reduced tyrosine phosphorylation of IRS-1 and PI3K/AKT pathway activation. These events are associated with a decrease in insulin stimulated GLUT 4 translocation (Dandona *et al*., 2004; Senn *et al*., 2003).

1.5. *In vitro* models of insulin resistance and their relevance in the search for treatments and prevention

1.5.1. Muscle

C2C12 cell line is a sub-clone originally obtained from the leg muscle of a normal C3H mouse (Yaffe and Saxel, 1977). In the presence of horse serum, C2C12 cells differentiate rapidly and produce extensive contracting myotubes. Therefore, they can be used for exercise studies, myogenesis and differentiation (Ahmadipour *et al*., 2012; Burattini *et al*., 2004; McMahon *et al*., 1994). Skeletal muscle accounts for about 70 % of the whole body's insulin stimulated glucose uptake and it is abundant in GLUT 4. C2C12 cell line has been demonstrated as a good model to study insulin stimulated glucose metabolism and changes in GLUT 4 activity under herbal stimulation (Ahmadipour *et al*., 2012; Nedachi and Kanzaki, 2006). Murine skeletal myoblasts (C2C12) have been used in insulin resistance studies, where insulin resistance was accomplished by treating cells with palmitate (Chavez and Summers, 2003; Li *et al*., 2015; Mazibuko *et al*., 2013; Tsuchiya *et al*., 2010), micro RNAs 29 and 135 (Honardoost *et al*., 2016; Zhou *et al*., 2016), inflammatory cytokines, such as TNF-α and IL-6 (Yang *et al*., 2012), and the PKC activator 12-*O*-tetradecanoylphorbol 13-acetate (Deng *et al*., 2012).

Palmitate-induced insulin resistance remains the most used method to study fatty acid-induced insulin resistance. Treating C2C12 and L6 (rat skeletal muscle cell line) cells with palmitate results in an increase in ceramide content in the intracellular matrix, leading to reduced insulin stimulated glycogen synthesis, together with insulin stimulated phosphorylation of GSK-3α through inhibition of AKT phosphorylation (Bikman and Summers, 2011; Chavez and Summers, 2012; Powell *et al*., 2003).

Treating C2C12 cells with palmitic acid reduces serine and threonine phosphorylation on ser473 and 308 respectively, while phosphorylating ser307 on IRS-1 (Gual *et al*., 2005; Hotamisligil *et al*., 1996; Ragheb *et al*., 2009). Ceramides, DAG and inflammatory cytokines (TNF-α and IL-6) induce effects that are similar to those produced by palmitate in the induction of insulin resistance (Chavez and Summers, 2003; Schmitz-Peiffer *et al*., 1999; Van der Poll *et al*., 1991; Wieser *et al*., 2013; Lovino *et al*., 2016). Palmitate treated skeletal muscle cells (C2C12 and L6) demonstrate enhanced mRNA and protein expression of TNF-α, together with NF-κB and PKC θ

leading to a reduction in GLUT 4 mRNA and glucose transport (Haghani *et al*., 2015; Jové *et al*., 2006). The use of PKC activators such as 12-O-tetradecanoylphorbol 13-acetate in the induction of insulin resistance further confirms the role of PKC in the pathogenesis of insulin resistance (Deng *et al*., 2012). *In vitro* knock-out studies demonstrate that inhibition of the expression of inflammatory cytokines and fatty acid metabolism in skeletal muscle could potentially improve insulin resistance (Haghani *et al*., 2015).

1.5.2. Liver

C3A cells are human hepatocytes sub-cloned from a hepatoma-derived HepG2 cell line commonly used for *in vitro* studies (Mavri-Damelin *et al*., 2008). C3A cells express liver-specific proteins and display morphological characteristics of human liver cells (Kelly, 1994; Mavri-Damelin *et al*., 2008). Hepatic insulin resistance has been studied in H4IIEC and HepG2 cell lines (Iwakami *et al*., 2011; Lin and Lin, 2008; Misu *et al*., 2010; Zhang *et al*., 2010; Zhao *et al*., 2016). High glucose concentrations, palmitic acid and hydrogen peroxide (H_2O_2) have been used to study insulin resistance in hepatocytes (Iwakami *et al*., 2011; Zhao *et al*., 2016). Palmitic acid treatment of hepatocytes does not only impair insulin signaling by suppressing insulin stimulated AKT activity (Zhang *et al*., 2010), but it also impairs the expression and activation of enzymes that are involved in gluconeogenesis and glycogenolysis (Konstantynowicz-Nowicka *et al*., 2015; Zhao *et al*., 2015). Palmitate treated hepatocytes show decreased expression of the enzymes phosphoenolpyruvate carboxykinase (PEPCK) and glucose 6-phosphatase (G-6-Pase), and increased expression of proteins involved in fatty acid transport, resulting in abnormal glucose metabolism (Dong *et al*., 2015; Konstantynowicz-Nowicka *et al*., 2015; Misu *et al*., 2010). Similar to other tissues that are a target for insulin resistance, palmitate treated cells also show an increase in ROS production, disturbed insulin signaling possibly through the activation of protein-tyrosine phosphatase 1B (PTP1B) (Rudich *et al*., 1998; Zhang and Kaufman, 2008; Zhang *et al*., 2015b).

1.5.3. Adipose tissue

The 3T3-L1 cell line is an immortalized fibroblast-like cell line isolated from non-clonal Swiss 3T3 cells of albino mice. Under appropriate hormonal inducers (insulin), glucocorticoids (dexamethasone) and cyclic AMP stimulants (3-isobutyl-1-

methylxanthine), 3T3-L1 cells can differentiate and resemble mature fat cells (adipocytes) (Arsenijevic *et al*., 2012). Differentiated 3T3-L1 cells express all proteins and morphological characteristics of mature fat cells (Poulos *et al*., 2010). They show sensitivity towards lipogenic (insulin) and lipolytic hormones (leptin and growth hormone) (Cao *et al*., 1991; Green and Kehinde, 1975; Poulos *et al*., 2010). Such characteristics make 3T3-L1 cells suitable for studying glucose metabolism, insulin action, obesity and other related factors *in vitro*.

Free fatty acids such as palmitic, lauric, myristic, linoleic, oleic, and arachidonic acid have been used in 3T3-L1 cells as inducers of insulin resistance (Jiao *et al*., 2009, 2011; Kim *et al*., 2015b; Mazibuko *et al*., 2015; Nguyen *et al*., 2012). Nguyen *et al* (2005) showed that FFA treated 3T3-L1 cells demonstrate decreased insulin-stimulated tyrosine phosphorylation of IRβ and a decrease in total protein concentrations. The increase in expression of NF-κB, which is a transcription factor for inflammatory proteins, and the activation of toll-like receptor 4 (TLR4), which is responsible for innate response of the immune system, provides a link between inflammation and insulin resistance in fatty acid induced insulin resistance of the adipose tissue (Kershaw and Flier, 2004; Suganami *et al*., 2007). The inhibitory effect of palmitic acid in insulin-resistant adipocytes could be linked to the activation of NF-κB and JNK, which induces the secretion of pro-inflammatory cytokines (TNF-α), thereby producing and amplifying proinsulin resistance signals (Shi *et al*., 2006; Song *et al*., 2006).

The use of high glucose concentrations and 4-hydroxynonenal (HNE) have been shown to induce insulin resistance, possibly through the induction of reactive oxygen species (ROS) production (Dasuri *et al*., 2013; Demozay *et al*., 2008; Marshall *et al*., 1991). The production of reactive oxygen species (ROS) in 3T3-L1 adipocytes leads to oxidative stress, downregulation of IRS-1/2 and reduced Glut 4 translocation (Dasuri *et al*., 2013; Demozay *et al*., 2008; Rudich *et al*., 1998). Studies conducted on adipocytes (3T3-L1 and rat primary adipocytes) have linked insulin resistance with Increased *O*-linked beta-*N*-acetylglucosamine (OGlcNAc) modification of IRS-1 and AKT, leading to the inhibition of insulin stimulated glucose uptake (Park *et al*., 2005). The adipose tissue secretes proteins and is also targeted by different proteins that are associated with insulin resistance (Guilherme *et al*., 2008; Kershaw and Flier, 2004; Makki *et al*., 2013). This makes the adipose tissue more than a storage tissue, but a

complex organ with a major role in the pathogenesis of insulin resistance (Kershaw and Flier, 2004). Oxidative stress and inflammation seem to be major pathways involved in adipose tissue insulin resistance and FFA appear to be inducers of these pathways (Makki *et al*., 2013; Nguyen *et al*., 2012; Thomson *et al*., 1997; Wakil and Abu-Elheiga, 2009). Inflammation present during fatty acid-induced insulin resistance provides a link between obesity and insulin resistance in other tissue such as the skeletal muscle (Guilherme *et al*., 2008; Karpe *et al*., 2011).

1.5.4. *In vivo* models of insulin resistance

The *db/db* C57BLKS mouse is a model of obesity, diabetes, and dyslipidemia (Bogdanov *et al*., 2014; Kobayashi *et al*., 2000). The db mutation is located on chromosome 4 of the leptin receptor gene and it is transmitted as an autosomal recessive gene (Bunner *et al*., 2014; Wang *et al*., 2014). The deficiency in the leptin receptor gene leads to faulty splicing of the leptin receptor and the production of non-functional proteins (Bunner *et al*., 2014). A deficiency in leptin signaling is characterized by high leptin and insulin levels, hyperphagia, which ultimately leads to obesity (Sharma *et al*., 2003). In the presence of the db gene, C57BLKS mouse strain develops severe diabetes, hence its use as a model for type 2 diabetes and insulin resistance (Mao *et al*., 2006).

1.5.5. Other models

Common examples of T2D *in vivo* models include *ob/ob* mice and Zucker *fa/fa* rats. The *ob/ob* or *ob* mouse is a model that presents a homozygous leptin mutation (Lep^{ob}) resulting in obesity (Drel *et al*., 2006). Obesity is characterized by an increase in the number and size of adipocytes. The model also presents mild hyperglycemia, which is a result of compensatory hyperinsulinemia, glucose intolerance, increased hormonal production from adrenal gland, high plasma insulin concentration together with impaired wound healing, which are all associated with T2D (King, 2012). The *ob/ob* mouse model presents signs of diabetes at four weeks (King, 2012).

Zucker *fa/fa* rats are the most used models of genetic obesity and diabetes (Kava *et al*., 1990). Zucker fa/fa also develop diabetes due to a mutation on the leptin gene causing obesity and diabetes. Zucker *fa/fa* rats present metabolic abnormalities that are observed in *ob/ob* and *db/db* mouse models, but with higher levels of glucose and insulin resistance in the skeletal muscle (Kava *et al*., 1990; King, 2012). Other known

models include the KK mouse, which develops diabetes as it ages (Ikeda, 1994). The NZO mouse, also known as the New Zealand obese mouse, presents a case of severe obesity with T2D only to the male strain (Ikeda, 1994; Radavelli-Bagatini *et al*., 2011).

1.6. Plants as sources of nutraceuticals – *A. phylicoides*

1.6.1. Classification of polyphenols and their characteristics

Polyphenols are a vast group of phytochemicals found in everyday plant-based foods; such as fruits, vegetables, whole grains, legumes, tea, cereal grains, cocoa and coffee. They are secondary metabolites that are produced by plants in response to stress (Beckman, 2000; Manach *et al*., 2004). Over 8000 phenolic structures have been identified (Bahadoran *et al*., 2013; Pandey and Rizvi, 2009). However, many of these compounds have not been characterized (Bahadoran *et al*., 2013; Manach *et al*., 2004). Polyphenols can be classified according to their structural diversity that ranges from simple phenolic acid to large polymeric macromolecules (Bahadoran *et al*., 2013; Pandey and Rizvi, 2009; Pietta *et al*., 2003). Phenolic acids, flavonoids and the less common stilbenes and lignans are the four major classification groups of polyphenols (Manach *et al*., 2004; Scalbert and Williamson, 2000).

1.6.1.1. Phenolic acids

Phenolic acids are categorized into 2 main classes: hydroxybenzoic acid derivatives (protocatechuic acid and garlic acid) and hydroxycinnamic acid derivatives (chlorogenic acid, caffeic acid, coumaric, para-coumaric acid, sinapic acid and ferulic acid) (Bahadoran *et al*., 2013; Robbins, 2003). The most frequently encountered compounds are caffeic acid found in coffee, fruits berries and cocoa beans (Manach *et al*., 2004; Pietta *et al*., 2003) and ferulic acid found in foods high in fiber such as wheat bran (Scalbert and Williamson, 2000). Herbal teas are also associated with a high content of phenolic acids (Joubert *et al.,* 2008). Compounds such as para-coumaric acid, chlorogenic acid, protocatechuic acid, and caffeic acid have been identified in herbal teas (Joubert *et al*., 2008; Padayachee, 2011). They have been shown to possess anti-oxidant properties, which they may exert through preventing the generation of radicals or the decomposition of radical to non-radical products (Gülçin, 2006; Lorenzo and Munekata, 2016; Semaming *et al*., 2015; Zang *et al*., 2000, 2003). Protocatechuic acid, ferulic acid and sinapic acid have been linked to anti-tumor and anti-hyperglycemic activity together with anti-aging activity (Semaming *et*

al., 2015; Srinivasan *et al*., 2007). Health benefits that have been linked to chlorogenic acid include anti-diabetic, anti-inflammatory and anti-bacterial activity (Farah *et al*., 2008). Chlorogenic acid also helps reduce the side effects accompanied by cholestasis through improving bile flow (Singh, 2011).

1.6.1.2. Flavonoids

The basic structure of flavonoids consists of two aromatic rings that are joined together by three carbon atoms forming an oxygenated heterocycle. They can be subdivided into seven subclasses namely: flavones, flavonols, flavanones, flavanonols, flavanols (or flavan-3-ols or catechins), anthocyanins and isoflavones (Manach *et al*., 2004; Pietta, 2000; Scalbert and Williamson, 2000). Flavonols, such as quercetin, have been shown to induce its anti-tumor properties through inducing apoptosis (Volate *et al*., 2005). Studies have also shown that the compound contains some cardioprotective properties (Jagtap *et al*., 2009). Moreover, quercetin has been shown to decrease basal glucose and insulin concentrations *in vivo* (Arias *et al*., 2014).

1.6.1.2.1. Isoflavones

Isoflavones include compounds with estrogen properties also known as phytoestrogens (Campos and Matos, 2010). These compounds include daidzein, glycitein and genistein, which have been identified in soy products and other legumes (Adlercreutz and Mazur, 1997; Bahadoran *et al*., 2013; Pietta, 2000). These chemical compounds are believed to reduce the risk of cancer (prostate cancer) and bone health (Messina, 1999; Setchell, 1998). It is believed that geistein exerts its anti-cancer activity through activating specific tyrosine kinases and also interfering with transduction mechanisms (Setchell, 1998). Soy has anti-inflammatory properties associated with a reduced risk of cardiovascular diseases and diabetes, these properties are attributed to the isoflavones it contains (Xu *et al*., 2015).

1.6.1.2.2. Flavones

Flavones are not as common as the other groups in fruits and vegetables; they mainly consist of glycosides. Edible sources of these compounds include parsley and celery. Large amounts of polyethoxylated flavones: tangerine, luteolin, nobiletin and sinensetin are contained in the skin of citrus fruits (Manach et al., 2004). Luteolin inhibits the migration and also induce apoptosis of vascular smooth muscle cells

associated with atherosclerosis (Jiang *et al*., 2013). This compound has also been associated with the prevention of memory loss, which it exerts by reducing inflammation in the brain (Theoharides *et al*., 2014, 2015; Yoo *et al*., 2013). It also reduce inflammation in the adipose tissue by suppressing macrophage activation (Theoharides *et al*., 2015).

1.6.1.2.3. Flavonones and Flavanols

Flavanones are glycosylated compounds that are found in large amounts in the white spongy part of citrus fruits (Majo *et al*., 2005). They are also found in fruits like tomato and aromatic plants such as mint (Manach et al*.*, 2004). Naringenin was shown to inhibit hepatic lipid accumulation, decrease blood glucose concentrations and also improve insulin secretion (Kawser Hossain *et al.,* 2016).

The richest source of flavanols is green tea and chocolate. They are also found in other foods such as apricots and beverages such as wine (Aherne and O'Brien, 2002). They exist in two forms: monomer form (catechins) and the polymer form (proanthocyanidins). The main flavanols in fruits are catechin and epicatechin, whereas gallocatechin, epigallocatechin, and epigallocatechin gallate is found in certain seeds of leguminous plants, in grapes and most abundantly in tea. Tea epicatechin and epigallocatechin gallate are highly stable, even when exposed to heat (Zhu *et al.,* 1997). Green tea catechins have been shown to lower body weight gain, triglyceride and cholesterol levels, making them an attractive drug candidate for weight loss (Cooper *et al*., 2005). Some health benefits of green tea are, stress lowering, antiviral, anti-carcinogenic and ultraviolet light skin protection properties (Cooper *et al*., 2005).

1.6.1.3. Anti-diabetic benefits

Phenolic acids such as chlorogenic have been intensely studied for their anti-diabetic benefits (Bahadoran *et al*., 2013). This compound acts in a similar fashion to metformin, which is by restoring the sensitivity of insulin-resistant cells, thereby improving glucose uptake (Deng *et al*., 2012; Meng *et al*., 2013). Not only does it mimic metformin, it has been shown to act in a similar manner to α-glucosidase inhibitors thereby suppressing postprandial hyperglycemia (Meng *et al*., 2013). In the liver, chlorogenic acid promotes the activity of CPT1 and enhances the rate of fatty acid oxidation (Mubarak *et al*., 2013; Sudeep *et al*., 2016). Protocatechuic acid improves

glucose uptake in adipocytes through the upregulation of peroxisome proliferator–activated receptor-γ. Cyclooxygenase-2 (Cox-2) is a pro-inflammatory enzyme that has been linked to insulin resistance (Chen *et al*., 2016). Diet induced together with palmitate induced insulin resistance have been shown to upregulate the expression of Cox-2 and toll-like receptor 2 (TLR-2) through the activation of NF-κB (Coll *et al*., 2010; Francés *et al*., 2015; López-Lázaro, 2009). The inhibition of Cox-2 has been shown to restore insulin sensitivity and also stimulate glucose uptake (Tian *et al*., 2011). Flavones, such as luteolin, inhibit the activation of NF-κB, which is responsible for the expression of inflammatory cytokines and inhibition of COX-2 and could potentially improve insulin resistance (López-Lázaro, 2009).

Green tea catechins have been shown to improve insulin-dependent glucose uptake in insulin-resistant skeletal muscle and adipose tissue by facilitating GLUT 4 translocation via AMPK pathway, thereby restoring insulin sensitivity (Ueda *et al*., 2008; Wu *et al*., 2004). In addition, the cinnamon phenolic compound naphthalene methyl ester of 3,4-dihydroxyhydrocinnamic acid (DHH105) showed enhanced phosphorylation of IR-β subunit and IRS-1 in adipocytes, resulting in the activation of phosphatidylinositol 3-kinase and AKT, thereby facilitating translocation of GLUT4 to the plasma membrane both *in vivo* and *in vitro* (Kim *et al*., 2006).

Eid *et al*., (2015) reported that quercetin stimulated glucose uptake in murine skeletal muscle cells C2C12, L6, murine H4IIE and human HepG2 liver cells through an insulin-dependent pathway that also involves AMPK (Eid *et al*., 2010, 2015). Activation of AMPK is known to increase glucose uptake by facilitating the translocation of GLUT4 transporters to the plasma membrane (Eid *et al*., 2010; Jeon, 2016). Adenosine monophosphate-activated protein kinase decreases hepatic glucose production by downregulating key gluconeogenesis enzymes such as phosphoenolpyruvate carboxylase (Hardie *et al*., 2012). Overall data demonstrate that polyphenols positively influence glucose metabolism in the adipose, liver, and skeletal muscle, and therefore appear to be a promising therapeutic candidate for the treatment of type 2 diabetes.

1.6.2. Overview of *A. phylicoides*

Athrixia phylicoides, also known as bush tea/Zulu tea, is one of the nine plants that are found in South Africa belonging to the genus Athrixia. *A. phylicoides* is an aromatic

shrub with woolly stems that grows in the eastern parts of South Africa (Mpumalanga, Limpopo, KwaZulu-Natal) and Swaziland. *A. phylicoides* blooms between the month of March and May, giving rise to light purple petals with bright yellow centers (Figure 1.3). *A. phylicoides* commonly grows in grassland and forest margin shrub areas, it can be used for medicinal and non-medicinal purposes (Pooley, 1998).

1.6.2.1. Traditional uses

South African locals use the leaves and twigs of the plant to make a refreshing beverage (infusion). The roots of the plant are used as a laxative and they can also be boiled and used as a cough remedy, which is a common practice amongst the Zulus (Joubert *et al*., 2008; Rampedi and Olivier, 2005). The herbal infusion can also be used for blood purification and the treatment of sores and burns. The local South African population living in the Gauteng province reported that they use *A. phylicoides* as a broom (Hutchings *et al*., 1996; Rampedi and Olivier, 2005). The VhaVenda people use this plant as a laxative and it is also believed that the plant carries some spiritual healing properties (McGaw *et al*., 2007). Hutchings *et al* (1996) and van Wyk and Gericke (2000) also reported that the VhaVhenda people brew the plant as an aphrodisiac. BaSotho use the plant to treat sore throats and coughs (Van Wyk *et al*., 2000).

Figure 1.3 Image of *A. phylicoides*. Figure taken from Pooley (2008)

1.6.2.2. Chemical composition of *A. phylicoides*

De Beer *et al* (2011) characterized the phenolic composition of an aqueous extract of *A. phylicoides* using High-Performance Liquid Chromatography with Diode-Array Detection (HPLC-DAD) and Liquid Chromatography–mass spectrometry (LC-MS) and

detected phenolic acids, flavonoids, and flavonols such as chlorogenic acid, 1,3-dicaffeoylquinic acid, 5-hydroxy-6,7, 8,3`,4`,5`-hexamethoxyflavon-3-ol and several hydroxycinnamic acid derivatives. The 6-hydroxyluteolin-7-O-β-glucoside and quercetagetin-7-O-β-glucoside were also identified using counter-current chromatography and liquid-liquid partitioning together with semi-preparative reversed phase HPLC (De Beer *et al*., 2011). Three additional compounds, 5-hydroxy-6,7,8,3`,4`,5`-hexamethoxyflavon-3-ol, 3-0-dimethydigicitrin and quercetin, were identified by Mashimbye *et al*. (2006). The most abundant polyphenolic compounds identified were 6-hydroxyluteolin-7-O-β-glucoside, followed by chlorogenic acid and protocatechuic acid (De Beer *et al*., 2011; Chellan *et al*., 2008).

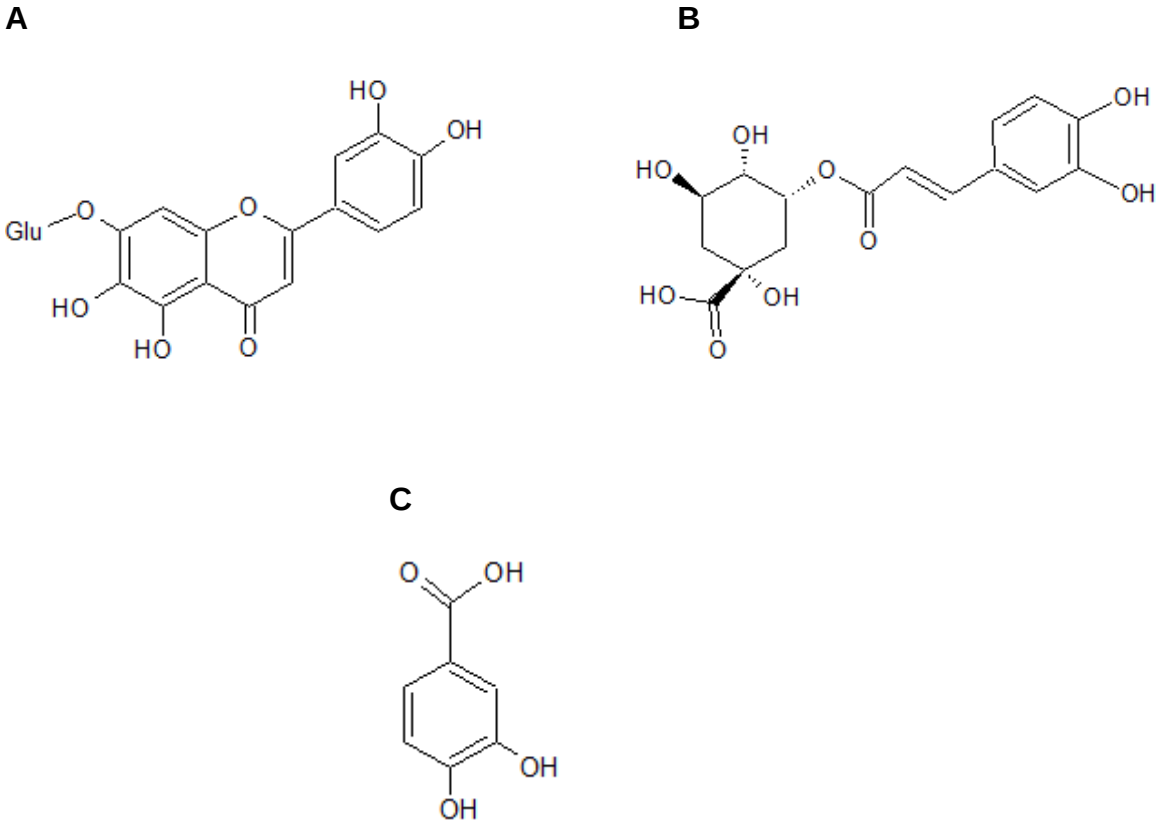

Figure 1.4 Selected phenolic compounds found in abundance in aqueous extracts of *A. phylicoides*.
(A) 6-hydroxyluteolin-7-O-β-glucoside, (B) chlorogenic acid and (C) protocatechuic acid.

1.6.2.3. Potential health benefits of *A. phylicoides*

Locals dwelling in rural and urban parts of South Africa also reported that they use *A. phylicoides* as a treatment for metabolic abnormalities such as hypertension and diabetes (McGaw *et al*., 2006). *In vitro* studies using an aqueous extract from *A. phylicoides* Chellan *et al* (2012) demonstrated enhanced glucose uptake and

utilization by Chang cells and C2C12 muscle cells. Following exposure to the extract, oxidation of ^{14}C-glucose to $^{14}CO_2$ increased significantly in both Chang cells and C2C12 muscle cells, while no effect was reported for 3T3-L1 adipocytes. The extract showed no cytotoxic effects *in vitro* and *in vivo* (Chellan *et al*., 2008, 2012) and it was suggested that it could improve glucose uptake via insulin dependent and insulin-independent pathways and protect against hyperglycemia-induced oxidative stress *in vitro* (Chellan *et al.,* 2012).

Some of the compounds found in *A. phylicoides* have been studied for their biological activity. Hypoglycemic effects of protocatechuic acid were shown in streptozotocin-induced diabetic rats, affecting enzymes involved in gluconeogenesis and glycolysis (Harini and Pugalendi, 2010). Chlorogenic acid also possesses anti-diabetic activity, such as suppression of hepatic gluconeogenesis (Hemmerle *et al*. 1997) and stimulation of glucose uptake through activation of AMPK in skeletal muscle (Ong *et al*. 2013). While the hypoglycemic effect of *A. phylicoides* was demonstrated by Chellan and colleagues (2012), its effect on insulin-resistant cells remains unknown. Investigation of the metabolic bioactivity in *in vitro* insulin-resistant models reflecting three tissues implicated in insulin resistance is likely to provide new knowledge and scientific evidence for the health-promoting effects of *A. phylicoides*.

Conclusion

It appears that free fatty acids play a major role in inducing insulin resistance. An increase of free fatty acids in the circulatory system has been implicated in inflammation, endoplasmic reticulum stress, ectopic fat deposition and many more abnormalities that are associated with insulin resistance. (Bollheimer *et al*., 1998; Hotamisligil *et al*., 1995; de Luca and Olefsky, 2008; Snel *et al*., 2012; Wieser *et al*., 2013; Yu *et al*., 2002; Zhang and Kaufman, 2008). Since the prevalence of T2D continues to rise also in South Africa, there is a need for investigating preventive mechanisms and safer alternatives, such as nutraceuticals, that can be included into a healthy life style.

1.7. Study Aims and Objectives

Hypothesis*: A. phylicoides* extract can protect against and/or ameliorate insulin resistance.

The proposed aims of the study were to investigate the effect of an aqueous extract of *A. phylicoides* on glucose metabolism in *in vitro* models of insulin resistance. Underlying mechanisms were elucidated by measuring changes in protein expression due to the plant extract. The effect of the extract on the development of diabetes in C57BLKS *db/db* mice was also be assessed.

In order to address the specific aim of the study, we:

- Established the effect *of A. phylicoides* extract on cell viability in the selected insulin-resistant cell models (dose finding).
- Investigated the effect of *A. phylicoides* extract on glucose uptake in palmitate-induced insulin-resistant cells at non-toxic concentrations.
- Investigated underlying mechanisms pertaining to glucose metabolism and insulin signaling using Western Blot analysis of selected proteins.
- Determined the effect of the extract on glucose metabolism in diabetic C57BLKS *db/db* mice

Chapter 2

2. **Materials and Methods**

2.1. Materials and methods

The plant was harvested from a natural population in the Bushbuckbridge area (Mpumalanga, South Africa) and identified by the South African National Botanical Institute. *Athrixia phylicoides* was supplied by Prof Jana Olivier (University of South Africa) and an aqueous extract was prepared by Dr Dalene De Beer from leaves and twigs according to the method described by Chellan *et al* (2012). The extract was prepared on a small scale, freeze-dried and characterized by Dr Christiaan Malherherbe (Agricultural Research Council of South Africa) using HPLC- DAD analysis according to the method described by De Beer *et al.* (2011) (Figure 2.1).

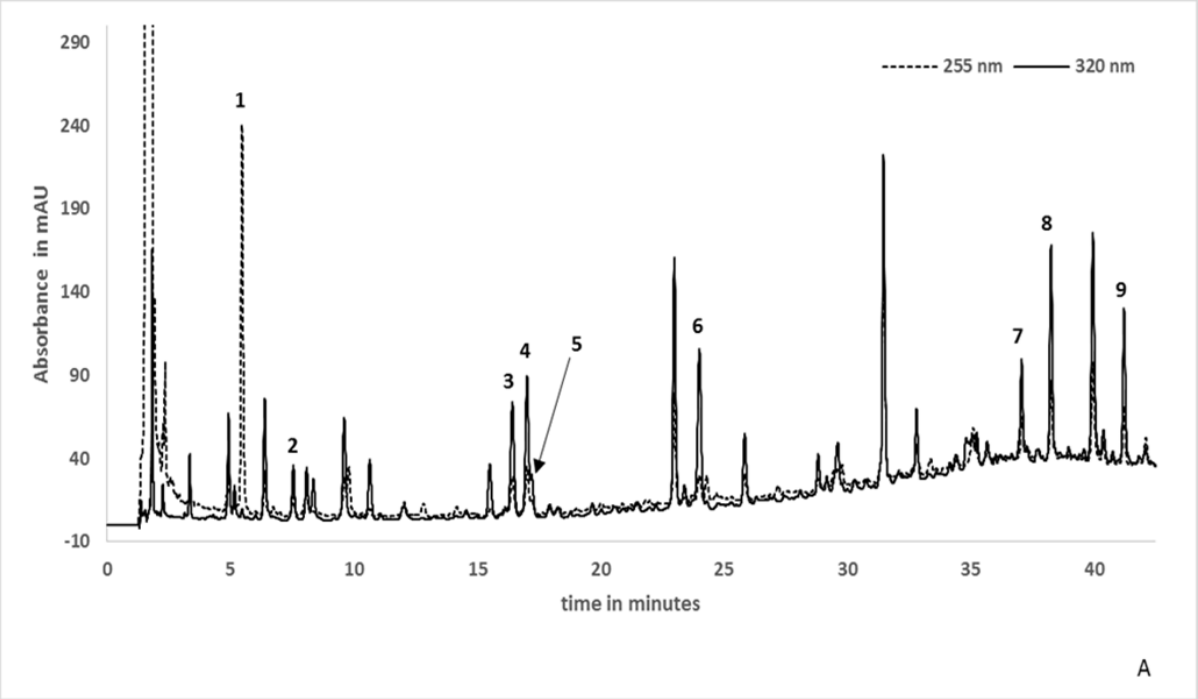

Figure 2.1 HPLC-DAD chromatogram with each peak identifying the prominent phenolic compounds in an aqueous extract of *A. phylicoides*
(1) Protocatechuic acid, (2) neochlorogenic acid, (3) Caffeic acid, (4) Chlorogenic acid, (5) Cryptochlorogenic acid, (6) para-coumaric acid, (7) 3,4-dicaffeoylquinic acid, (8) 3,5-dicaffeoylquinic acid, (9) 4,5-dicaffeoylquinic acid.

Table 2.1: List of reagent, catalogue numbers and suppliers

Material	Supplier	Catalogue no
1,1-Dimethylbiguanide hydrochloride (Metformin)	Sigma-Aldrich	D150959-5g
1,4-Dithiothreitol	Sigma-Aldrich	3483-12-3
2-deoxy-[3H]-D-glucose	Amersham	ART 0200C
3-(4,5-dimethylthiazol-2-yl)-2,5-di phenyltetrazolium bromide (MTT)	Sigma-Aldrich	M2003
Bovine serum albumin (BSA) fatty acid free	Capricorn Scientific	BSA-FAF-1U
Bradford reagent	Bio-Rad	500-0201
Serum albumin bovine serum (BSA)	Bio-Rad	100-10SB
Cell culture tested water	Lonza	BE17-724Q
Crystal Violet powder	Sigma-Aldrich	548-62-9
Dexamethasone	Sigma-Aldrich	D4902
Dimethyl sulfoxide (DMSO)	Sigma-Aldrich	D4540
Dulbecco's phosphate buffered saline (DPBS)	Lonza	BE17-513F
Dulbecco's modified eagle's medium (DMEM)	Lonza	BE12-604F
Dulbecco's modified eagle's medium (DMEM) without phenol red	Sigma-Aldrich	BE12-604F
Eagle's modified essential medium (EMEM)	Lonza	BE12-662F
Metformin	Sigma Aldrich	D150959
Ethyl alcohol	Sigma-Aldrich	E7023-500ml
Fetal Bovine Serum	GIBCO	1050-064
Glycine	Sigma-Aldrich	G7126
HEPES	Lonza	17-737E
Horse serum	Highveld Biological	308
Human insulin solution	Sigma-Aldrich	I9278-5ML
Insulin ELISA kit	Merck Millipore	EZRMI-13K
Isobutyl-1-methylxanthine (IBMX)	Sigma-Aldrich	I5879-1G
Isopropanol	Sigma-Aldrich	19516
LabAssayTM Glucose	Wako Pure Chemical Industries, Ltd	298-65701
L-glutamin	Lonza	G8540
New Born Calf Serum (NBCS)	Biochrom	BC/S0125-H

Oil red O powder	Sigma-Aldrich	1320-06
Palmitic Acid	Sigma-Aldrich	P5585-10G
para-Nitrophenylphosphate	Sigma-Aldrich	SRE 0026
Protein-tyrosine phosphatase 1B (PTP1B)	Abcam	Ab51277
Sodium dodecyl sulfate (SDS)	USB Incorporated	77504 500ML
Trisodium citrate	Sigma-Aldrich	6132-04-3
Trypan blue	Sigma-Aldrich	T93595
Trypsin	Lonza	17-161F

Table 2.2: Reagents and preparation of stock solutions

Reagents / stock solution	Weight/volume
Krebs-Ringer bicarbonate HEPES buffer (KRBH) • 115 mM NaCl [M_W=58.44] • 24 mM $NaHCO_3$ [M_W=84.01] • 5 mM KCl [M_W=74.55] • 1 mM $MgCl_2$ [M_W=95.21] • 2.5 mM $CaCl_2$ [M_W=110.98] • BSA 0.1 % (w/v) • 1M HEPES [M_W=238.3] • 8 mM Glucose • TC water Filter sterilize using a 0.22µm filter unit	 3.36 g 1.008 g 0.186 g 0.048 g 0.139 g 0.5 g 5 ml 720.64 g Make up to the mark using a volumetric flask (500 ml)
1N NaOH stock solution • NaOH M_W= 39.997] • TC water	1.8g 45 ml
2N NaOH stock solution • NaOH M_W= 39.997] • TC water	3.6 g 45 ml
Bradford lysis buffer • 10 % SDS stock • 2N NaOH stock • TC water	500 µl 2.5 ml 47 ml
50 % ethanol solution (45 ml) • ethanol (absolute) • TC water	22.5 ml 22.5 ml
3-isobutyl-1-methylxanthine (IBMX) stock • IBMX • 50 % ethanol	57.9 mg 5.21 ml
Dexamethasone 10mM stock • Dexamethasone [M_W=392,461] • 100 % ethanol	3.92 mg 1 ml

Reagents / stock solution	Weight/volume
Full growth medium for C2C12 • FBS (final FBS concentration-10 %) • DMEM with phenol red	 4.5 ml 40,5 ml
Full growth medium C3A • FBS (final concentration – 10 %) • L-glutamine (final concentration 2 mM) EMEM	 4.5 ml 450 µl 40.050 ml
Full growth medium 3T3-L1 • NCS (final concentration-10 %) • DMEM	 4.5 ml 40 ml
Adipocyte differentiating medium • FBS (final concentration 10%) • dexamethasone1 µM • insulin1 µg/ml • IBMX (0.5 mM) • DMEM	 3.5ml 3.5 µl 3.5 µl 350 µl 34.643 ml
Adipocyte maintenance medium • FBS (final concentration -10 %) • 1 µg/ml insulin • DMEM	 3.5 ml 3.5 µl 31.15 ml
Myocyte differentiating medium • Horse serum (final concentration- 2 %) • DMEM	 900 µl 44.1 ml
3-(4,5-dimethylthiazol-2-yl)-2,5-diphenyltetrazolium bromide (MTT solution) (2 mg/ml stock) • MTT • TC water Dissolve and filter sterilize using a syringe driven filter unit 0.22µm	 90 mg 45 ml
Palmitic acid 150 mM stock • Palmitic acid [M_W=256.42] • Ethanol (100 %)	 57.69 mg 1500 µl
• **Sorenson's buffer (pH 10.5)** 0.1M glycine [MW=75.07] • 0.1M NaCl [M_W=58.44] • TC water	 0.75 g 0.584 g 100 ml
1 % (w/v) Oil Red O stock solution • ORO powder • isopropanol	 1 g 100 ml
0.7 % Oil Red O working solution • 1 % ORO solution • Distilled water	 7 ml 3 ml
2 % Crystal Violet stock solution • Crystal violet powder • TC grade water	 2 g 100 ml

Reagents / stock solution	Weight/volume
Crystal violet working solution • 2 % Crystal violet stock solution • Distilled water	 250 µl 49.750 ml
Citric acid stock solution (250 ml) • 50 mM citric acid monohydrate (M_W 210.14 • ddH_2O	 2.63 g 250 ml
Trisodium citrate solution stock solution (250 ml) • sodium citrate tribasic dehydrate [M_W=294.10] • ddH_2O	 3.689 mg 250 ml
Citrate buffer working solution Adjust pH of trisodium citrate using citric acid (pH=6) Dissolve: • trisodium citrate [Mw=294.10] • 1 mM Ethylenediaminenttraacetic acid (EDTA) [M_W=372.24] • 0.1 M Sodium chloride [M_W=58.44] **Store at -4ºC**	 7.35 g 186.12 mg 2.9 g
1,4-Dithiothreitol (DTT) stock solution • 1 mM DTT [M_W=154.25] • Citrate buffer Mix by vortexing	 30.8 mg 20 ml
para-Nitrophenylphosphate (Pnpp) stock solution • 10 mM pNPP [M_W=371.1] • 50 mM Citrate buffer	 75 mg 20.21 ml
Protein-tyrosine phosphatase 1B (200 µg/ml stock solution • PTP1B enzyme • 50 mM Citrate buffer	 100 µl 400 µl

2.2. *In vitro* study

2.2.1. Muscle cell insulin resistance model

As a model for the insulin target muscle tissue, the murine skeletal muscle cell line C2C12 (ECACC catalogue number 91031101) was used. Cells were cultured and maintained in Dulbecco's Modified Eagle Medium (DMEM) supplemented with 10 % Fetal Bovine Serum (FBS). Cells were sub-cultured every 2 days once they reached 70 % confluency for a maximum of 10 passages. Cells were incubated at 37 °C with 5 % CO_2 and humidity (standard culture conditions).

Cells were cryopreserved by freezing in Dulbecco's Modified Eagle's Medium (DMEM) containing 20 % fetal bovine serum (FBS) and 7.5 % dimethyl sulfoxide (DMSO) to serve as cryoprotectant. Cells were thawed by placing them in a water-bath (37 °C). Immediately after thawing, the cell suspension was transferred into 50 ml tubes containing 9 ml of pre-warmed growth media (DMEM supplemented with 10 % FBS). This was followed by centrifuging cells at 200 g for 5 min. The supernatant was removed by aspiration and the cell pellet was re-suspended in fresh media and mixed by gentle pipetting up and down. Thereafter, cells were counted by staining 20 µl of cell suspension with 20 µl 0.4 % (w/v) trypan blue solution. The solution was mixed by pipetting up and down. The mixture was pipetted into the counting chambers of a hemocytometer and the number of cells was counted under an inverted light microscope (Olympus CKX41, Olympus, Tokyo, Japan) using the 10X magnification lens. Cells were counted in all 9 squares of the hemocytometer, the average was determined and it was multiplied by a factor of two and the volume of each square (10 000) in order to determine the number of viable cells per milliliter.

2.2.1.1. Sub-culturing and seeding for experiments

Once cells had reached a confluency of 70 %, media was aspirated and cells were washed with 12 ml of pre-warmed DPBS. Cells were trypsinized by the addition of 2 ml (75 cm^2 flask) trypsin, followed by incubation for 5 min (under standard culture conditions) in order to detach the cells from the growth surface of the flask. A light microscope (Olympus CKX41, Olympus, Tokyo, Japan) was used to confirm detachment of the cells from the growth surface, followed by the addition of 8 ml fresh media to deactivate the trypsin. Thereafter, cells were centrifuged for 5 min at 200 g. The supernatant was gently removed by aspiration, making sure not to disturb the

pellet. Cells were re-suspended in 5 ml fresh media and an aliquot of the suspension was used to count the number of cells. Cells were counted as described in section 2.1.1.2. After counting, cells were seeded into 75 cm^2 flask for maintenance, 25 cm^2 flasks for western blots and into multi-well plates for assays (Table 2.3).

Table 2.3: Seeding densities for C2C12 experiments in different plates and flasks

Cell line	Plate/flask type	concentration/ml	Cell density	Volume/well
C2C12	96 well plate	50 000 cell/ml	5 000 cells/well	100 µl
	48 well plate	42 500 cells/ml	17 000 cell/well	400 µl
	25 cm^2 flask	80 000 cells/ml	400 000 cells/flask	5 ml

2.2.1.2. C2C12 myocyte differentiation

C2C12 cells were seeded into a 96 well plate (TC treated flat bottom, Eppendorf, Hamburg, Germany) for cytotoxicity assays or 48 well plate (Corning® CellBIND®, Corning Corp., St Louis, USA) for glucose uptake and grown to confluence for 48 hrs. To achieve differentiation of C2C12 cells, growth media was replaced with differentiation media (Table 2.1, DMEM containing 2 % horse serum) after for a further 2 days, in order to reduce proliferation and initiate the formation of myotubules.

2.2.1.3. Induction of insulin resistance in C2C12 resistance and treatments of cells with extract

Insulin resistance was induced by treating cells with freshly prepared palmitic acid (750 µM) in DMEM without phenol red, containing 5 mM glucose and 2 % fatty acid free BSA. The palmitic acid was prepared from a stock solution (150 mM palmitic acid) and it was diluted with an equal amount of 100 % ethanol before adding to a 2 % fatty acid-free BA in DMEM, yielding a final concentration of 750 µM and 1 % ethanol. A solvent control (1 % ethanol) was prepared with 100 % ethanol and both solutions were incubated in a water bath at 37 ºC for 2 hrs in order to conjugate the palmitic acid with the BSA. After 2 hrs of incubation, the solution was filter sterilized using 0.22 µm Milex® syringe driven filter unit (Merck Millipore, Massachusetts, USA). The cells were then treated with 400 µl of the solutions under standard culture conditions for 16 hrs based on a study by Mazibuko *et el*. (2013).

After the induction of insulin resistance, C2C12 cells were washed and serum-starved with 400 µl of pre-warmed Dulbecco's phosphate buffered saline (DPBS) for 1 hr,

under standard culture conditions to avoid interference from serum proteins during the assay. After serum-starving, cells were treated with 2 concentrations of *A. phylicoides* (10 and 100 µg/ml) prepared from a 10 mg/ml stock solution and 1 µM metformin dissolved in Krebs Ringer bicarbonate HEPES buffer (KRBH) (Table 2.2) containing: 2 % BSA,1 % ethanol, 750 µM palmitic acid and 8 mM glucose. Palmitic acid and ethanol were diluted as described in Table 2.2. The cells were treated with 400 µl of the treatments and incubated under standard culture conditions for 3 hours. Thirty minutes before the end of the incubation time insulin was added to yield a 2 µM final concentration and the cells were incubated for a further 30 min (Figure 2.2).

2.2.1.4. Determination of cytotoxicity using - MTT Assay

Cells were seeded into a 96 well plate (Tissue culture treated flat bottom, Eppendorf, Hamburg, Germany) and they were differentiated after reaching 100 % confluency. After differentiation, they were serum starved for an hour followed by treatment with different concentrations of *A. phylicoides* (0.01, 0.1, 1 and 2 mg/ml), which were dissolved in KRBH containing 8 mM glucose. Thereafter, cells were incubated under standard culture conditions for 3 hrs. Treated cell were subjected to an MTT assay in order to determine toxicity/viability. The MTT assay is a colorimetric assay that detects metabolic activity by means of NADPH-dependent cellular oxidoreductase enzyme. In living cells, the NADPH-dependent cellular oxidoreductase enzymes reduce the tetrazolium dye MTT 3-(4,5-dimethylthiazol-2-yl)-2,5-diphenyltetrazolium bromide to its insoluble formazan, which is indicated by a purple color (Mosmann, 1983).

Medium from the treated cells was removed and the cells were washed with 100 µl of pre-warmed DPBS. This was then followed by the addition of 100 µl of 1 mg/ml of the MTT solution into each well followed by incubation at 37 ºC for 30 min. Thereafter medium containing MTT was removed from the wells, 200 µl of Dimethyl sulfoxide (DMSO) and 25 µl of Sorenson's glycine buffer (0.1 M glycine + 0.1 M NaCl, pH 10.5) were added into each well. The solution was gently mixed by pipetting up and down and the absorbance was measured at the wavelength of 570 nm using a microtiter plate reader (BioTek® ELX800, BioTek, Vermont, USA). Results were expressed as percentage of control.

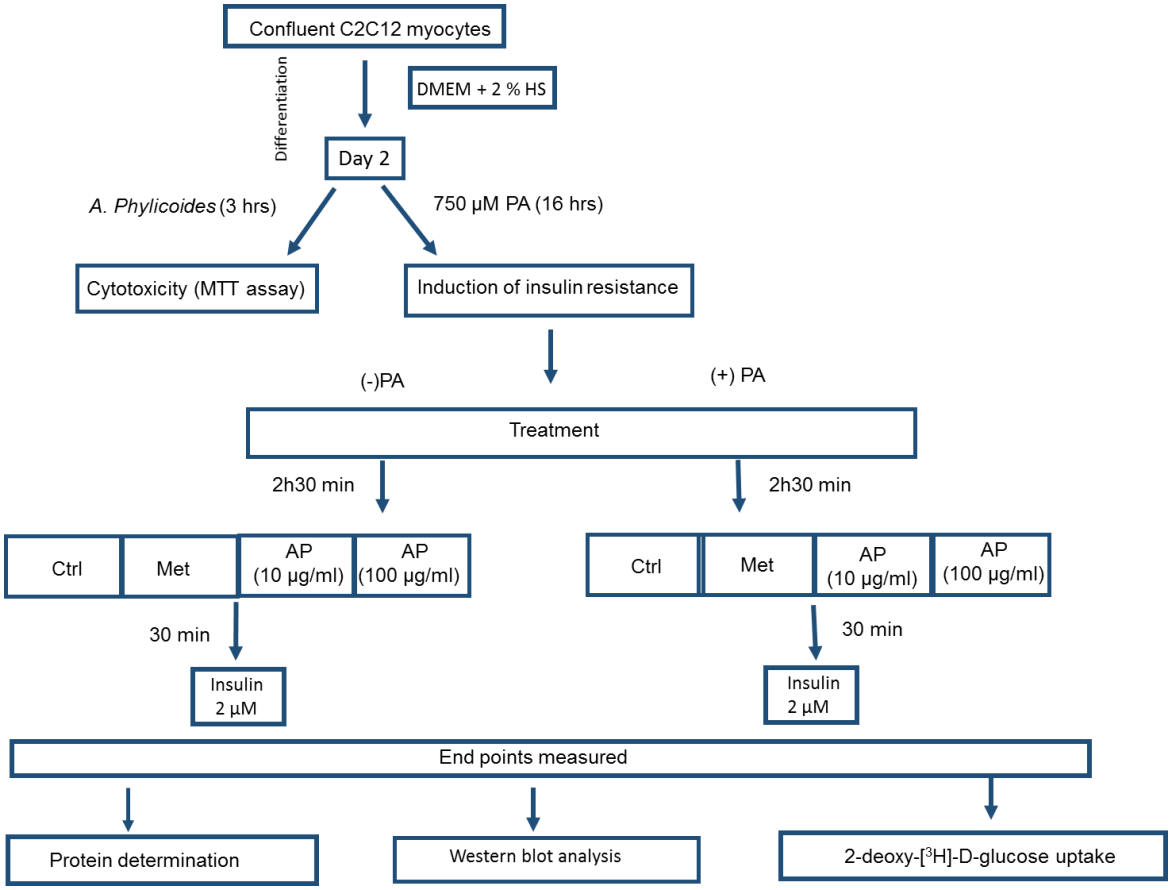

Figure 2.2: Experimental outline for C2C12 cell line.
PA - palmitic acid, Ctrl - control, Met - metformin, AP - *A. phylicoides*

2.2.1.5. Glucose uptake assay using 2-deoxy-[^{3}H]-D-glucose

The 2-deoxy-[^{3}H]-D-glucose uptake assay involves adding 2-deoxy-[^{3}H]-D-glucose to cells and measuring its intracellular concentrations using a scintillation counter. To measure the intracellular concentrations of 2-deoxy-[^{3}H]-D-glucose, treatments were removed after 3 hrs and the media was replaced with 125 µl glucose free KRBH containing and 0.5 µCi/ml 2-deoxy-[^{3}H]-D-glucose with or without insulin (2 µM). Cells were incubated under standard culture conditions. Thereafter, cells were washed twice with 250 µl of ice cold DPBS in order to stop the reaction and also wash off excess glucose that might have remained. Cells were lysed by adding 500 µl of lysis buffer (0.1 M NaOH + 0.1 % SDS) into each well followed by incubation at 37 ºC in an orbital shaker for 1h30 min for cell lysis. Scintillation fluid was prepared by adding 400 µl double distilled water (ddH_2O), 400 µl sample and 2 ml of Ready Gel Ultima Gold into scintillation vials (6 ml miniature size, PerkinElmer, Waltham, USA). The remaining samples were stored in the plates at -20 ºC for Bradford assay. The scintillation cocktail was mixed by inverting vials until the samples were clear. Vials were placed

into a liquid scintillation analyzer (2200 CA, Parkard Tricarb series, PerkinElmer, Waltham, USA) and left in the analyzer for a minimum of 1hr to equilibrate to room temperature and darkness. Samples were read using a program that allows quantification of ^{3}H-isotope. The counter efficiency was calculated using counts per minute (CPM) and disintegrations per minute (DPM). Values obtained were used to calculate the specific radioactivity on a GraphPad online radioactivity calculator (www.graphpad.com/quickcalcs/radcalcform.cfm) radioactivity calculator. The CPM average of each well was divided by the specific radioactivity and multiplied by the amount of sample loaded, in order to obtain cpm/fmol. The concentrations obtained were normalized by protein values in order to obtain fmol/mg. Results were reported as the percentage of control.

2.2.1.6. Protein determination Bradford assay

The Bradford assay is a spectroscopic method that is used to determine total protein concentration in a lysate. It is based on the absorbance shift of the dye Coomassie Brilliant Blue G-250, which changes color to blue when it comes into contact with assayed proteins. Binding of the assayed protein to the dye stabilizes the blue form of the dye allowing the concentration of the protein to be measured by absorbance of the complex formed. The ionic form of the dye (blue) has an absorbance maximum at 590 nm (Bradford, 1976).

The assay was conducted in a 96 well clear assay plate (polystyrene Greiner Bio-one, Frickenhausen, Germany). The standard was prepared by serially diluting bovine serum albumin (BSA) in lysis buffer. A concentration range between 0.031 to 1 mg/ml was used. Each well contained 5 µl of the serially diluted sample, followed by the addition of the protein samples in the remaining wells. Thereafter, 250 µl of the Bradford agent was added into each well, followed by a 5 min incubation in the dark (room temperature). The absorbance was measured at a wavelength of 570 nm in a BioTek® ELX800. The standard curve was used to determine total protein concentrations expressed as mg/ml.

2.2.1.7. Protein analysis (Western Blots)

Table 2.4: Materials for Western blot analysis

Material	Supplier	Catalogue number
Laemli sample buffer	Bio-Rad	161-0737
Trizma® base	Sigma-Aldrich	T1503-1KG
Glycine	Sigma-Aldrich	G7126-1KG
Nacl	Sigma-Aldrich	S7653-1KG
Tween-20	Sigma-Aldrich	58980C
Hybond-P PVDF membrane	Amersham	RPN1416F
Whatman paper	Merck Millipore	3031-915
Clarity™ western ECL substrate	Bio-Rad	170-5060
Instant skimmed milk powder	Spar	N/A
Methanol (analytical grade)	VWR Chemicals	1070182511
Restore™ PLUS Western blot stripping buffer	Thermo Scientific	46430
Ponceau S stain	Sigma Aldrich	P23295
10X tris/glycine/SDS buffer	Bio-Rad	161-0772
Mini-PROTEIN® TGX™ gels	Bio-Rad	456-1034
LumiGLO Reserve™	KPL	54-71-000
BSA standard	Bio-Rad	500-0007
Dc reagent A	Bio-Rad	500-0114
Dc reagent B	Bio-Rad	500-0113
Dc reagent S	Bio-Rad	500-0115
Stainless steel beads	Qiagen	69989
Precision plus protein WesternC marker	Bio-Rad	161-0382

Precision protein strep Tactin-HRP conjugate	Bio-Rad	161-0381
Glucose transporter 4 (GLUT4)	Cell Signaling	2213
Total threonine kinase B (AKT)	Cell Signaling	4685
Phosphorylated threonine kinase B (AKT ser473)	Cell Signaling	4060
Beta actin	Santa Cruz	Sc-2318
PMSF	Fluka	78830
Tween 20	Sigma-Aldrich	58980C
Phosphorylated 5'adenosine monophosphate activated protein kinase (AMPK ser172)	Cell Signaling	2535
Total 5'adenosine monophosphate activated protein kinase (AMPK)	Cell Signaling	3523

Table 2.5: Stocks and buffer preparation for Western blot analysis

Solutions	**Volume**
Transfer buffer (1L) • 25 mM Tris (MW=121) • 192 mM glycine (MW=75.07) • ddH_2O • 100 % Methanol	 3.03 g 14.41 g 800 ml 200 ml
10 X Tris buffered saline (TBS) (pH=7.6) • 200 mM Tris (Mw) • 1.37 M NaCl (Mw) Dissolve in 1 L ddH_2O	 24.22 g 80.06 g
Tris buffered saline with TWEEN 20 (TBST) • 10X TBS • ddH_2O • Tween-20	 100 ml 900 ml 1 ml
1X running buffer (1L)	

• Dilute of 10X tris/glycine/SDS • ddH_2O	100 ml 900 ml
5 % blocking solution • Instant skimmed milk powder • 1X TBST	 5 g 100 ml
2.5 % blocking solution • Instant skimmed milk powder • 1X TBST	 2.5 g 100 ml
Sample buffer (4X) • 900 µl of Laemli sample buffer • 100 µl of β-mercaptoethanol	 950 µl 50 µl

2.2.1.7.1. Protein isolation from cells

Skeletal muscle cells (C2C12) were grown and differentiated in 25 cm^2 flasks. Treatments were prepared as described in section 2.1.1.5. Each flask was treated with 5 ml of the treatments, incubated under standard culture conditions for 3 hrs and insulin (2 µM) was added for the last 30 min. Thereafter, cells were washed with 5 ml DPBS and 300 µl of lysis buffer was added into each flask. Cells were lifted off the surface using a scraper and the lysate was transferred into 2 ml tubes. Samples were stored at -20 ºC until they were needed.

The cell lysate was thawed on ice. Thereafter, a stainless ball was added into every sample. The samples were loaded on a pre-cooled tissue lyser blocks and they were lysed in a tissue lyser (Qiagen, Hilden, Germany) at 25 Hertz for 60 seconds. Thereafter, the samples were removed from the tissue lyser block and placed on ice for 60 sec. This step was repeated 5 times to ensure proper lysis. Thereafter, samples were centrifuged (Thermocentrifuge, Eppendorf, Hamburg, Germany) for 15 min at 15 7890 g (4 ºC) and the supernatant was carefully removed and transferred into fresh 1.5 ml tubes.

2.2.1.7.2. Protein quantification (RD CDTM assay)

The reducing agent and detergent compatible (RD CD) assay is a colorimetric assay that is based on the Lowry protocol. The assay determines protein concentrations contained in each sample in the presence of a reducing agent and detergents. Standard BSA solution with the following concentrations: 0.125, 0.25, 0.5, 0.75, 1, 1.5, and 2 mg/ml were added into each well (5 µl). A small aliquot (5 µl) of the samples was added into the remaining wells. Thereafter, 20 µl of reagent S was added into 1000 µl of reagent A. Reagent A (25 µl) and 200 µl of reagent B were added into each well containing the sample and the standard respectively. The plate was incubated in the dark for 10 min and the absorbance was measured at a wavelength of 630 nm using a BioTek® ELX800 plate reader. Protein concentrations were determined using a standard curve and they were expressed as mg/ml.

2.2.1.7.3. Gel electrophoresis

Protein samples were diluted and mixed with a 4X sample buffer (1:3). Samples were transferred to a heating block and heated at 95 ºC for 5 min in order to denature the proteins. After heating, samples were centrifuged briefly and returned to ice. Thereafter, 12 µl of precision plus westernC standard was loaded on the first lane of the 10 % sodium dodecyl sulfate polyacrylamide gel electrophoresis (SDS-PAGE) gel, followed by the addition of sample (30 µg for AKT and AMPK, 60 µg for GLUT 4) on the next lanes. The gel electrophoresed for 70 min at 150 V until the pink band marking 25 kDa ran off.

Figure 2.3: Mini-PROTEAN® Tetra Cell Systems and power pacTM used for gel electrophoresis.

2.2.1.7.4. Transfer of gel to a polyvinylidene fluoride membrane (PVDF) for Western blots

The polyvinylidine fluoride (PVDF) was pre-soaked in 100 % methanol for 5 min. Thereafter, the PVDF membrane, filter paper and fiber pads were equilibrated by soaking in transfer buffer for 20 min. The electrophoretic transfer was assembled on top of the negative electrode side (black) the following order: fiber pad, filter paper, gel PVDF membrane, filter paper and fiber pad. The cassette was closed and placed (negative and positive electrode facing the corresponding side in the tank) into the tank filled with transfer buffer and an ice pack to provide a cool environment and also prevent temperature fluctuations during the transfer process. The transfer was performed for 75 min at 160 V/4 ºc on top of a stirrer.

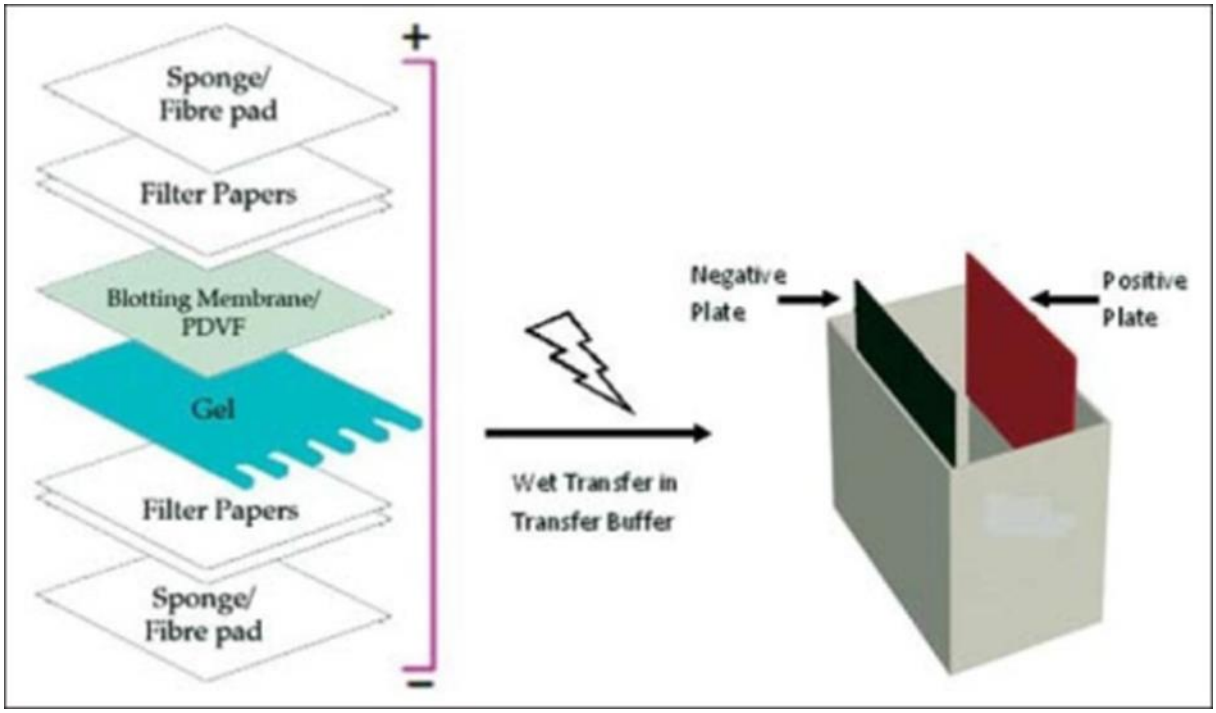

Figure 2.4: Schematic representation of a transfer sandwich used to transfer proteins from a gel (Mahmood and Yang, 2012).

2.2.1.7.5. Ponceau staining

Ponceau S stain is a sodium salt of thiazo dye that can be used for rapid reversible detection of proteins on PVDF membrane. The membranes were stained on an orbital shaker for 5 min. After confirming that the bands were clearly visible, the stain was removed by washing the membrane with 1 x tris-buffered saline (TBS) and TWEEN 20 (TBST).

2.2.1.7.6. Blocking and labelling of antibody

To block non-specific binding, the membrane was submerged in 5 % non-fat milk dissolved in 1X TBST for 2 hrs on an orbital shaker. After blocking, the membrane was incubated with the primary antibody in 1X TBST (see table 2.5) at 4 ºC on a shaker for 16 hrs. After 16 hrs of incubation, the membrane was washed with 1X TBST (thrice for 10 min) in order to remove excess primary antibody. Thereafter, the membrane was incubated with the secondary antibody in 2.5 % non-fat milk dissolved in 1X TBST at room temperature for 90 min. Secondary antibody dilutions were prepared as recommended by manufacturer (Table 2.6). This was followed by washing the membrane with 1X TBST (3 times for 10 min). Thereafter, 2 ml of ClarityTM western ECL substrate was added onto the membrane and left in the dark for 5 min.

Chemilumescence was detected using Chemidoc-XRS imager. Blots were analyzed using quantity one 1D software from Bio-Rad. Beta actin was used as a housekeeping protein.

Table 2.6: List of primary and secondary anti-bodies, percentage of gel used and dilution used for Western blot analysis.

Differentiated C2C12 muscle cells	**% gel**	**Dilution**
Phosphorylated 5'adenosine monophosphate activated protein kinase (AMPK)	10	1:800
Glucose transporter 4 (GLUT4)	10	1:500
Phosphorylated Threonine kinase B (AKT ser 473)	10	1:1000
Total Threonine kinase B (AKT)	10	1:1000
Total 5'adenosine monophosphate activated protein kinase (AMPK ser 172)	10	1:800
Donkey anti-Rabbit	10	1:4000:
Goat NTI-mouse	10	1:4000
Beta actin	10	1:800

2.2.2. Human liver cells (C3A) cell culture

The cells were cultured and maintained in EMEM with 2 mM L-glutamine and 10 % FBS. Cells were sub-cultured every 4 days and they were used within a maximum of 20 passages to avoid mutations. After seeding for experiments, cells were refreshed every 48 hrs for 4 days until they had reached a confluency of 80 % and they were incubated under standard culture conditions. Cells were thawed, counted and seeded as described in section 2.2.1.1 after they had reached 80 % confluency.

Table 2.7 : Seeding densities for experiments in flasks and plates for C3A cells

Cell line	Plate/flask type	Concentration/ml	Cell density	Volume/well
C3A	96 well plate	110 000 cells/ml	11 000 cells/well	100 µl
	48 well plate	110 000 cells/ml	33 000 cells/well	300 µl

2.2.2.1. Cytotoxicity assay

Cells were treated with different concentrations of *A. phylicoides* and subjected to an MTT assay as described in section 2.2.1.4. For assay purposes, the different concentrations (0.01, 0.1, 1 and 2 mg/ml) of *A. phylicoides* were dissolved in DMEM without phenol red and pyruvate containing 8 mM glucose and cells were incubated for 3 hrs under standard culture conditions.

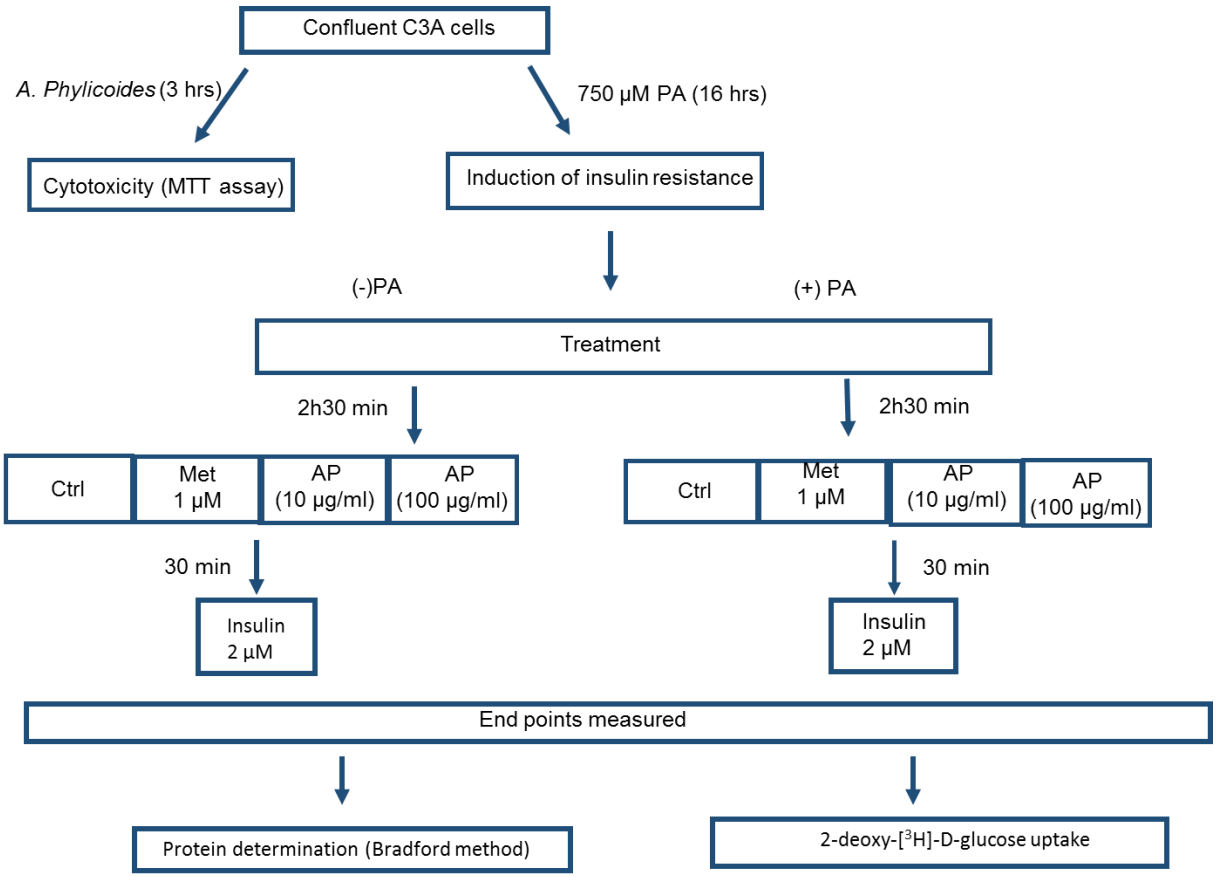

Figure 2.3: Experimental outline for C3A cell line.
PA - palmitic acid, Ctrl - control, Met - metformin, AP - *A. phylicoides.*

2.2.2.2. Induction of insulin resistance and treatment with extracts

Treatments for inducing insulin resistance were prepared and dissolved in DMEM as described in section 2.2.1.3. The cells were incubated under standard cell culture conditions for 16 hrs in order to induce insulin resistance. After 16 hrs, treatments were prepared as described above (see section 2.2.1.3) in DMEM containing 8 mM glucose. The cells were treated with 300 µl of the treatments and incubated under standard culture conditions for 3 hours and insulin was added to yield a 2 µM final concentration 30 minutes before the end of the incubation time (see Figure 2.3)

Glucose uptake assay using 2-deoxy-[^{3}H]-D-glucose uptake method. Treatments were removed from cells and washed with 250 µl of ice cold DPBS, thereafter, they were treated as described in section 2.2.1.5. Treatments were prepared in glucose free DMEM containing 0.5 µCi/ml 2-deoxy-[^{3}H]-D-glucose with or without 2 µM insulin.

2.2.2.3. Protein determination-Bradford assay

Total protein concentration was determined using the Bradford assay. Standards and actual protein concentrations in a lysate were determined as described in section 2.2.1.6.

2.2.3. 3T3-L1 adipocytes as a model of insulin resistance

Pre-adipocytes 3T3-L1 cell line (ATTC Cat No. CL-173) were grown and maintained in DMEM supplemented with 10 %new born calf serum (NCS). After reaching a 70 % confluency, the cells were sub-cultured and seeded into 96 well plates (TC treated flat bottom, Eppendorf, Hamburg, Germany tissue and Corning® CellBIND®, sigma Aldrich, St Louis, USA) for MTT assays and Oil Red O stain (4000 cells/well, 20 000 cells/ml), respectively, and 75 cm^2 flask maintenance (splitting ratio of 1:6).

2.2.3.1. Adipocyte differentiation

After 3T3-L1 fibroblasts had reached a confluency of 100 %, the growth medium was replaced with differentiating medium (DMEM containing 10 % FBS, 1 µM Dexamethasone, 0.5 mM 3-isobutyl-1-methylxanthine and 1 µg/ml insulin). Cells were refreshed with freshly prepared differentiating medium every 24 hrs for 3 days. Thereafter, the differentiating medium was replaced by adipocyte maintenance medium (refer to table 2.1). The cells were refreshed with freshly prepared adipocytes maintenance medium every 24 hrs for two days. After 2 days, adipocyte maintenance medium was replaced by normal growth medium (DMEM supplemented with 10 % FBS), which was changed daily for 3 days. Full differentiation was confirmed by observing fully formed lipid droplets in each well under an inverted light microscope (Olympus CKX41, Olympus, Tokyo, Japan).

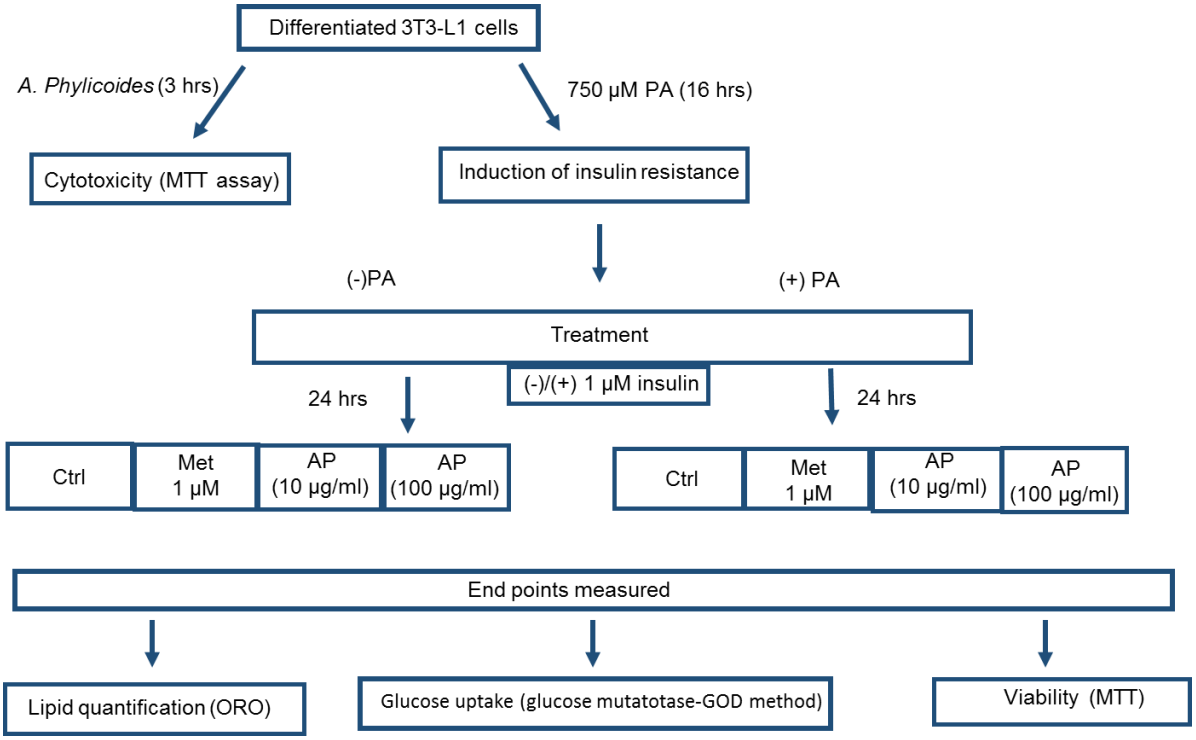

Figure 2.4: experimental outline for 3T3-L1 cell line.
PA - palmitic acid, Ctrl - control, Met - metformin, AP - *A. phylicoides*

2.2.3.2. Induction of insulin resistance and treatment

Insulin resistance was induced as described in section 2.2.1.3. Cells were serum starved and treated as described above (2.2.1.3). Treatments were dissolved in DMEM without phenol red containing 25 mM glucose, 2 % BSA, 1 % ethanol, with and without 1µM insulin and with and without 750 µM palmitic acid. Treated cells were incubated for 24hrs under standard culture conditions. Treatment blanks, which are leftovers of all the different treatments that were prepared, were added into a clear plate (polysterine TPP® 96 U-base, Zellkultur und labortechnologies, Switzerland) and they were incubated under the same conditions as the cells.

2.2.3.3. Glucose uptake assay using mutarotase-GOD method

LabAssay™ glucose kit was used to conduct uptake assays. The enzyme mutarotase converts α-D-glucose to β-D-glucose. The enzyme glucose oxidase oxidizes β-D-glucose yielding hydrogen peroxide. Hydrogen peroxidase reacts with phenol and 4-aminoantipyrine in the presence of hydrogen peroxide, yielding a red pigment. Glucose can then be assayed by measuring the absorbance of the red pigment.

After 24 hrs, treatments were removed from the wells and transferred into a clear plate (polystyrene TPP® 96 U-base, Zellkultur und labortechnologies, Switzerland). A standard curve was prepared according to manufacturer's recommendations yielding 6 different concentrations (50, 100, 200, 300, 400 and 500 mg/dl). Treatments, treatment blanks and standards (2 µl) were added to the assay plate, followed by 300 µl of the chromogen reagent. The plate was incubated at 37 °C for 5 min and the absorbance was measured at a wavelength of 490 nm using BioTek® ELX800 plate reader (BioTek, Vermont, USA).

2.2.3.4. Lipid quantification using Oil Red O staining

The Oil Red O (ORO) stain is a fat-soluble dye with a maximum absorbance at 518 nm. The stain can be used to stain triglycerides, frozen lipid sections and freshly prepared samples of mammalian cells. After media was removed from the cells, the cells were washed with 100 µl of DPBS. In order to fix the cells, DPBS was removed and replaced by 50 µl of neutral buffered formalin (10 % v/v), followed by a 15 min incubation at room temperature. Thereafter, neutral buffered formalin was removed and cells were washed twice with 100 µl of DPBS. After washing, 50 µl of 0.7 % (v/v) ORO was added and incubated at room temperature for 30 min. After incubation, the ORO staining solution was removed and cells were washed 3 times with ddH_2O. Double distilled water was aspirated, followed by the addition of 50 µl of isopropanol into each well. The plate was gently agitated by gentle tapping the plate on the side in order to aid the extraction of the ORO stain. The extracted ORO stain (50 µl) was transferred to a clear assay plate and the absorbance was measured at 490 nm in a BioTek® ELX800 plate reader. After extracting the ORO stain, all wells were washed with 50 µl of 70 % ethanol. The ethanol was aspirated and it was followed by the addition of 80 µl of 0.5 % crystal violet (CV) stain into each well. Stained cells were incubated at room temperature for 5min. After 5 min, the staining solution was aspirated and cells were washed 3 times with 80 µl of DPBS. The DPBS was removed by aspiration and this was followed by the addition of 70 % ethanol (50 µl). The stain was extracted by gently tapping the plate on the side. Thereafter, 80 µl of the extracted stain was transferred into an assay plate and the absorbance of the plate was measured at 570 nm in a BioTek® ELX800 plate reader. Results for both stains were expressed as percentage of control. The CV stain is a measure of viability, therefore values obtained from the absorbance were used to normalize the ORO stain.

2.2.3.5. Cytotoxity assay-MTT assay

Mature 3T3-L1 adipocytes were subjected to an MTT assay to assess viability after they were treated with different concentration of *A. phylicoides* for 3 hrs without the addition of insulin. Treatments were prepared in DMEM containing 25 mM glucose and cells were treated as described in section 2.2.1.4. The absorbance was read at 570 nm in a BioTek® ELX800 plate reader. Results were calculated and expressed as percentage of control.

2.2.4. PTP1B enzyme assay

Protein tyrosine phosphatase 1B (PTP1B) is a member of tyrosine phosphatase (PTPase) family of proteins. Protein Tyrosine Phosphatase 1B directly dephosphorylates activated IRS-1, among other target proteins, on its tyrosine residues. The PTP1B assay is based on the ability of the enzyme to dephosphorylate the substrate *p*-nitrophenyl phosphate (*p*NPP) yielding *para*-nitrophenol, which is of yellow color. The absorbance of *para*-nitrophenol can be measured at a wavelength of 450 nm. For the purpose of this assay, *A. phylicoides* was dissolved in TC water to yield a concentration of 10 mg/ml (10 mg in 1000 µl TC water) and it was diluted to 8 different concentrations using 50 mM citrate buffer (50, 25, 12.5, 6.25, 3.13, 1.56, 0.78, 0.39 µg/ml) Thereafter, 30 µl of citrate buffer was added to an assay plate (polystyrene, Micro F-bottom, Greiner bio-one, Frickenhausen, Germany), followed by 10 µl of 10 mM DTT, 10 µl of 10 mM of *p*NPP and 25 µl of the extract extracts or sodium with and without the addition of 25 µl of the PTP1B enzyme. Controls were prepared in a similar manner, without the addition of the extract, with and without the addition of the enzyme. All samples were prepared in duplicates. The plate was incubated for 30 min at 37 ºC. After incubation, 50 µl of 1M sodium hydroxide was added to all wells in order to stop the reaction. The absorbance was read at 405 nm using a BioTek® ELX800 plate reader (BioTek, Vermont, United States of America). The inhibitory effect was determined by calculating the half maximal inhibitory concentration (IC_{50}) using GraphPad Prism version 6.

2.2.5. Statistical analysis

Statistically significant differences for the cytotoxicity results were analyzed using One-Way ANOVA on GraphPad Prisms 6.0 (San Diego, USA). For the glucose uptake data, a 2-way ANOVA with a 2x2 factorial design was applied and each treatment, i.e.

controls, metformin and the extract at different concentrations, was analyzed separately for interactions and main effects between the two factors insulin and palmitic acid. Both insulin and palmitic acid had two levels, i.e. (-) and (+) insulin or palmitic acid. ANOVA tables with the relevant data are presented in Addendum 1. The Western Blot results were analyzed by 3-way ANOVA with a 3x2 design, with the factors insulin, palmitic acid and treatment (extract) each with two levels. A $p<0.05$ was considered statistically significant and Tukey-Kramer test was used for post hoc multiple comparisons. The Two- and Three-Way ANOVAs were conducted by Dr S Riedel-van Heerden using NCSS version 11.0.7 (NCSS LLC., Kaysville, USA).

2.3. *In vivo* experiments

In order to assess the overall effect of the extract on glucose metabolism and insulin resistance and to also confirm *in vitro* findings, an *in vivo* model of type 2 diabetes (C57BLKS *db/db* mice model) was used. Metformin (300 mg/kg), a first line agent for the management of type 2 diabetes, which falls under biguanide class of drugs, and vildagliptin (5 mg/kg), a new line of anti-diabetic agents that falls under the class dipeptidyl peptidase-4 inhibitors (DPP-4 inhibitors), were used as positive controls. An aspalathin enriched rooibos plant extract (SB1 60 mg/kg) was used as a reference. Two concentrations of the extract were selected based on literature (Chellan *et al*., 2008).

2.3.1. Ethics statement

Ethical approval for this study was granted by the Ethics Committee at the Medical Research Council of South Africa (ECRA, see Addendum 2). The study was performed in accordance with the principles and guidelines of the South African Medical Research Council as outlined in Guidelines on Ethics for Medical Research Council.

2.2.2. C57BLKS *db/db* mice housing and maintenance

Diabetic C57BLKS *db/db* mice were bred and housed at the South African Medical Research Council PUDAC unit. Thirty-six (36) six-week-old male obese diabetic *db/db* and six lean male mice were randomly selected and assigned into groups of 6. They were housed in individual cages where they had free access to food (standard rodent diet ground into powder) and water. On fasting days, food was removed from the cages. Mice were maintained under a 12 hr light/dark cycle at 22 °C. Prior to the

beginning of the study, all selected mice were weighed and fasted in order to record their baseline fasting plasma glucose levels. Food intake was monitored daily, fasting plasma glucose levels and water intake were monitored weekly. Body weights were measured every other day.

Table 2.8: Treatment groups and their corresponding to daily doses

Groups	**Treatments**
Normal control (non-diabetic)	Vehicle equivalent daily
Diabetic control	Vehicle equivalent daily
Vildagliptin	5 mg/kg/d
Metformin	300 mg/kg/d
Rooibos (SB1)	60 mg/kg/d
A.phylicoides I	20 mg/kg/d
A.phylicoides II	200 mg/kg/d

2.3.2. Preparation of treatments

Food was prepared weekly and the daily dose of each treatment was calculated and adjusted weekly according to the average of body weights in each treatment group. The treatments (metformin and vildagliptin tablets and AP 20, 200 mg/kg/day, Table 2.8) were mixed into the powdered standard rodent pellet. Obese control and lean controls received no treatment with their food. Each mouse was given 10 g of food daily. Food that remained was stored at room temperature under desiccation.

2.3.3. Food and water intake

In order to determine daily food intake, food was weighed before it was given to the mice. The remaining food was weighed and recorded the next day before new food could be given to each mouse. Water intake was monitored weekly, each week animals were given 250 ml of water and the amount of water left was measured after each week. Total water intake was calculated by subtracting the amount of water left from the amount of water that was given to each mouse.

2.3.4. Fasting plasma glucose concentrations

Fasting plasma glucose levels were measured weekly after an overnight fasting period. Blood was collected by pricking the tail of the mice with a needle. Thereafter, the sample was loaded onto a glucose strip inserted in a glucometer. Values obtained

from the glucometer were recorded and the average glucose concentration of each group was calculated.

2.3.5. Oral glucose tolerance test (OGTT)

Oral glucose tolerance tests were conducted on day 29 as described by Mazibuko (2014) with minor modifications. Mice were fasted overnight (16 hrs) and fasting plasma glucose concentrations were measured as described in (section 2.3.4). Thereafter, treatments were administered to mice by oral gavage. Treatments were freshly prepared by dissolving the daily dose of all extracts and control agents in ddH_2O. Obese and lean control groups received ddH_2O with no treatments. An hour after administering treatments, the mice received 2 g/kg glucose through oral gavage. Blood glucose concentrations were measured at time intervals 30, 60 and 120 min.

2.3.6. Terminations

Mice were anaesthetized on day 31 by inhaling 2 % fluothane (AstraZeneca Pharmaceuticals, Johannesburg, South Africa). A mid-line abdominal incision was made and blood was collected from the abdominal aorta and transferred to a serum separating tube (SST). Serum samples were prepared by centrifuging the blood obtained from mice and the samples were sent to PathCare laboratories for lipid profiling. Lipids analyzed were cholesterol, HDL-cholesterol and triglycerides. The liver was harvested and fixed in 10 % buffered formalin for histological analysis.

2.3.7. Serum insulin determination

Enzyme-linked immunosorbent assay (ELISA) is a technique used to assay proteins such as hormones and antibodies in a liquid sample. The assay involves the use of an antibody that is bound to a surface/plate. Antigens that are contained by the assayed sample bind the immobilized antibody. This is followed by the addition of a detection enzyme-linked antibody. Soon after the substrate is added, the enzyme changes it to a detectable form, which is directly correlated with the amount of antigen bound. For the purpose of this assay, a Rat/Mouse 96-well plate ELISA kit was used and serum samples were not diluted. Samples and standards (10 µl) were loaded into an ELISA plate coated with mouse monoclonal anti-rat insulin antibodies, which allowed the protein (insulin) of interest to bind. Thereafter, 80 µl of detection antibody was added into each well, the plate was covered with a plate sealer and incubated at room

temperature for 2 hrs on an orbital shaker (500 rpm). After 2 hrs, the wells were washed with 300 µl of wash buffer (diluted according to the manufacturer's recommendation). Thereafter, 100 µl of enzyme solution was added to each well, the plate was sealed and incubated for 30 min at room temperature on a shaker. The enzyme was removed and washed 6 times with 300 µl of wash buffer. After washing, 100 µl of the substrate were added into each well and the plate was incubated at room temperature (on an orbital shaker) for 20 min. Thereafter, a stop solution (100 µl) was added in order to terminate color development and the absorbance was measured at a wavelength of 450 nm using a BioTek® ELX800 plate reader.

2.3.8. Histological tissue processing and analysis

Tissues fixed in 10 % buffered formalin were trimmed into small pieces (<5 mm) and placed into histology cassettes. The cassettes were placed into a tissue processor overnight (Leica TP 1020, Leica Microsystems, Nussloch, Germany). During the processing, the tissues were moved through different concentrations of ethanol in an ascending order (70 % for 1.5 hrs, 2 x 96 % for 1 hr each and 3x 100 % for 1 hr each) and 3 changes of xylene for 1 hr. Thereafter, tissues were saturated with molten paraffin wax for 2 hrs (2x). Processed tissues were then fixed in paraffin wax and sections were cut (5 µm) using rotary microtome (Leica RM 2125 RM, Leica Microsystems, Nussloch, Germany). The sections were place in a water bath set at ± 40 °C and thereafter placed onto 3-aminopropyltriethoxysilane (APES) coated slides. Slides were incubated at 65 °C for 30 min to facilitate effective adherence of the tissue to the slides. Liver sections were prepared by Mr D Linden from the Biomedical research and innovation platform (BRIP) of the South African Medical research council (SAMRC).

2.3.8.1.H & E staining of liver sections

Hematoxylin and eosin stain is a staining procedure that can be used to visualize different elements in a tissue section. It involves the use of hemalum, which stains the nuclei of cells blue, and a counterstain known as eosin, which highlights other components of the cytoplasm. Liver sections were dewaxed by placing slide in xylene 3 times for 10 min, followed by hydrating in ascending ethanol concentrations (2 x 100 %, 96 % and 70 %) for 2 min each. Excess stain was rinsed of by dipping slides in water 20 times. After rinsing, the slides were placed in hematoxylin stain for 12 min

and the stain was rinsed off with running water. Thereafter, the slides were submerged in 1 % aqueous eosin stain for 3 min. This was followed by rinsing off the stain in running water. The slides were cleared by dipping each one of them in xylene 20 times. A cover slip was fixed on top of the slide. Staining procedures were done by Ms C Chapman from the Biomedical Research and Innovation Platform (BRIP) of the South African Medical research council (SAMRC).

2.3.8.2.Steatosis scoring

Histological analysis of liver sections was conducted using the NASH Clinical Research Network Scoring System. Liver sections were scored for steatosis twice in 2 regions: portal and central vein area (Trak-Smayra *et al*., 2011). Both areas were scored according to changes observed (Micro, Medio and Macrovesicular changes), they were awarded a score from 0-3. A score of 0 indicated <5 %, a score of 1 indicates between 5 and 33 %, while a score of 2 indicated between 33 and 66 % and a score of 3 >66 %. Macrovesicular changes represent an advanced form of steatosis where the nucleus is totally displaced and the cytoplasm is replaced by a big droplet of fat. For mediovesicular changes, the nucleus is still in the center of the cell and the cytoplasm contains small drops of fat. Microvesicular changes are a mild form of steatosis that can be identified by mall intracytoplasmic fat vacuoles. The first scoring round was done by Dr C.J.F Muller and the second round was conducted by Miss Charity Masilela.

2.3.9. Statistical analysis

Statistical analysis was done using GraphPad Prism 6.0 (San Diego, USA). A one-way ANOVA with a multiple comparison Dunnett's test was used for statistical analysis.

Chapter 3

3. Results

3.1. *In vitro* assessment of the effect of an aqueous extract of *A. phylicoides* on insulin resistance

In this study the effect of *A. phylicoides* in insulin-resistant (muscle cell (C2C12), adipocytes (3T3-L1) and human liver cells (C3A) was assessed. To achieve this, cell viability and glucose uptake assays were performed using similar protocols as described previously (Mazibuko, 2014). Furthermore, genes involved in insulin signaling (p-AKT and GLUT4) and non-independent insulin signaling (p-AMPK) were assessed by Western blot analysis.

3.1.1. *In vitro* assessment of *A. phylicoides* on cell viability, glucose uptake and the regulation of glucose metabolism associated proteins using skeletal muscle cells (C2C12)

3.1.1.1. Dose finding for *A. phylicoides* extract in differentiated skeletal muscle cells (C2C12)

To investigate the optimum concentration with no cytotoxic effect, a dose finding study was conducted in normal C2C12 muscle cells using MTT assay as described in section 2.2.1.4. Briefly, normal C2C12 muscle cells were treated with *A. phylicoides* at a concentration range of 0.01 to 2 mg/ml. Statistical analysis was conducted using one-way ANOVA and post hoc Turkey Kramer test. While no concentrations induced changes in viability when compared to the control, the 2 and 0.1 mg/ml concentrations significantly decreased viability in comparison to the 0.01 mg/ml treatment group (Figure 3.1). There was no dose-dependent response, therefore, doses that are closer to what could be achieved *in vivo* (10 and 100 µg/ml) were chosen for all *in vitro* experiments.

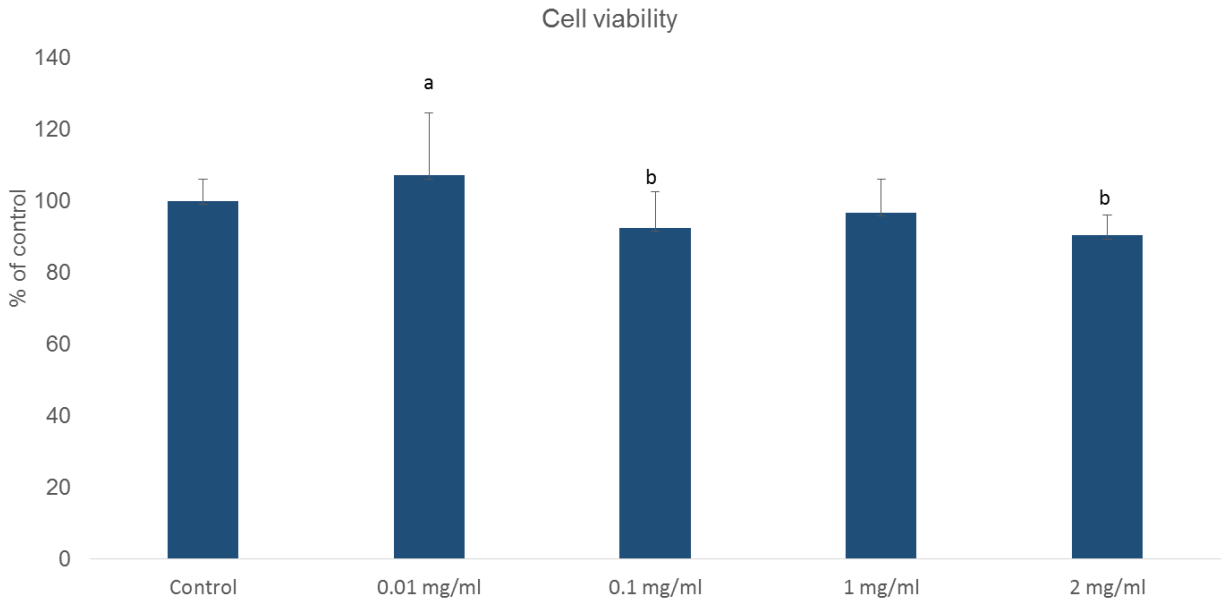

Figure 3.1: Effect of *A. phylicoides* on cell viability in C2C12 muscle cells.
Cells were, cultured in Krebs Ringer bicarbonate HEPES buffer supplemented with 8 mM glucose and 0.1 % BSA. Cells were treated with or without *A. phylicoides* (0.01 to 2 mg/ml) for 3 hrs. Cell viability was measured using an MTT assay. A one way ANOVA Tukey Kramer test was used for statistical analysis. Results are expressed as the mean of three independent experiments relative to the control at 100 % ± standard deviation. Different letters denote statistical differences between treatments at $p<0.05$. Abbreviations: ANOVA-analysis of variance; HEPES- 2-[4-(2-hydroxyethyl)piperazin-1-yl]ethanesulfonic acid, MTT- 3-(4,5-dimethylthiazol-2-yl)-2,5-diphenyltetrazolium bromide; BSA-bovine serum albumin.

3.1.1.2. Effect of *A. phylicoides* on glucose uptake in differentiated insulin-resistant skeletal muscle cells (C2C12)

Glucose uptake was measured using the 2-deoxy-[^{3}H]-D-glucose uptake method in order to determine the effect of *A. phylicoides* (see section 2.2.1.5). Statistical analysis was conducted using two-way ANOVA, where each treatment, i.e. control, metformin and the different extract concentrations, was analyzed individually for palmitic acid and insulin effects and interactions (Figure 3.2). For the control, a significant interaction between palmitic acid and insulin treatment was observed, where in the absence of palmitic acid, insulin significantly increased ($p<0.05$) glucose uptake (Figure 3.2). On the other hand, palmitic acid significantly decreased ($p<0.05$) glucose uptake in insulin treated cells.

No statistically significant interaction was observed for metformin. Overall, a significant increase ($p<0.05$) in glucose uptake was observed when cells were treated with insulin regardless of the presence of palmitic acid. Palmitic acid significantly decreased ($p<0.05$) glucose uptake in the presence and absence of insulin (Figure 3.2).

A statistically significant interaction was observed for the low dose (10 µg/ml) of the extract, where a significant increase ($p<0.05$) in insulin-stimulated glucose uptake in the absence of palmitic acid was demonstrated. However, insulin had no effect on glucose uptake in the presence of palmitic acid.

No statistically significant interaction was observed for the highest concentration (100 µg/ml) of the extract, however, a significant increase in insulin-stimulated glucose uptake was observed regardless of palmitic acid treatment (Figure 3.2).

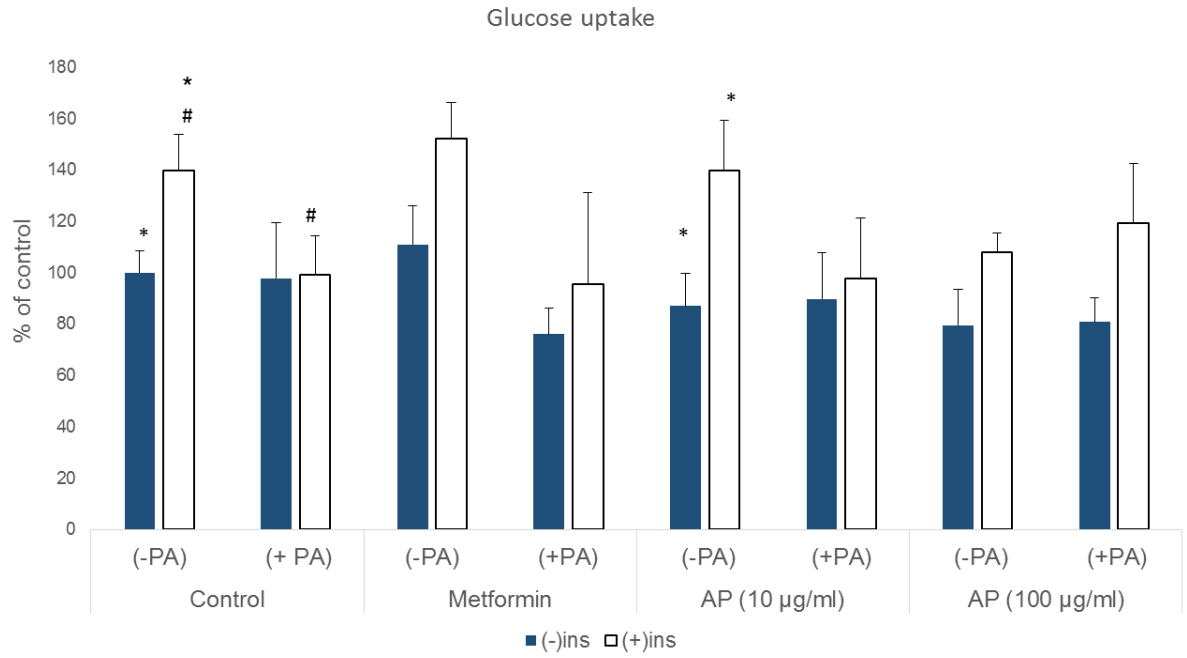

Figure 3.2: Effect of *A. phylicoides* on glucose uptake on insulin-resistant C2C12 muscle cells. C2C12 muscle cells were cultured in Krebs Ringer bicarbonate HEPES buffer with 8 mM glucose, 2 % BSA, 1% ethanol with 750 µM palmitate (+PA) or without palmitate (-PA) for 16 hrs. Thereafter, cells were treated with or without *A. phylicoides* (10 and 100 µg/ml) for 3 hours. Metformin (1µM) was used as positive control. Thereafter, cells were stimulated with insulin for the last 30 min. Glucose uptake was measured using [^{3}H]-2-deoxy-D-glucose. A two-way ANOVA with post hoc Tukey Kramer test was used for statistical analysis, where each treatment, i.e. control, metformin and the different extract concentrations, was analyzed individually for palmitic acid, insulin effects and interactions. Statistically significant interactions are indicated in the graph when $p<0.05$. Within each treatment, groups with the same sign (# and *) differ significantly from each other. Significant main effects are described in the text. Results are expressed as the mean of three independent experiments relative to the control at 100 % ± standard deviation. Abbreviations: BSA - bovine serum albumin; (-)ins - without insulin; (+)ins - with insulin; HEPES-2-[4-(2-hydroxyethyl)piperazin-1-yl]ethanesulfonic acid; ANOVA - analysis Of variance.

For the Western blot analysis of proteins involved in insulin signaling and glucose uptake, only one concentration was selected (100 µg/ml), as it was shown to alleviate insulin resistance.

3.1.1.3. Effect of *A. phylicoides* on phosphorylation of AMPK in differentiated insulin-resistant skeletal muscle cells

Adenosine monophosphate kinase (AMPK) is a master energy regulator that is highly expressed during stress. The enzyme is responsible for restoring cellular ATP levels by activating glucose uptake and β-oxidation (Mihaylova and Shaw, 2011). Therefore, it is possible that the aqueous extract of *A. phylicoides* could modulate glucose uptake through the phosphorylation and activation of AMPK. Results (Figure 3.3) were analyzed using three-way ANOVA. Overall, no statistically significant interactions were observed for phosphorylated AMPK (Figure 3.3 A) and total AMPK (Figure 3.3 B), all treatments (palmitic acid, insulin and the extract) showed no effect.

For phosphorylated to total AMPK (p-AMPK/t-AMPK) ratio, there were no statistically significant interactions observed. Only main effects were observed where the treatment (100 µg/ml) significantly increased p-AMPK/t-AMPK ratio regardless of the presence of both insulin and palmitic acid (Figure 3.3 C)

A

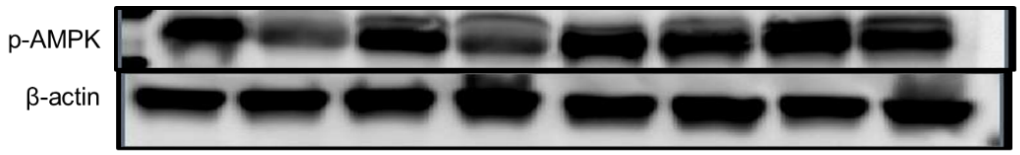

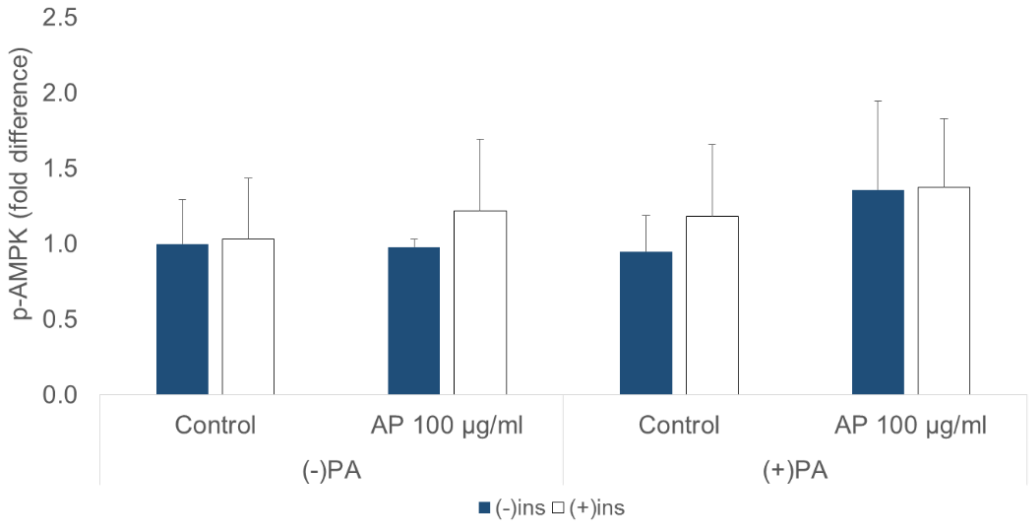

B

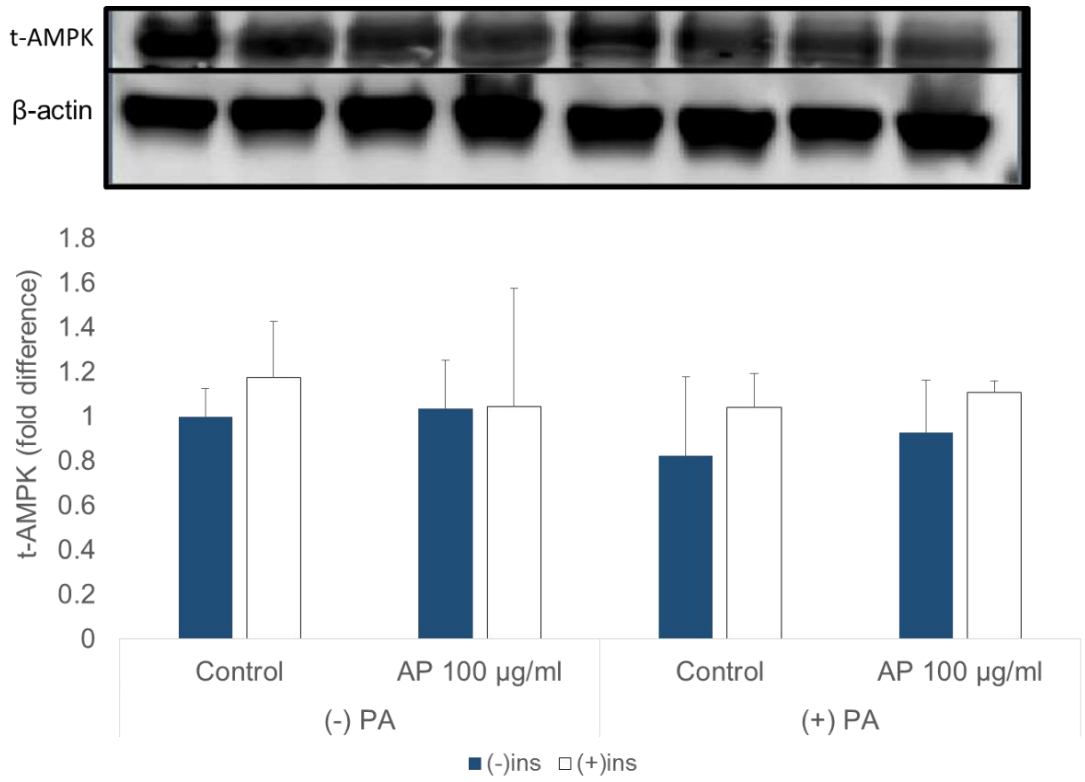

C

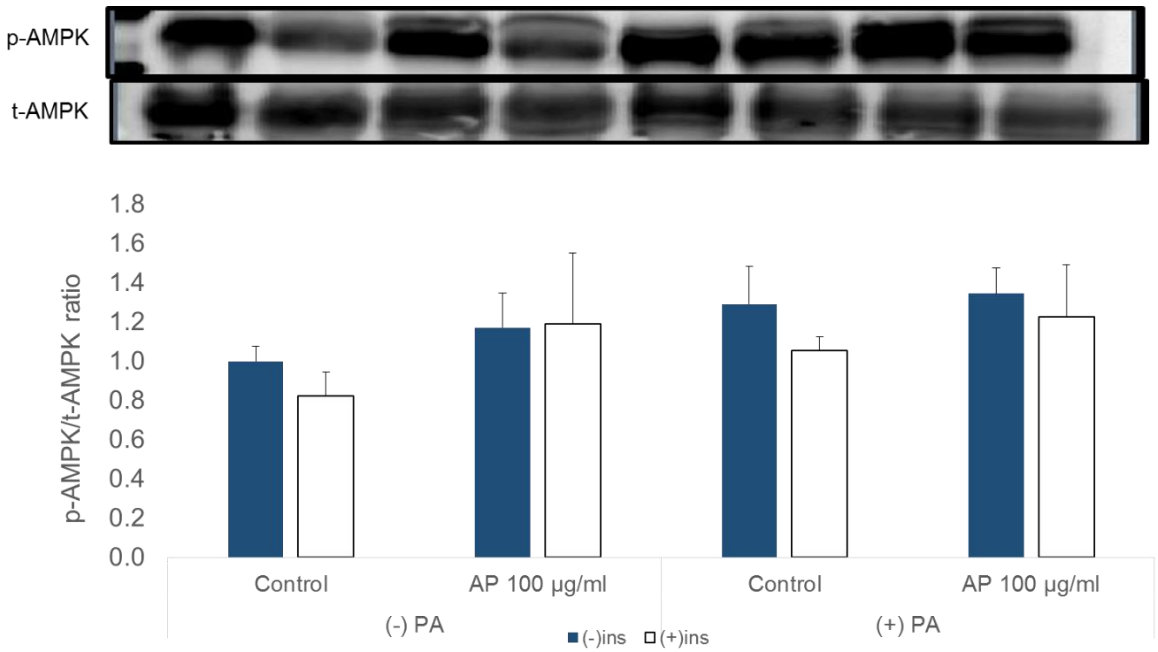

Figure 3.3: Effect of *A. phylicoides* on the expression and phosphorylation of adenosine monophosphate kinase protein (AMPK) expression and phosphorylation.
C2C12 muscle cells were, maintained in Krebs Ringer bicarbonate HEPES buffer with 8 mM glucose, 2 % BSA, 1 % ethanol with 750 µM palmitate (+PA) or without palmitate (-PA) for 16 hrs, thereafter they were treated with *A. phylicoides* (100 µg/ml) for 3 hrs. Thereafter, cells were stimulated with Insulin (2 µM) for the last 30 min. Cells were lysed and subjected to Western blot analysis. (A) Reports the

phosphorylation levels of AMPK (p-AMPK), (B) total AMPK (t-AMPK) and (C) is the phosphorylated to total AMPK ratio (p-AMPK/t-AMPK). The ratio of p-AMPK/t-AMPK was used to estimate the level of AMPK activation. Statistical analysis was conducted using three-way ANOVA with a 3x2 design, where $p<0.05$ was designated as statistically significant. Significant main effects are described in the text. Results are expressed as the mean fold of 2 (3 for p-AMPK) independent experiments relative to control ± standard deviation. Abbreviations: (-)ins – without insulin; (+)ins - with insulin: HEPES - 2-[4-(2-hydroxyethyl)piperazin-1-yl]ethanesulfonic acid; ANOVA - Analysis Of Variance, BSA-bovine serum albumin.

3.1.1.4. Effect *of A. phylicoides* on phosphorylation of AKT in differentiated insulin-resistant skeletal muscle cells

Protein kinase B (AKT) is a serine/threonine-specific protein kinase that has been associated with GLUT 4 translocation and other cellular processes (Hundal *et al*., 2000; Whiteman *et al*., 2002). Western blot analysis was used in order to elucidate whether the extract improve glucose metabolism in insulin-resistant skeletal muscle cells by increasing the expression and phosphorylation of AKT**.** Results (Figure 3.4 A) demonstrated no statistically significant interaction, however, insulin significantly ($p<0.05$) increased the phosphorylation of AKT regardless of palmitic acid and extract treatments.

Overall, palmitic acid and extract treatment significantly decreased ($p<0.05$) the phosphorylation of AKT. There were no statistically significant interactions or main effects observed for total AKT (t-AKT) (Figure 3.4 B).

For the ratio of phosphorylated to total AKT, no significant interactions were observed (Figure 3.4 C). A significant increase ($p<0.05$) was only detected when cells were treated with insulin regardless of the presence of the extract or palmitic acid.

A

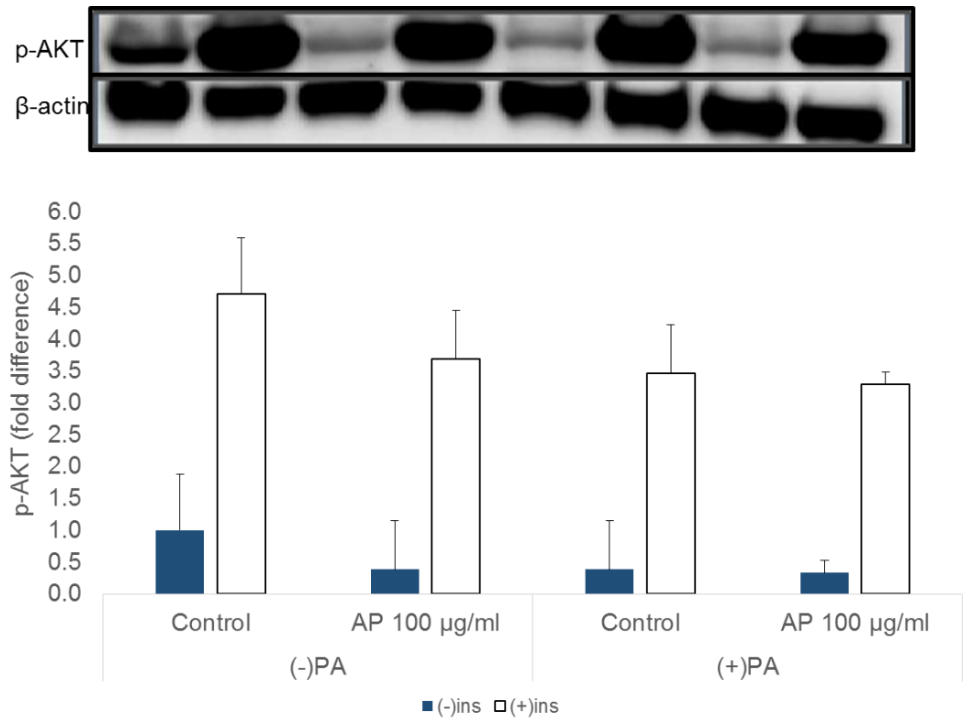
p-AKT
β-actin
p-AKT (fold difference)
6.0
5.5
5.0
4.5
4.0
3.5
3.0
2.5
2.0
1.5
1.0
0.5
0.0
Control
AP 100 μg/ml
Control
AP 100 μg/ml
(-)PA
(+)PA
(-)ins
(+)ins

B

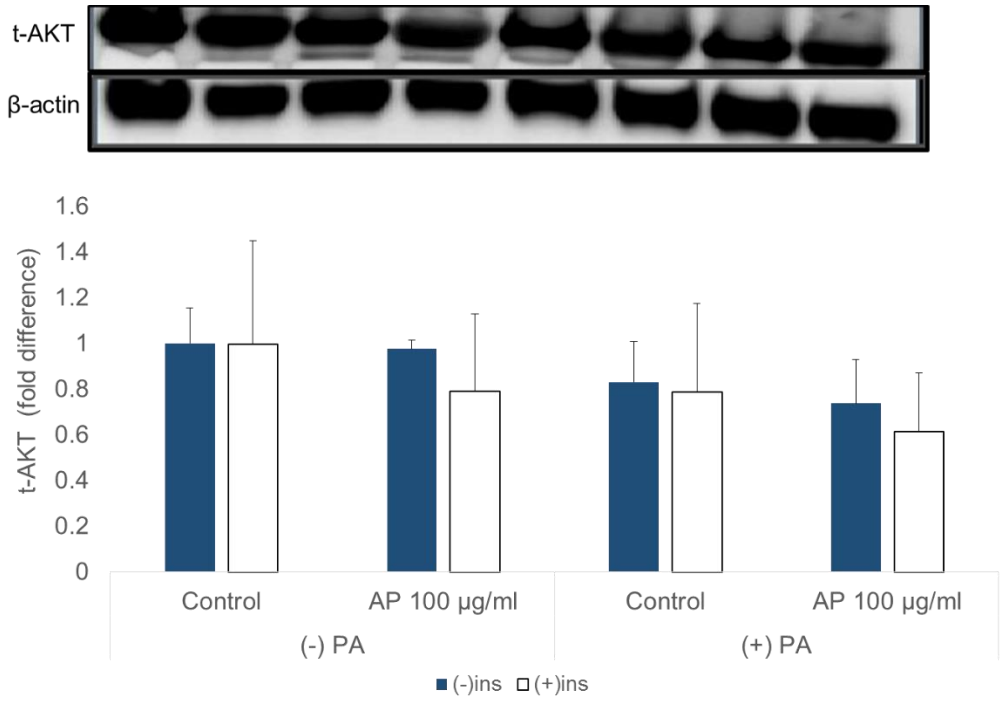
t-AKT
β-actin
t-AKT (fold difference)
1.6
1.4
1.2
1
0.8
0.6
0.4
0.2
0
Control
AP 100 μg/ml
Control
AP 100 μg/ml
(-) PA
(+) PA
(-)ins
(+)ins

C

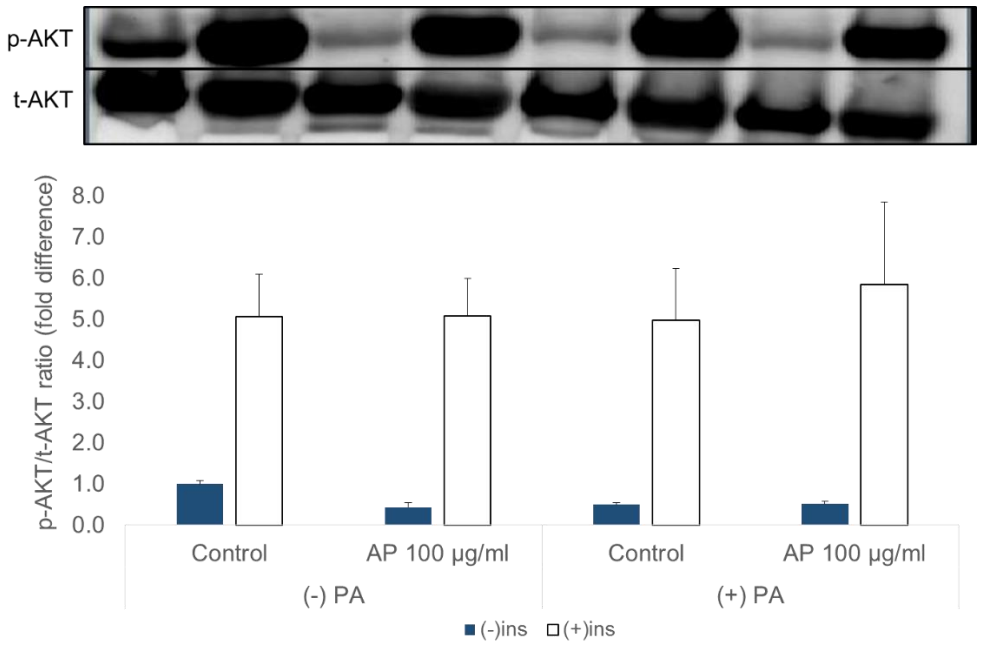

Figure 3.4: Effect of *A. phylicoides* on expression and phosphorylation of protein kinase B (AKT).
C2C12 muscle cells were, maintained in Krebs Ringer bicarbonate HEPES buffer with 8 mM glucose, 2 % BSA, 1 % ethanol with 750 µM palmitate (+PA) or without palmitate (-PA) for 16 hrs, thereafter they were treated with *A. phylicoides* (100 µg/ml) for 3 hrs. Thereafter, cells were stimulated with Insulin (2 µM) for the last 30 min. Cells were lysed and subjected to Western blot analysis. (A) Reports the phosphorylation levels of AKT (p-AKT), (B) total AKT (t-AKT) and (C) is the phosphorylated to total AKT ratio (p-AKT/t-AKT). The ratio of p-AKT/t-AKT was used to estimate the level of AK activation. Statistical analysis was conducted using three-way ANOVA with a 3x2 design, where $p<0.05$ was designated as statistically significant. Significant main effects are described in the text. Results are expressed as the mean fold of 2 (3 p-AKT) independent experiments relative to control ± standard deviation. Abbreviations: (-)ins - without insulin; (+)ins - with insulin: HEPES - 2-[4-(2-hydroxyethyl)piperazin-1-yl]ethanesulfonic acid; ANOVA - Analysis Of Variance; BSA - bovine serum albumin.

3.1.1.5. Effect of *A. phylicoides* on glucose GLUT 4 expression

Glucose transporter type 4 (GLUT 4) is an insulin regulated protein that is responsible for transporting glucose across the plasma membrane of tissues such as the muscle and adipose tissue (Huang and Czech, 2007b; Olson, 2012). The extract of *A. phylicoides* could potentially increase glucose uptake in insulin sensitive cells by upregulating the expression and translocation of GLUT 4. Results showed no statistically significant differences in the expression of GLUT 4 in the presence of the extract, insulin or palmitic acid (Figure 3.5).

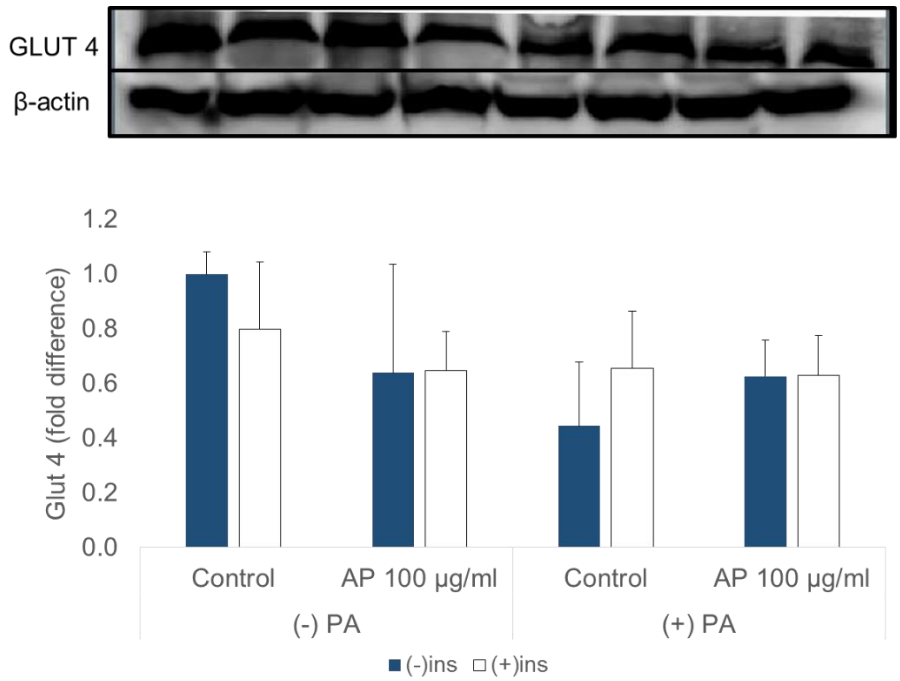

Figure 3.5: Effect of *A. phylicoides* on Glucose transporter 4 (GLUT 4) expression and phosphorylation.
C2C12 muscle cells were, maintained in Krebs Ringer bicarbonate HEPES buffer with 8 mM glucose, 2 % BSA, 1 % ethanol with 750 µM palmitate (+PA) or without palmitate (-PA) for 16 hrs, thereafter they were treated with *A. phylicoides* (100 µg/ml) for 3 hrs. Thereafter, cells were stimulated with Insulin (2 µM) for the last 30 min. Cells were lysed and subjected to Western blot analysis. Statistical analysis was conducted using three-way ANOVA with a 3x2 design, where $p<0.05$ was designated as statistically significant. Results are expressed as the mean fold of two independent experiments relative to control ± standard deviation. Abbreviations: (-)ins - without insulin; (+)ins - with insulin: HEPES - 2-[4-(2-hydroxyethyl)piperazin-1-yl]ethanesulfonic acid; ANOVA - Analysis Of Variance, BSA - serum bovine albumin.

3.1.2. *In vitro* assessment of *A. phylicoides* on cell viability and glucose uptake in human liver cells (C3A)

3.1.2.1. Cytotoxicity assessment of *A. phylicoides* in human liver cells (C3A)

Human liver cells (C3A) were treated with different concentrations of *A. phylicoides* ranging from 2 to 0.01 mg/ml. An MTT assay was used to determine the effect of the extract on cell viability. A one-way ANOVA with post hoc Tukey Kramer test revealed that the extract had no effect on cell viability at the concentrations tested (Figure 3.6). As a result, 10 and 100 µg/ml were selected as working concentrations that could be achieved *in vivo.*

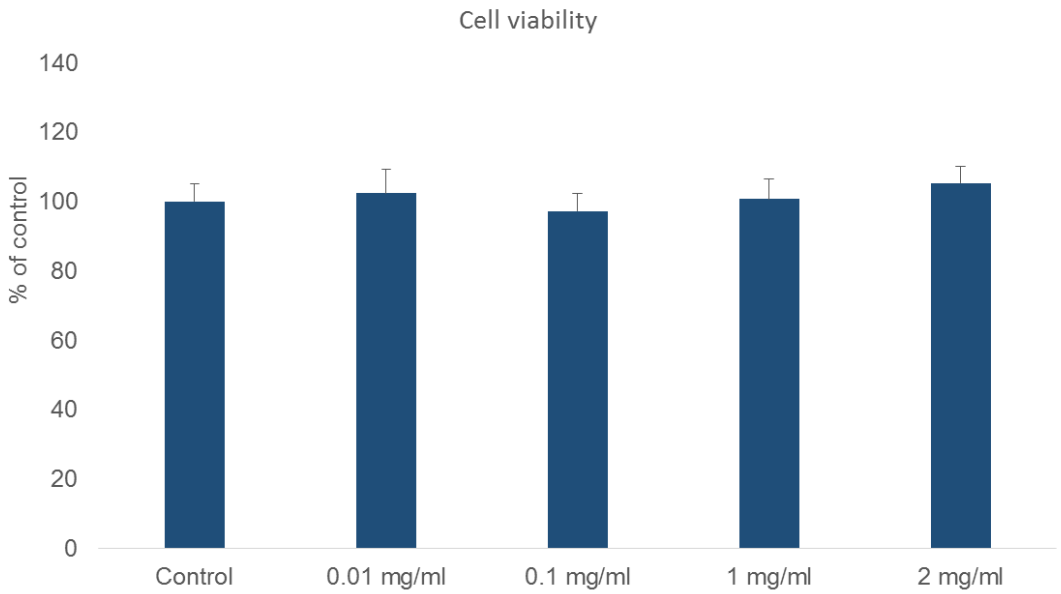

Figure 3.6: Effect of *A. phylicoides* on cell viability in normal C3A human liver cell line.
C3A liver cells were treated with Dulbecco's modified eagle's medium without phenol red, supplemented with 8 mM glucose and 2 % BSA. Cells were treated with or without *A. phylicoides* (0.01 to 2 mg/ml) for 3 hrs. Cells viability was measured using an MTT assay. A one-way ANOVA with post hoc Tukey Kramer test was used for statistical analysis where $p<0.05$ was designated as statistically significant. Results are expressed as the mean of three independent experiments relative to the control at 100 % ± standard deviation. Abbreviations: MTT - 3-(4,5-dimethylthiazol-2-yl)-2,5-diphenyltetrazolium bromide; ANOVA -analysis of variance, BSA - bovine serum albumin.

3.1.2.2. Effect of *A. phylicoides* on glucose uptake in insulin resistant human liver cells (C3A)

In order to determine the effect of the extract on glucose uptake in C3A liver cells, 2-deoxy-[^{3}H]-D-glucose uptake method (see section 2.2.2) was used and the results were analyzed using two-way ANOVA, where the treatments were analyzed separately. There were no statistically significant interactions observed in any of the treatment groups. Overall, insulin significantly increased glucose uptake ($p<0.05$) for all treatments in the presence and absence of palmitic acid (Figure 3.7).

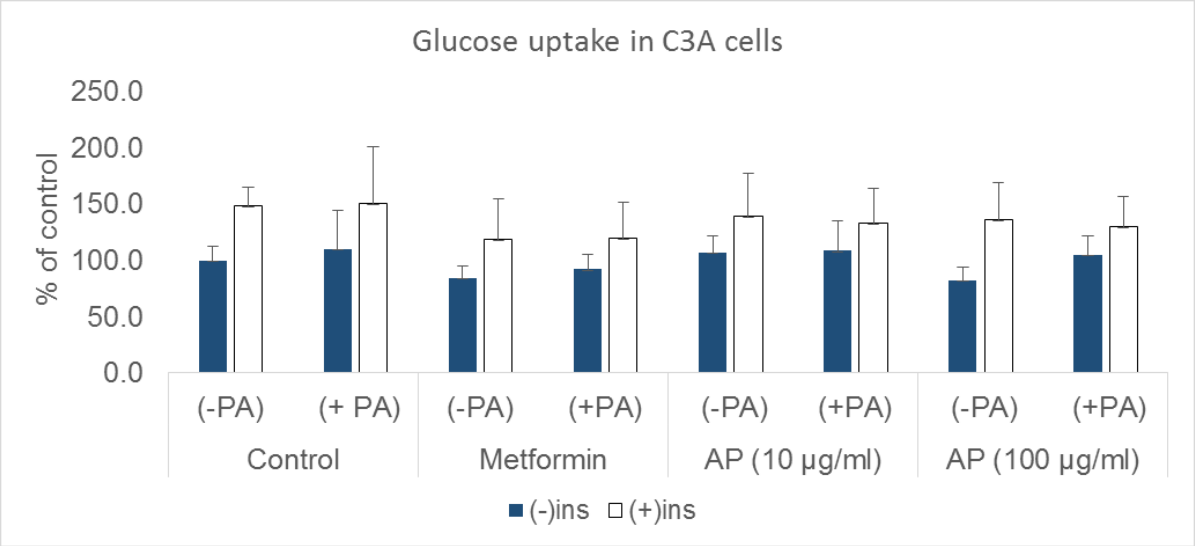

Figure 3.7: Effect of *A. phylicoides* on glucose uptake on insulin-resistant C3A human liver cells. C3A muscle cells were cultured in Dulbecco's modified eagle medium buffer with 8 mM glucose, 2 % BSA, 1 % ethanol with 750 µM palmitate (+PA) or without palmitate (-PA) for 16 hrs. Thereafter, they were treated with or without *A. phylicoides* (10 and 100 µg/ml) for 3 hrs. Metformin (1µM) were used as positive control. Thereafter, cells were stimulated with (2 µM) insulin for the last 30 min. Glucose uptake was measured using [3H]-2-deoxy-D-glucose. A two-way ANOVA with post hoc Tukey Kramer test, with a 2x2 design was used where $p<0.05$ was designated as statistically significant. Results are expressed as the mean of three independent experiments relative to the control at 100 % ± standard deviation. Abbreviations: (-)ins - without insulin; (+)ins - with insulin; HEPES - 2-[4-(2-hydroxyethyl)piperazin-1-yl]ethanesulfonic acid; ANOVA - Analysis Of Variance; BSA - bovine serum albumin.

3.1.3. *In vitro* assessment of *A. phylicoides* on cell viability, glucose uptake and lipid accumulation in adipocytes (3T3-L1)

3.1.3.1. Cytotoxicity assessment of *A. phylicoides* in differentiated adipocytes

An MTT assay was used in order to assess viability in adipocytes (3T3-L1). A range of concentrations (0.01 to 2 mg/ml) of *A. phylicodes* was used to treat cells. A one-way ANOVA post hoc Tukey Kramer test was used for statistical analysis. A significant decrease in cell viability was observed across all concentrations in comparison to the control. A concentration of 2 mg/ml significantly decreased viability in comparison to all treatment groups. The viability of cells treated with 0.01 and 0.1 mg/ml concentrations of *A. phylicoides* was significantly higher ($p<0.05$) compared to 1 mg/ml treatment group (Figure 3.8). Although viability was significantly decreased across all treatment groups, the concentrations 0.1 and 0.01 mg/ml were able to maintain cell viability above 80 % and were therefore chosen for the glucose uptake experiments.

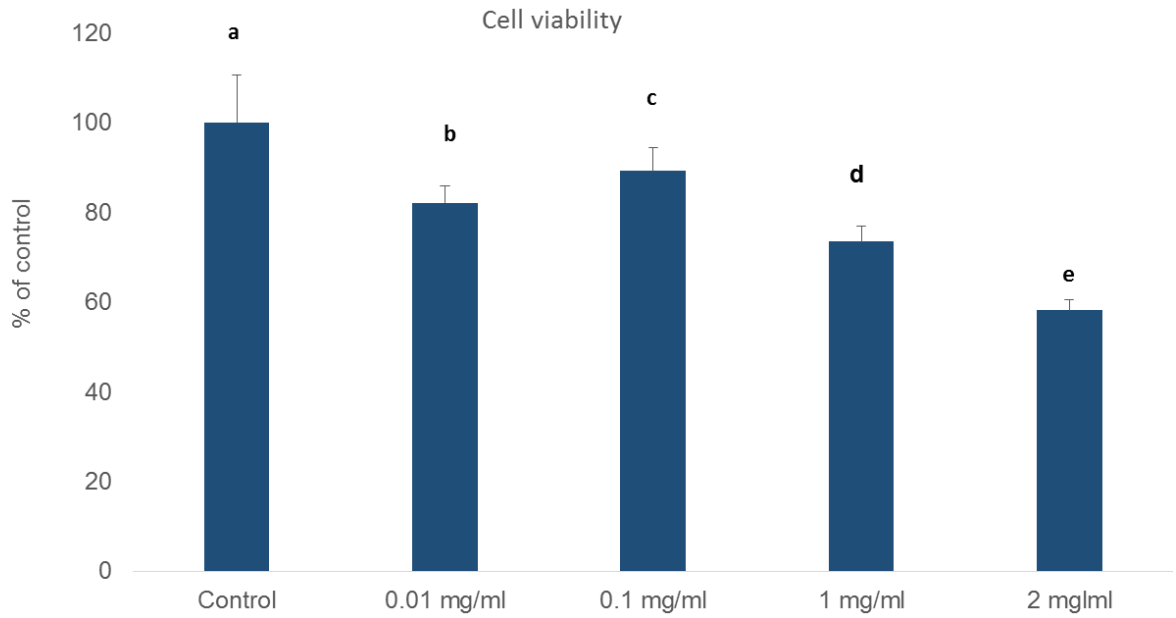

Figure 3.8: Effect of *A. phylicoides* on cell viability in normal 3T3-L1 cells.
3T3-L1 adipocytes were treated with Dulbecco's modified eagle's medium supplemented with 25 mM glucose for 24 hrs with or without *A. phylicoides* (0.01 to 2 mg/ml). Cell viability was measured using the MTT assay. A one-way ANOVA with post hoc Tukey Kramer test was used for statistical analysis. Results are expressed as the mean of three independent experiments relative to the control at 100 % ± standard deviation. Different letters denote statistical differences between treatments at $p<0.05$. Abbreviations: MTT- 3-(4,5-dimethylthiazol-2-yl)-2,5-diphenyltetrazolium bromide; ANOVA - analysis of variance.

3.1.3.2. Cytotoxicity assessment of the different treatments in 3T3-L1 cells

The effect of insulin, palmitic acid and the extract were analyzed using two-way ANOVA. Cells were treated as described in section 2.2.3.2. No statistically significant interactions were observed for palmitic acid and insulin in all groups. Insulin significantly increased ($p<0.05$) viability regardless of the presence of palmitic acid in the control, metformin, 10 µg/ml treatment groups. Palmitic acid showed no significant effect, while insulin significantly increased viability both in the absence and presence of palmitic acid for the 100 µg/ml (Figure 3.9).

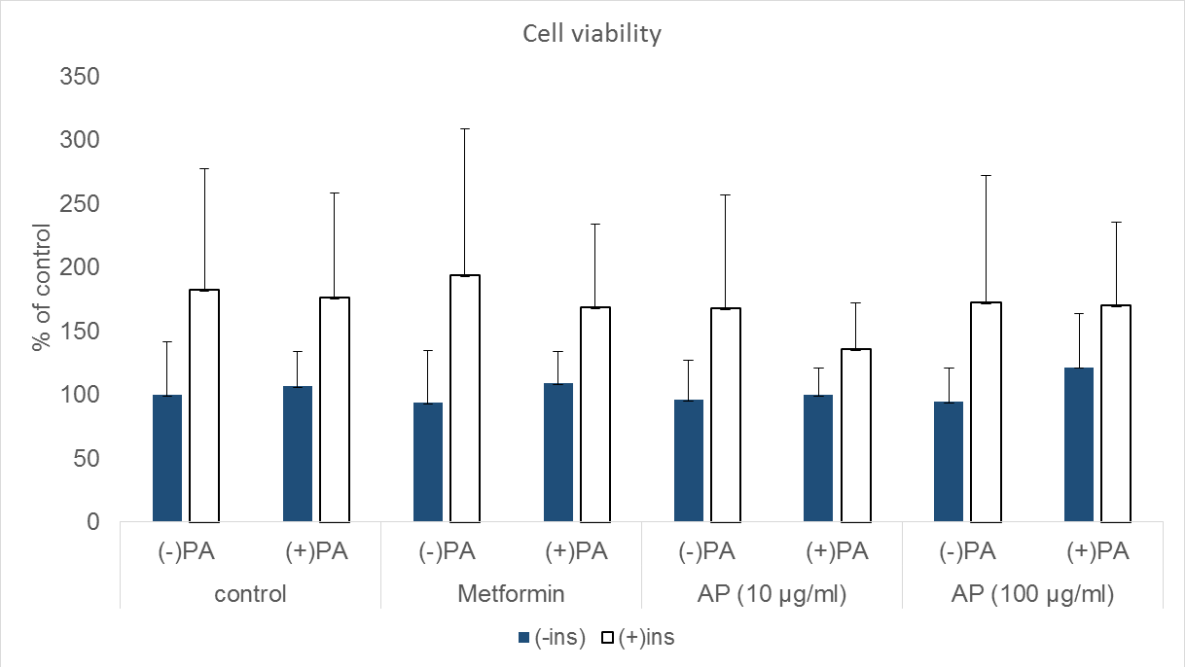

Figure 3.9: Effect of *A. phylicoides* on viability in insulin-resistant 3T3-L1 adipocytes.
3T3-L1 cells were cultured in Dulbecco's modified eagle medium buffer with 8 mM glucose, 2 % BSA, 1 % ethanol with 750 µM palmitate (+PA) or without palmitate (-PA) for 16 hrs. Thereafter, they were treated with or without *A. phylicoides* (10 and 100 µg/ml) for 24 hrs with (+ins) or without (- ins) 1 µM insulin stimulation. Metformin (1 µM) were used as positive control. Cell viability was measured using MTT. A two-way ANOVA post hoc Tukey Kramer test with a 2x2 design was used for statistical analysis, where $p<0.05$ was designated as statistically significant. Significant main effects are described in the text. Results are expressed as the mean of two independent experiments relative to the control at 100 % ± standard deviation. Abbreviations: (-)ins - without insulin; (+)ins - with insulin; ANOVA - Analysis Of Variance; MTT - 3-(4,5-dimethylthiazol-2-yl)-2,5-diphenyltetrazolium bromide; BSA - bovine serum albumin.

3.1.3.3. Effect of *A. phylicoides* on glucose uptake and lipid accumulation in differentiated insulin-resistant adipocytes (3T3-L1)

In adipocytes (3T3-L1), glucose uptake was measured using glucose oxidase method. In the control group, results showed no statistical interaction and neither insulin nor palmitic acid had any effect on glucose uptake. In the metformin group, a statistically significant interaction was observed between palmitic acid and insulin, where insulin significantly increased ($p<0.05$) glucose uptake in the absence of palmitic acid. No statistically significant interaction was observed for the lowest concentration (10 µg/ml) of the extract, however, palmitic acid significantly increased ($p<0.05$) glucose uptake (main effect) while insulin showed no overall effect. There was no statistically significant interaction and both insulin and palmitic acid showed no significant effect on glucose uptake when the cells were treated with the highest concentration of the extract (Figure 3.10 A).

Lipid accumulation was determined by staining cells with Oil Red O. No statistically significant interactions were observed between palmitic acid and insulin for any of the treatments. For the control, a significant decrease ($p<0.05$) in lipid accumulation was observed in the presence of palmitic acid regardless of insulin treatment. For the highest concentration (100 µg/ml) of the extract, a significant decrease in lipid accumulation was observed in the palmitate treated cells regardless of the presence of insulin (Figure 3.10 B).

A

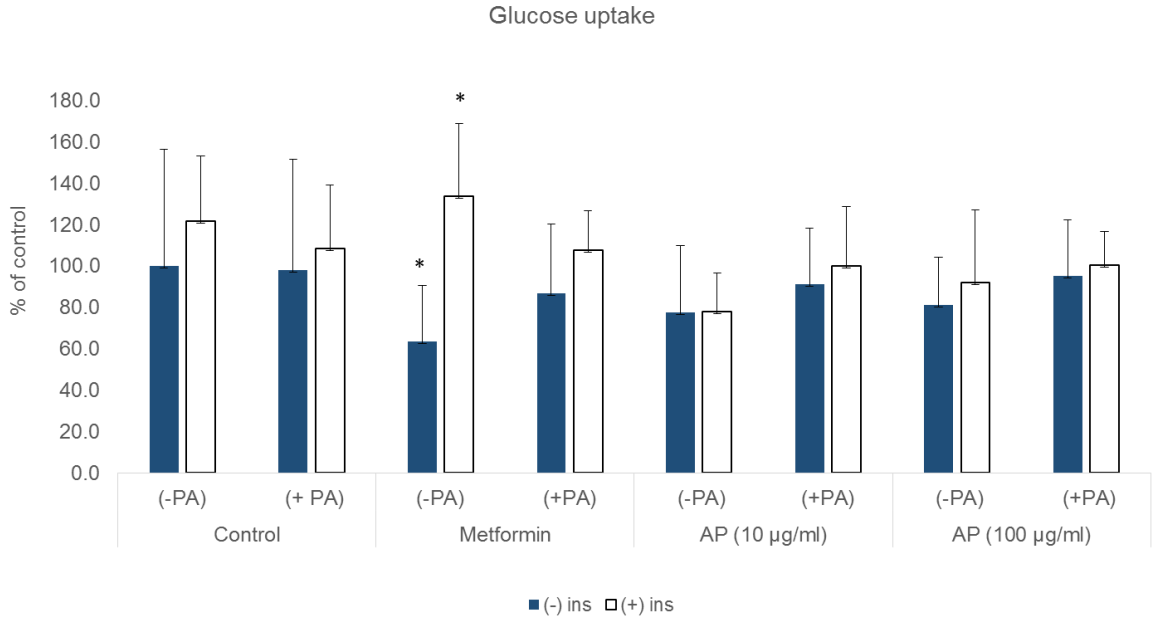

B

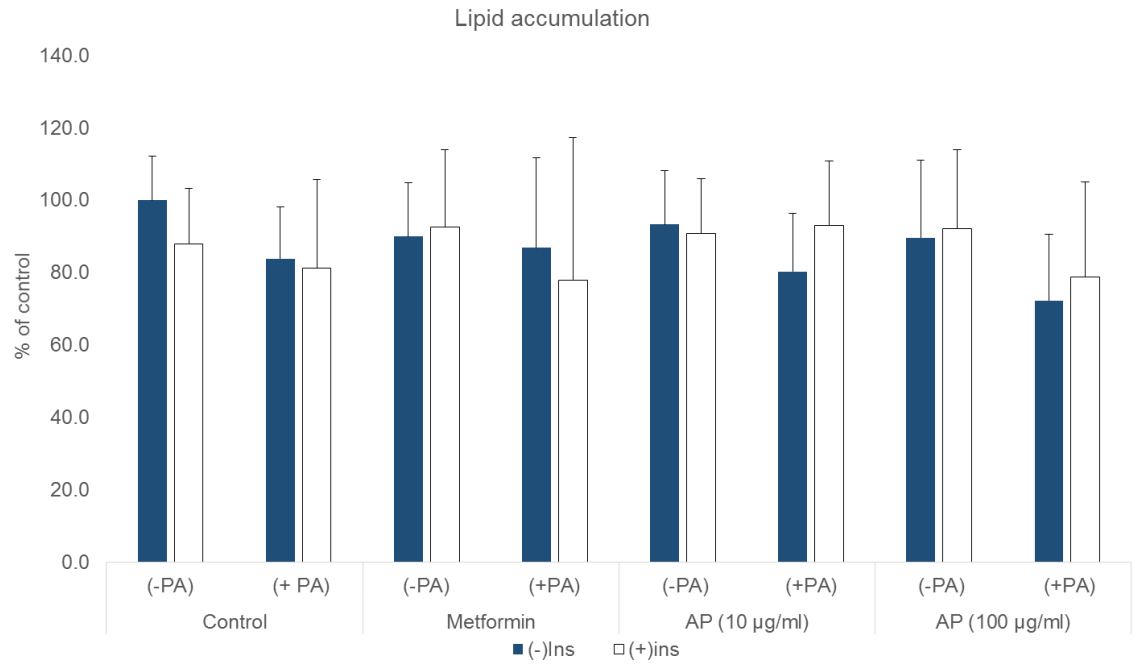

Figure 3.10: Effect of *A. phylicoides* on glucose uptake and lipid accumulation in 3T3-L1 adipocytes.
3T3-L1 cells were cultured in Dulbecco's modified eagle medium buffer with 8 mM glucose, 2 % BSA, 1 % ethanol with 750 µM palmitate (+PA) or without palmitate (-PA) for 16 hrs. Thereafter, they were treated with or without *A. phylicoides* (10 and 100 µg/ml) for 24 hrs with (+ins) or without (- ins) 1 µM insulin stimulation. Metformin (1µM) were used as positive control. Glucose uptake (A) was measured using a glucose oxidase method, lipid accumulation (B) was measured using oil red O staining. A two-way ANOVA post hoc Tukey Kramer test, where each treatment, i.e. control, metformin and the different extract concentrations, was analyzed individually for palmitic acid and insulin effects and interactions. Statistically significant interactions are indicated in the graph when $p<0.05$. Within each treatment, groups with * differ significantly from each other. Significant main effects are described in the text. Results are expressed as the mean of three independent experiments relative to the control at 100 % ± standard deviation. Abbreviations: BSA - bovine serum albumin; (-)ins - without insulin; (+)ins - with insulin; ANOVA - Analysis Of Variance.

3.1.4. Inhibitory effect of *A. phylicoides* on the activity of PTP1B

Protein tyrosine phosphatase 1B (PTP1B) is negative regulator of insulin signaling, which acts by dephosphorylating the insulin receptor and thereby inhibiting its association with substrates such as the insulin receptor substrate protein (IRS). Therefore, it was of interest to investigate the inhibitory effect of *A. phylicoides* on the activity of PTP1B. Eight different concentrations (serial dilutions) of the aqueous extract of *A. phylicoides* (50, 25, 12.5, 6.25, 3.13, 1.56, 0.78, 0.39 µg/ml) were used to determine the concentration of the extract at which the response is reduced by 50 % (IC_{50}) (Figure 3.11). The assay was conducted as described in section 2.2.4.

Athrixia phylicoides showed inhibitory effects against the PTP1B enzyme as it has an IC_{50} value of 7.3±1.1 µg/ml.

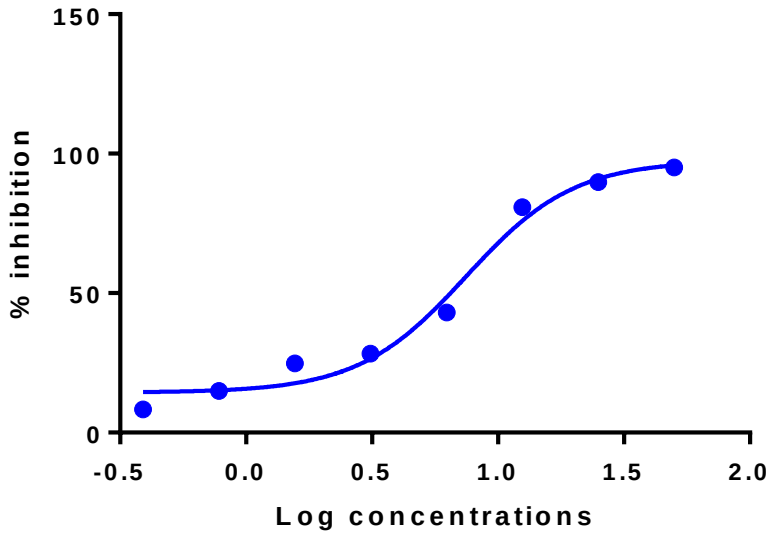

Figure 3.11: Potent inhibitory effect of *A. phylicoides* on PTP1B**.**
The extract (50 µg/ml) was serially diluted in citrate buffer to yield 8 different concentrations. Citrate buffer (50 Mm), 1,4-Dithiothreitol (DTT) (1 mM), para-Nitrophenylphosphate (1 mM), each concentration of the extract and the enzyme were added into each well and incubated in for 30 min. The reaction was stopped by adding NaOH (1M). Results are expressed as the percentage of inhibition. Abbreviations: PTP1B - Protein-tyrosine phosphatase 1B.

3.2. Assessment of anti-diabetic potential of *A. phylicoides in vivo*

3.2.1. Treatment dose received by each experimental group

C57BLKS *db/db* mice were given 10 g of food each day. Prior to the start of the treatments, food intake was measured to assess average daily intake and food was subsequently prepared to deliver the daily dose in 6 g. Table 3.1 illustrates the intended dose and the delivered dose during the 30-day treatment period. When removing the days where the animals were fasted for blood glucose measurements, the treatment doses are very close to the intended dose. The group fed the high dose of the extract, however, did not reach the targeted dose. Results are expressed as mean ± standard deviation of 6 mice.

Table 3.1: Representation of the intended dose, actual dose and the dose after subtracting fasting days in the different treatment groups

Group	Intended dose mg/kg/day	average daily dose mg/kg/day	daily dose* mg/kg/day
Vildagliptin	5	4.63 ± 0.15	5.32 ± 0.17
Metformin	300	261.61 ± 24.80	297.34 ± 27.30
SB1	60	53.11± 3.30	60.53± 3.25
AP1 20 mg/kg	20	17.37 ± 1.35	19.90 ± 1.48
AP2 200 mg/kg	200	161.70 ± 16.03	184.12 ± 19.06

* Average daily dose excluding the days when mice were fasted for blood glucose measurements (once per week).

3.2.2. Effect of an aqueous extract of *A. phylicoides* in food and water intake and body weight gain

The weekly average water consumption of each group over a period of 30 days was calculated and compared between obese and lean control groups. Results showed a significant increase ($p<0.05$) in water intake for the obese control group when compared to the lean (128.2 ± 15.9 vs 69.0 ± 8.2 ml). All treatments showed no effect on water consumption when they were compared to the obese control (Figure 3.12 A)

The average food intake of each group over a period of 30 days was calculated. Results showed a significant increase ($p<0.05$) in the obese control group in comparison to the lean control group (25.4 ± 20.1 vs 40.1 ± 3.8 g/100 g body weight). However, all treatments (metformin, vildagliptin, SB1 and AP) showed no effect when they were compared with the obese control group (Figure 3.12 B).

The lean control group was compared to the obese group (Figure 3.12 C) and results showed a significant increase ($p<0.05$) in body weight gain for the obese group (-0.8 ± 1.5 vs 1.8 ± 1.8 g). All other treatments showed no effect on body weight gain after four weeks of treatment.

A

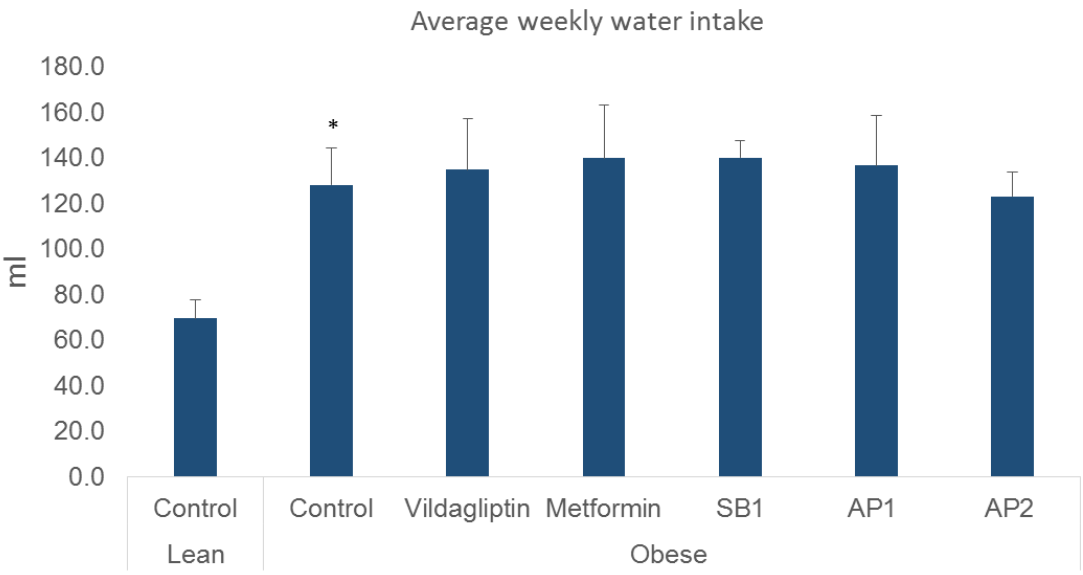
Average weekly water intake
ml
180.0
160.0
140.0
120.0
100.0
80.0
60.0
40.0
20.0
0.0
*
Control
Lean
Control
Vildagliptin
Metformin
SB1
AP1
AP2
Obese

B

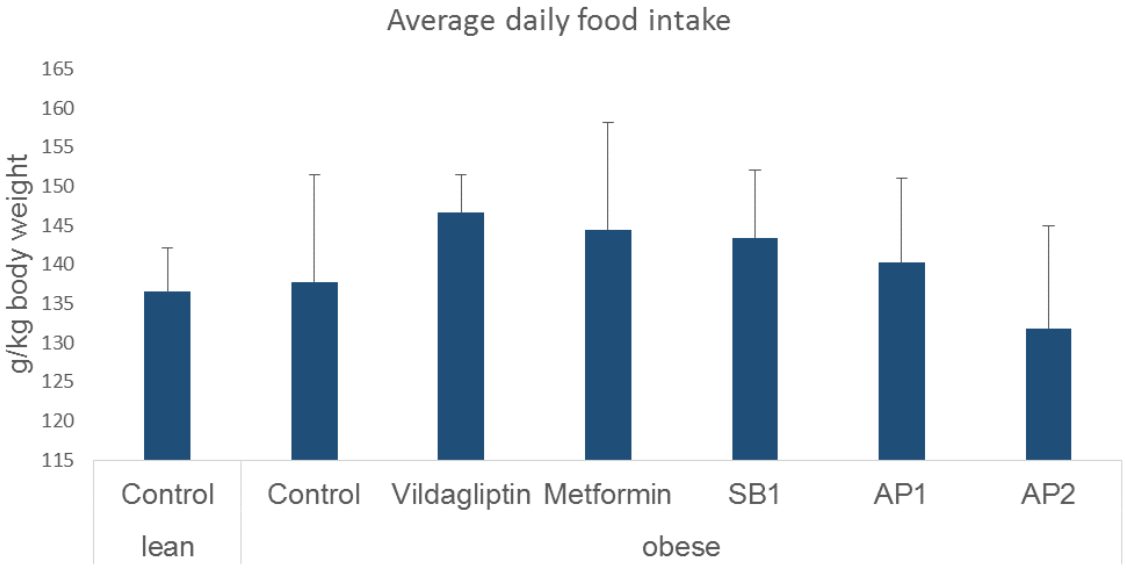
Average daily food intake
g/kg body weight
165
160
155
150
145
140
135
130
125
120
115
Control
lean
Control
Vildagliptin
Metformin
SB1
AP1
AP2
obese

C

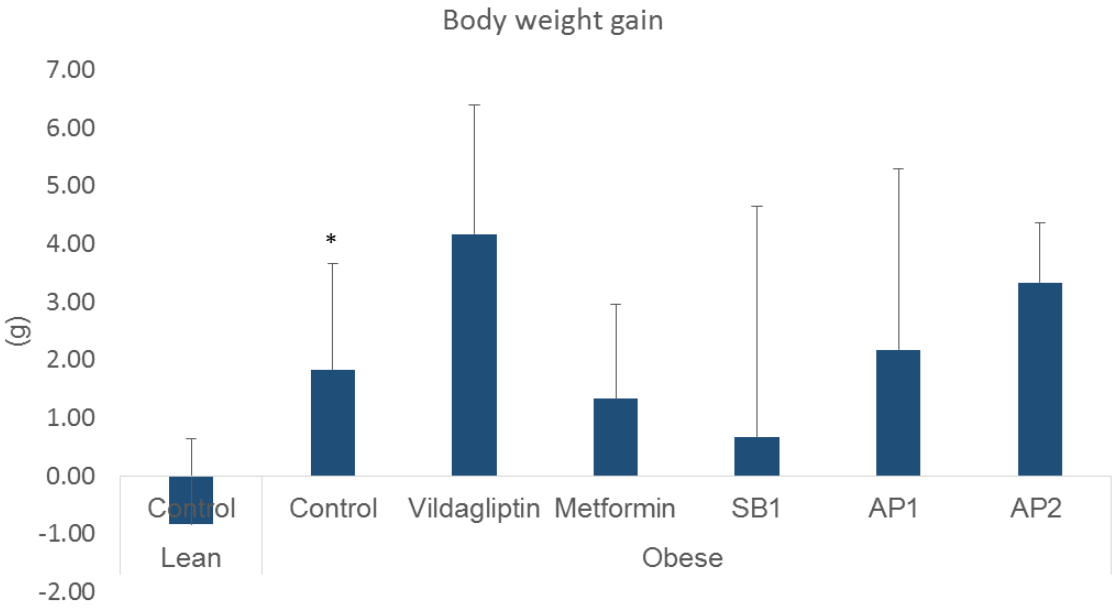

Figure 3.12: Average water, food intake together with body weight gain of each treatment group. Six weeks old C57BLKS *db/db* mice were are signed into group of 6. Six lean mice were used as a control. Mice were treated with vildagliptin (5 mg/kg), metformin (300 mg/kg), aspalathin enriched rooibos extract (SB1 60 mg/kg), and two concentration of *A. phylicoides* (AP1 20 and 200 mg/kg) for 4 weeks. Water intake was monitored weekly, food intake was monitored daily and body weight gain was calculated using the first and last body weight of each animal. (A) reports average weekly water intake, (B) food intake and (C) is the average body weight of each group. Statistical analysis was conducted using one-way ANOVA (Dunnett's test for obese vs all treatment groups, a t-test for lean vs control). Mean ± Standard deviation, where * represents statistical significance between lean and obese control groups at p <0.05. Abbreviations: AP - *Athrixia phylicoides*; SB1 - aspalathin enriched rooibos extract, ANOVA - analysis of variance

3.2.3. Effect of *A. phylicoides* weekly on 16 hr fasting plasma glucose concentrations

Fasting plasma glucose levels were measured weekly. A significant increase was observed ($p<0.05$) in fasting plasma glucose levels in the obese group in comparison to the lean group for week one (6.2 ± 1.6 vs 11.5 ± 1.8 mmol/l), week two (3.6 ± 0.6 vs 9.8 ± 4.59 mmol/l), week three (7.2 ± 1.7 vs 12.1 ± 4.5 mmol/l) week 4 (4.3 ± 0.7 vs 16.2 ± 4.9 mmol/l). Metformin, SB1 and the two concentrations of the extract showed no effect throughout the four weeks (Figure 3.13 B, C and D) compared to the obese control group. However, after the first week (Figure 3.13 A), metformin significantly increased ($p<0.05$) fasting plasma glucose levels in comparison to the obese control group (11.5 ± 1.8 vs 18.2. ±3.4 mmol/l).

A

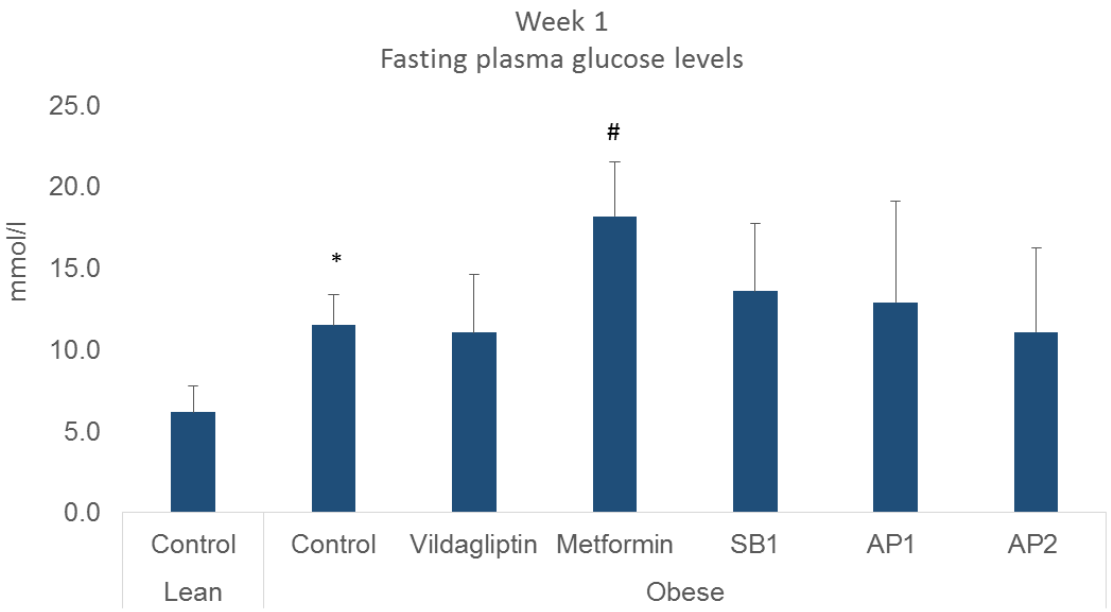
Week 1
Fasting plasma glucose levels
25.0
20.0
15.0
10.0
5.0
0.0
mmol/l
*
#
Control
Control
Vildagliptin
Metformin
SB1
AP1
AP2
Lean
Obese

B

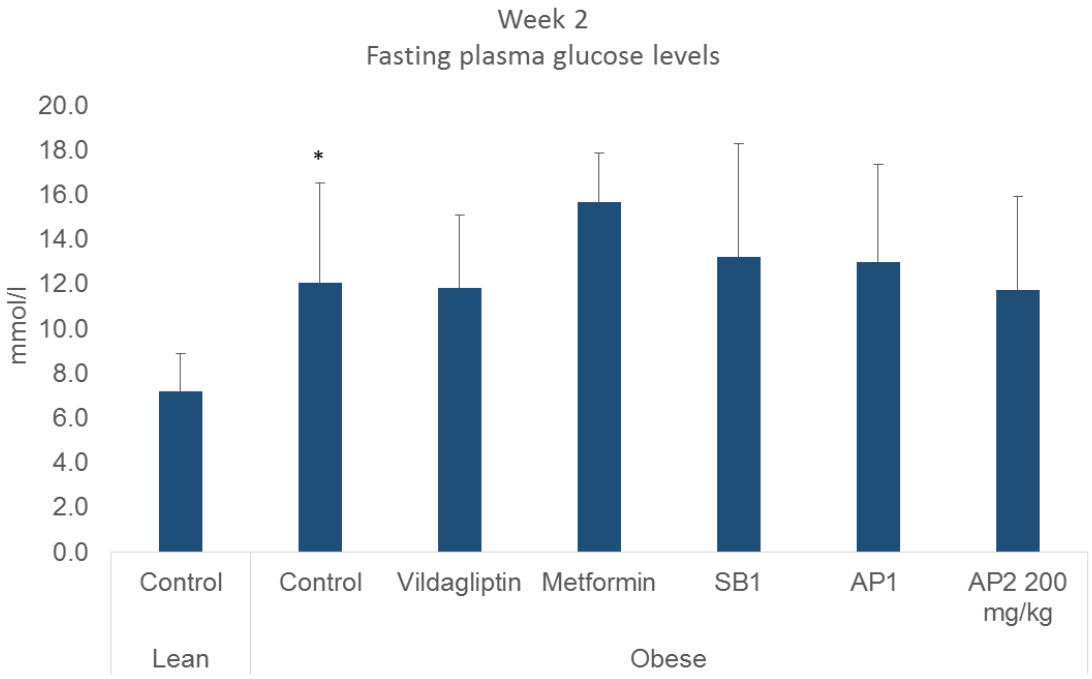
Week 2
Fasting plasma glucose levels
20.0
18.0
16.0
14.0
12.0
10.0
8.0
6.0
4.0
2.0
0.0
mmol/l
*
Control
Control
Vildagliptin
Metformin
SB1
AP1
AP2 200 mg/kg
Lean
Obese

C

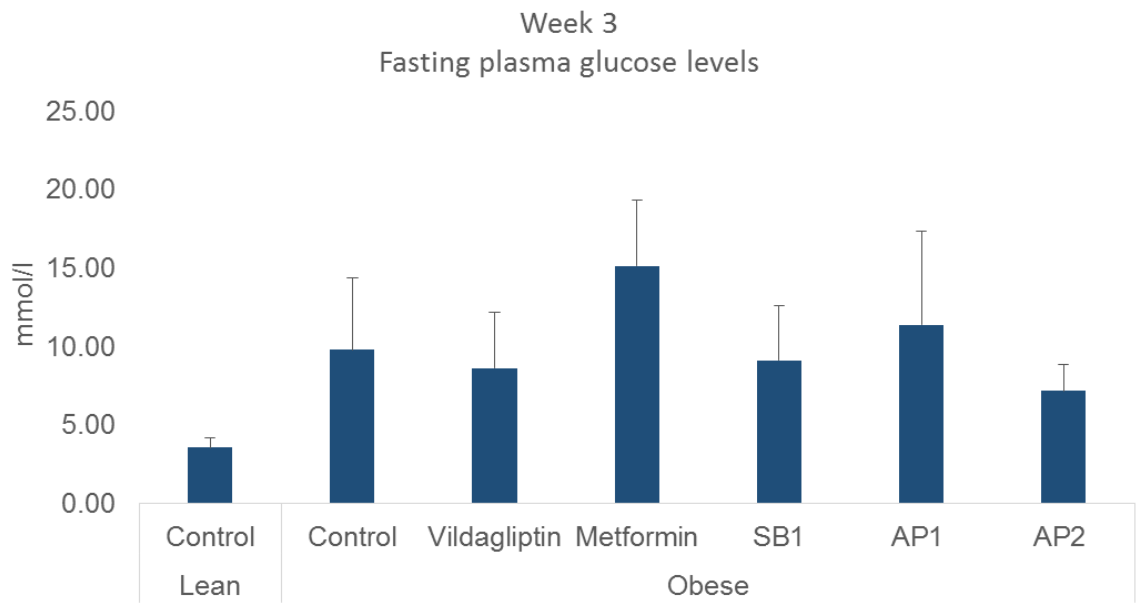

D

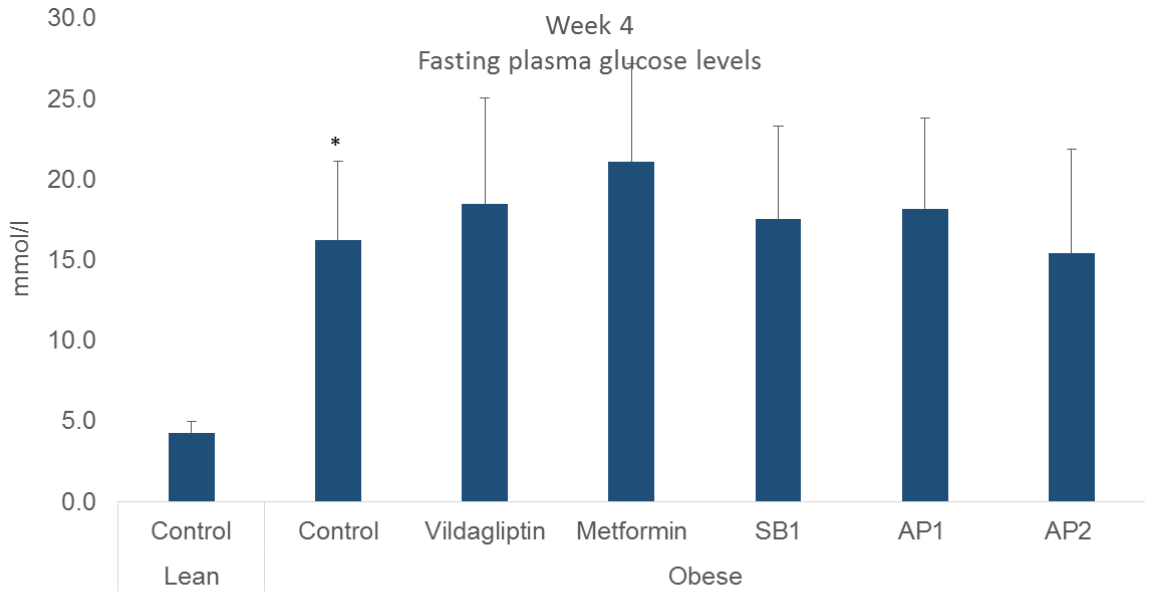

Figure 3.13: **Fasting plasma glucose concentrations measured weekly after a 16 hour fasting period.**
Six weeks old C57BLKS *db/db* mice were are signed into group of 6. Six lean mice were used as a control. Mice were treated with vildagliptin (5 mg/kg), metformin (300 mg/kg), aspalathin enriched rooibos extract (SB1 60 mg/kg), and two concentration of *A. phylicoides* (AP1 20 and 200 mg/kg) for 4 weeks. Fasting plasma glucose levels were monitored weekly. Figure A shows fasting plasma glucose levels measured after week 1, (B) week 2, (C) week 3 and (D) represents week 4. Statistical analysis was conducted using one-way ANOVA (Dunnett's test for obese vs all treatment groups, a t-test for

lean vs control). Mean ± Standard deviation, where * represents statistical significance between lean and obese control groups and # represents a statistically significant difference between obese control group and obese treatment groups at p <0.05. Abbreviations: AP-*Athrixia phylicoides*; SB1-aspalathin enriched rooibos extract, ANOVA analysis of variance

3.2.4. Effect of *A. phylicoides* on oral glucose tolerance

An oral glucose tolerance test (OGGT) is designed to assess impaired glucose tolerance, where glucose is administered orally and its disposal is monitored over time. Glucose (2 g/kg) was administer to mice and their blood glucose levels were monitored after 30, 60 and 120 min. After 30 minutes, an increase in blood glucose is expected, which should return to baseline within 120 min. At the first time point (30 min), 5 mice in the obese control group presented with glucose levels above the detection limit of the glucometer (33.3 mmol/l) and could therefore not be quantified. Similarly, 5 mice in the vildaglitpin group, 3 in the metformin group, 4 in the SB1 group, all mice in the low dose AP and 5 in the high dose *A. phylicoides* group were above the detection limit. At the second time point (60 min) 4 mice in the obese group presented with high glucose concentrations that were above the limit that could be detected by the glucometer. Similarly, 5 in the vildagliptin group, 1 in the metformin group, 3 in the SB1 group, 5 in the AP1 group and 4 in the AP2 group were above the detection limit.

A decrease in glucose levels was observed after 120 min, where only 1 animal out of 6 in the metformin, SB1, AP1 and AP2 groups had glucose levels higher than the detection limit (Figure 3.14). Statistical analysis and area under the curve calculations were not conducted due to the lack of quantitative data.

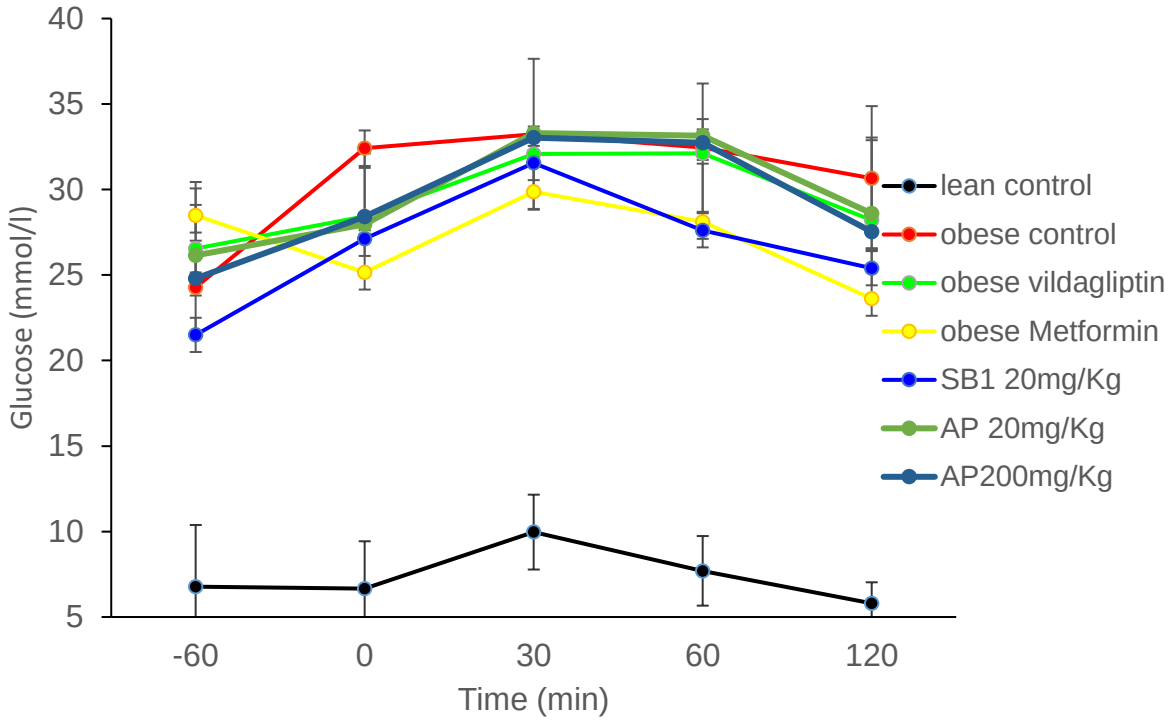

Figure 3.14: Oral glucose tolerance test after a 16 hours fasting period.
Six weeks old C57BLKS *db/db* mice were are signed into group of 6. Six lean mice were used as a control. Mice were treated with vildagliptin (5 mg/kg), metformin (300 mg/kg), aspalathin enriched rooibos extract (SB1 60 mg/kg), and two concentration of *A. phylicoides* (AP1 20 and 200 mg/kg) for 4 weeks. Mice were fasted for 16 hrs, followed by oral administration of treatment. An hour later, 20 mg/kg of glucose was administered. Thereafter, glucose levels were monitored over different time points (30, 60, and 120 min). All treatments showed no effect on glucose concentrations at the time points 30 and 60 min. Glucose concentrations decreased after 120 min. No statistical analysis was conducted.

3.2.5. Effect of *A. phylicoides* on organ weights (liver and adipose tissue)

The liver and retroperitoneal fat were harvested at the end of the treatment period (day 31) and they were weighed (refer to section 2.3.6). Vildagliptin, metformin, SB1 and the two concentrations of AP had no effect on liver and retroperitoneal fat weights in comparison to the obese control group. A significant increase ($p<0.05$) in liver weight was observed in the obese group in comparison to the lean group (0.04 ± 0.00 vs 0.05 ± 0.01 g/g body weight) g/g body weight (Figure 3.15 B). A significant increase ($p<0.05$) was observed in retroperitoneal fat when the lean group was compared to the obese control group (0.01 ± 0.00 vs 0.03 ± 0.00 g/g body weight). The other treatments (metformin, vildagliptin, SB1 and AP) showed no effect in both liver and retroperitoneal fat weights (Figure 3.15 A and B).

A

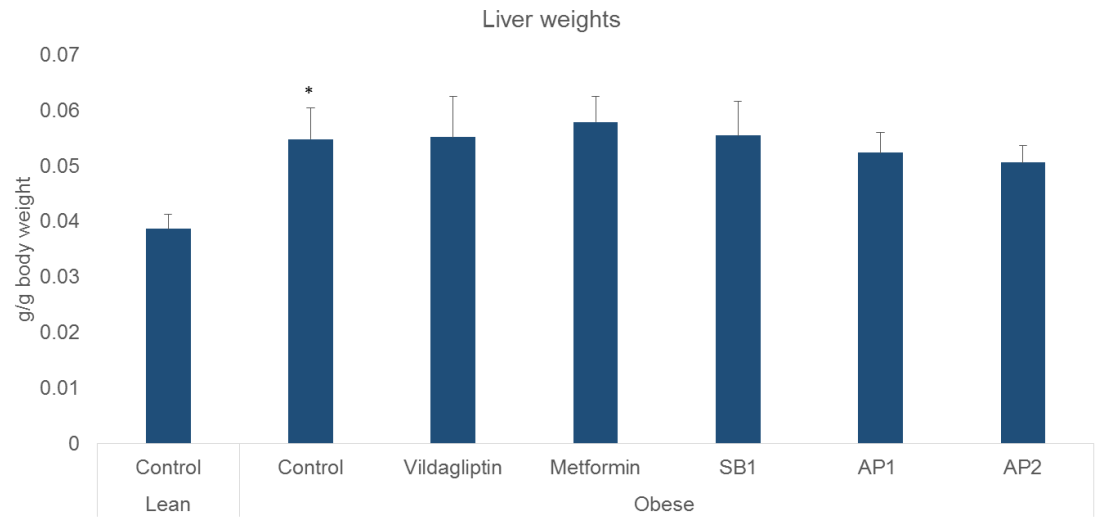

B

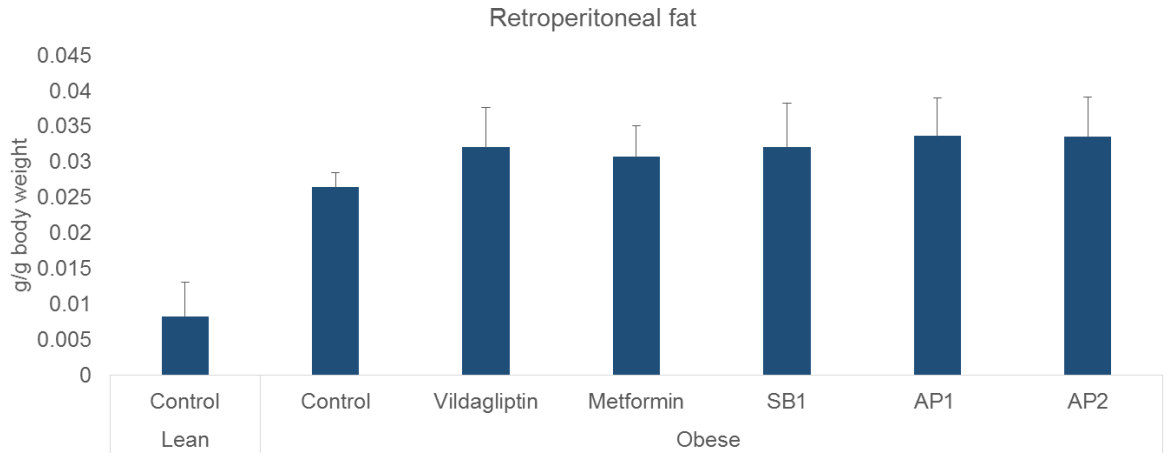

Figure 3.15: Effect of *A. phylicoides* on liver and retroperitoneal fat weights.
Six weeks old C57BLKS *db/db* mice were are signed into group of 6. Six lean mice were used as a controls. Mice were treated with vildagliptin (5 mg/kg), metformin (300 mg/kg), aspalathin enriched rooibos extract (SB1 60 mg/kg), and two concentration of *A. phylicoides* (AP1 20 and 200 mg/kg) for 4 weeks. Organs were harvested from *db/db* mice on termination day. (A) Reports the average liver weights per group and (B) is the average retroperitoneal fat weights per group. Statistical analysis was conducted using one-way ANOVA (Dunnett's test for obese vs all treatment groups, a t-test for lean vs control). Results are the mean ± Standard deviation, where * represents statistical significance between the lean and obese control groups at $p<0.05$. Abbrevations: SB1-aspalathin enriched rooibos extract; AP-*Athrixia phylicoides*; ANOVA analysis of variance.

3.2.6. Effect of *A. phylicoides* on serum insulin concentrations and insulin sensitivity in *db/db* mice

Serum insulin concentrations were measured by ELISA and they were used to calculate the Homeostatic model assessment of insulin resistance (HOMA-IR index). The HOMA-IR index is a widely used technique applied in the assessment of insulin sensitivity using fasting plasma glucose and insulin concentrations (Wallace *et al*., 2004). No statistically significant changes were observed in serum insulin concentrations across all treatment groups (metformin, vildagliptin, SB1, and AP) in comparison to the obese control group. Vildagliptin, metformin and SB1 markedly reduced serum insulin concentrations in comparison to the obese control group (Figure 3.16 A).

Vildagliptin, metformin and SB1 markedly improved insulin sensitivity in *db/db* mice. Both concentrations of the extract showed no effect in improving insulin sensitivity (Figure 3.16 B)

A

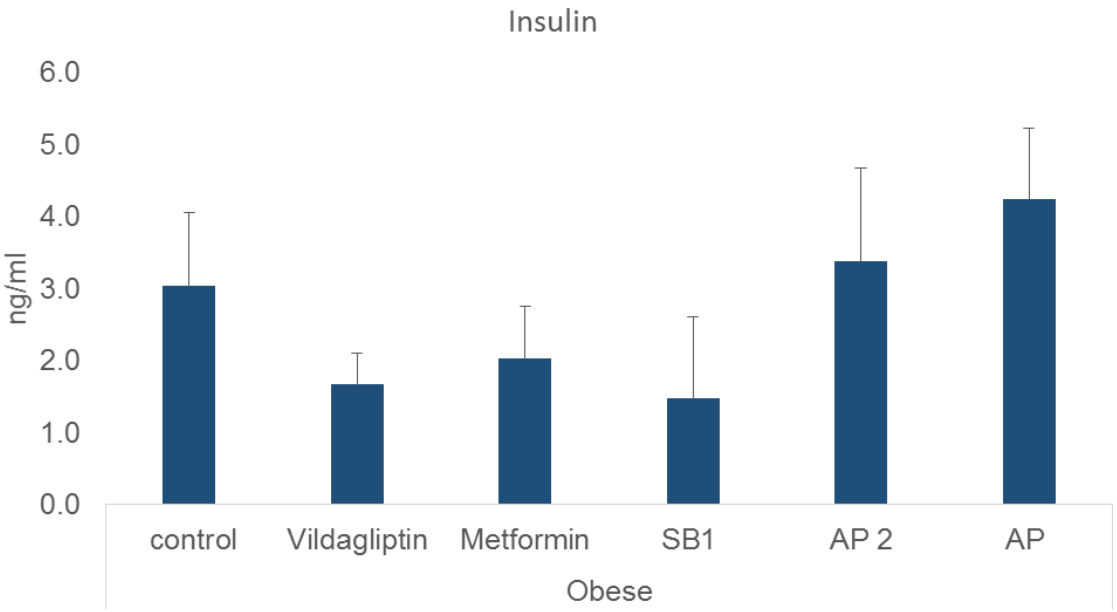

B

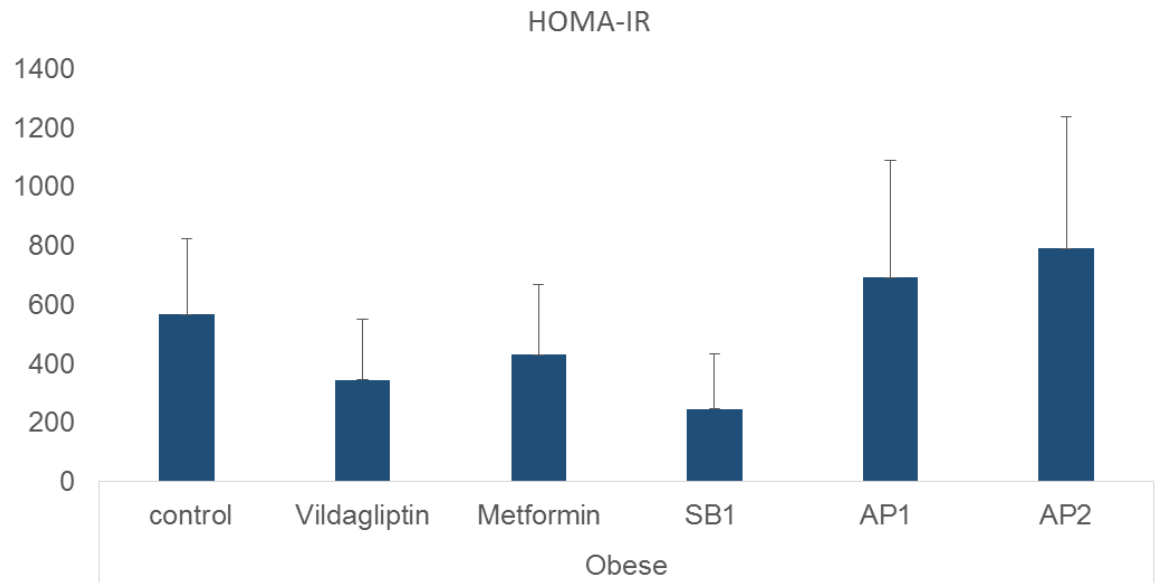

Figure 3.16: Serum insulin concentrations and insulin sensitivity measured by the HOMA-IR index.
Six weeks old C57BLKS *db/db* mice were are signed into group of 6. Six lean mice were used as a controls. Mice were treated with vildagliptin (5 mg/kg), metformin (300 mg/kg), aspalathin enriched rooibos extract (SB1 60 mg/kg), and two concentration of *A. phylicoides* (AP1 20 and 200 mg/kg) for 4 weeks. Serum insulin concentration were measured using ELISA. Concentrations obtained for the insulin together with baseline glucose (from oral glucose tolerance test) were used to calculate the HOMA-IR index. (A) Reports serum insulin concentrations and (B) is the HOMA-IR index. Statistical analysis was conducted using one-way ANOVA (Dunnett's test) and a t-test for lean vs control). Results are the mean ± Standard deviation, where statistical significance was considered at $p<0.05$. Abbreviations: SB1-aspalathin enriched rooibos extract; *AP-Athrixia phylicoides*; ANOVA analysis of variance.

3.2.7. Effect of *A. phylicoides* on serum lipid concentration in diabetic *db/db* mice

Serum cholesterol concentration was significant increased ($p<0.05$) in the obese control group when compared to the lean (2.20 ± 0.20 vs 3.52 ± 0.29 mmol/l). Metformin, vildagliptin, SB1 as well as the two concentrations of the extract showed no effect (Figure 3.17 A).

A significant increase ($p<0.05$) in HDL-cholesterol concentration was observed in the obese control group when it was compared to the lean group (1.67 ± 0.14 vs 2.46 ±0.41mmol/l) (Figure 3.17 B). Comparing SB1, vildagliptin and the extract to the obese control demonstrated no HDL-cholesterol lowering effects. Metformin showed a significant increase ($p<0.05$) in HDL-cholesterol concentration (2.46 ± 0.41 vs 3.15 ± 0.33 mmol/l).

Serum triglyceride levels significantly increased ($p<0.05$) in the obese group in comparison to the lean (0.80 ± 0.10 vs 1.95 ± 0.70 mmol/l). No significant serum triglyceride lowering effects were observed in vildagliptin, metformin, SB1, as well as the two concentrations of AP.

A

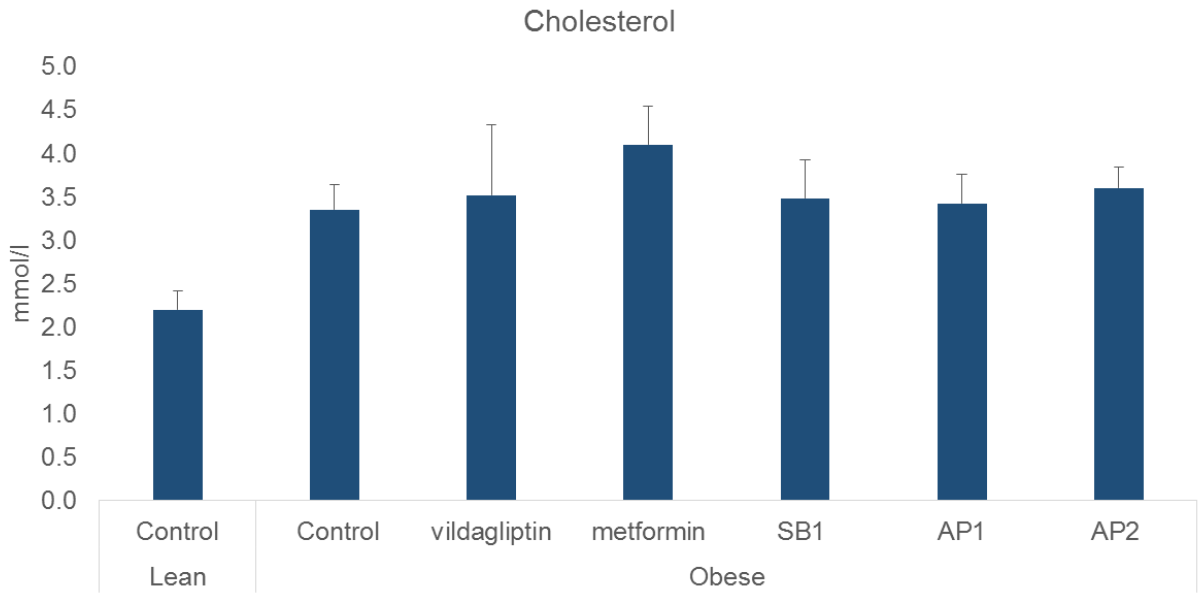

B

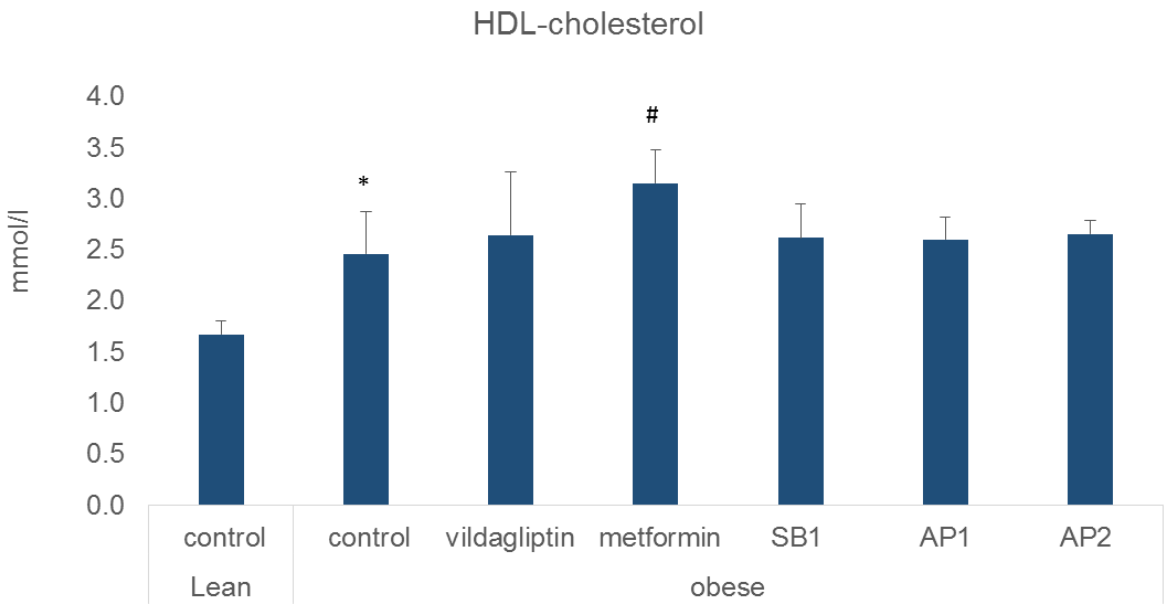

C

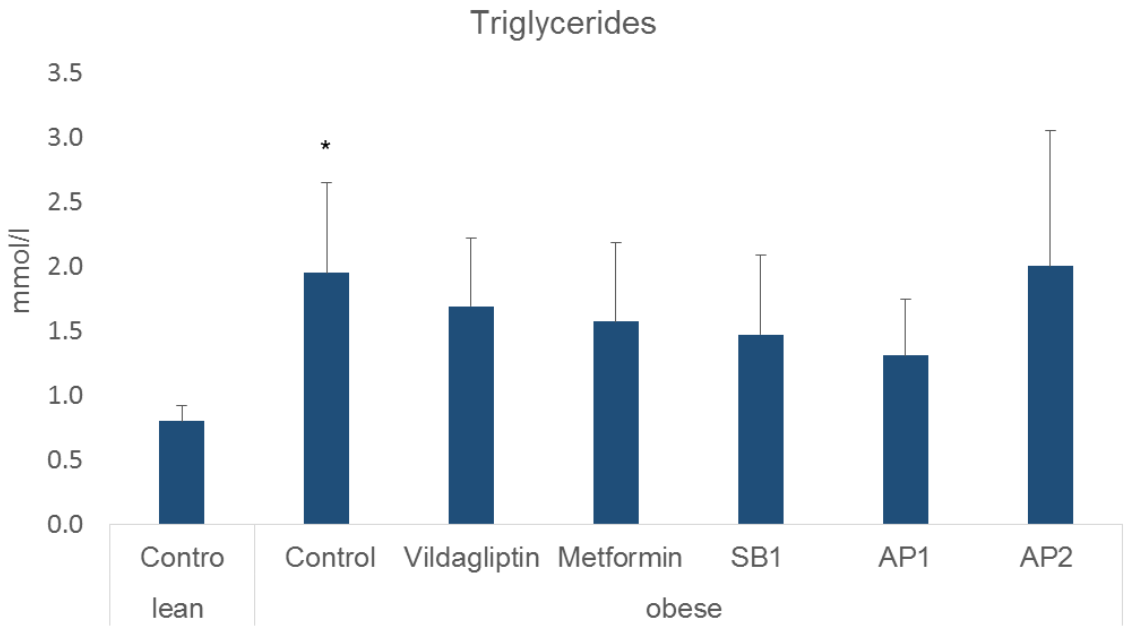

Figure 3.17: Effect of *A. pylicoides* on serum cholesterol, high density lipoprotein-cholesterol (HDL-cholesterol) and triglyceride concentrations.
Six weeks old C57BLKS db/db mice were are signed into group of 6. Six lean mice were used as a control. Mice were treated with vildagliptin (5 mg/kg), metformin (300 mg/kg), aspalathin enriched rooibos extract (SB1 60 mg/kg) and two concentration of *A. phylicoides* (AP1 20 and 200 mg/kg) for 4 weeks. (A) Reports serum cholesterol concentration, (B) serum HDL-cholesterol and (C) is triglyceride concentrations. Statistical analysis was conducted using one-way ANOVA (Dunnett's test for obese vs all treatment groups, a t-test for lean vs control), where * represents a comparison between lean and obese control groups and # represents a comparison between obese control group and the obese treatment groups at $p<0.05$.

3.2.8. Effect of *A. phylicoides* on steatosis in *db/db* mice

The effect of *A. phylicoides* was investigated in liver sections harvested from *db/db* mice. Liver sections were scored as follows: Macrovesicular changes represent a form of steatosis where the cytoplasm of the liver cell is completely displaced by a lipid droplets. Mediovesicular changes were characterized by medium sized lipid droplets occupying the cytoplasm of hepatocytes. Macrovesicular and mediovesicular changes represent advanced steatosis, while microvesicular changes presented by very small lipid droplets in the cytoplasm are considered as the mild form of steatosis. Liver sections were scored in two regions (central and portal vein area) and the scores were combined by calculating the average of each group. There were no macrovesicular changes observed in the treatment groups, however, one out of the six animals in the obese control group presented with macrovesicular changes. The higher dose of the

extract (AP2) lowered the incidence of mediovesicular changes markedly but not significantly. Taken together with the absence of macrovesicular changes, this suggests that AP2, at the given dose, improved the degree of steatosis (Figure 3.18).

A

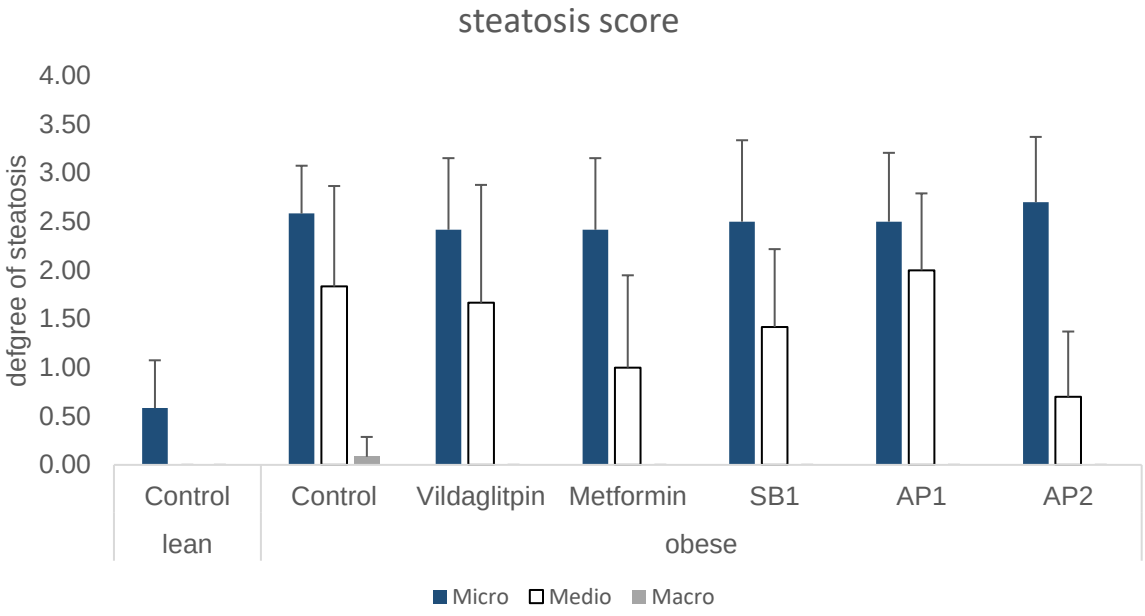

B

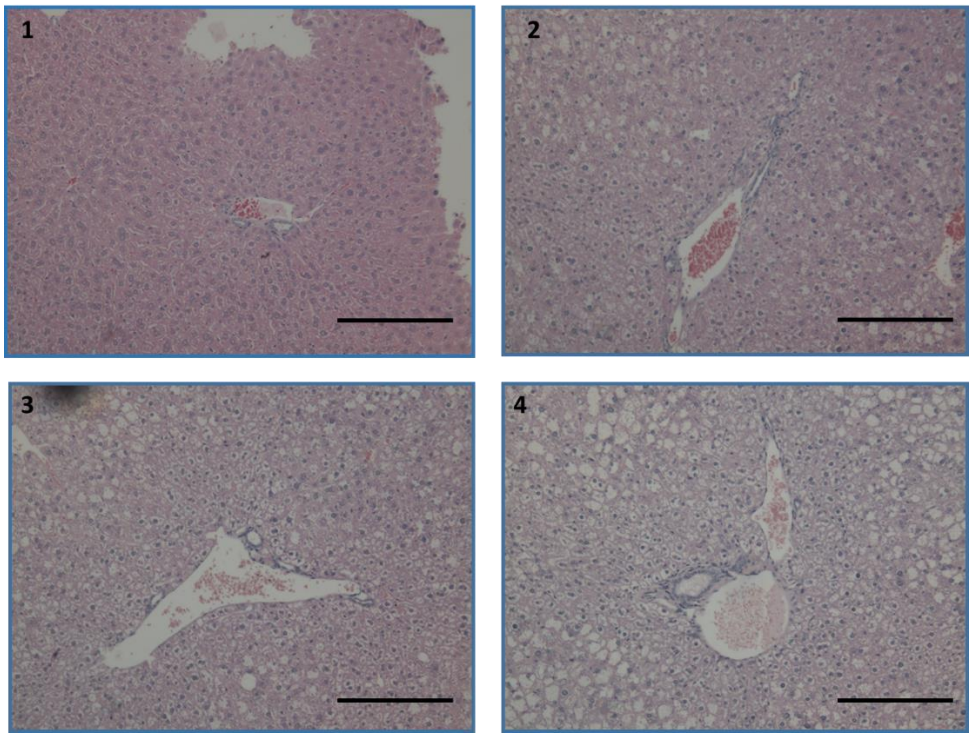

Figure 3.18: Degree of steatosis analyzed in the portal and central vein area of liver sections. Six weeks old C57BLKS *db/db* mice were are signed into group of 6 with 6 lean mice as controls. Mice were treated with vildagliptin (5 mg/kg), metformin (300 mg/kg), aspalathin enriched rooibos extract (SB1 60 mg/kg) and two concentration of *A. phylicoides* (AP 20 and 200 mg/kg) for 4 weeks. The Non-alcoholic steatohepatitis (NASH) scoring system was used to analyze the degree of steatosis in liver sections. (A) reports the quantified combined scores from the central vein and portal vein area, (B) is a representation of the steatosis scores where: (1) lean control group represents a score of 0 for microvesicular, mediovesicular and macrovesicular changes; (2) metformin group represents a score of 1 for microvesicular changes, 1 for mediovesicular and macrovesicular changes, (3) vildagliptin represents a score of 2 for microvesicular, 2 for mediovesicular and 0 for macrovesicular changes and (4) obese control group represents 0 for microvesicular, 1 for mediovesicular and 2 for macrovesicular changes. Histomicrographs were captured at 100 X magnification. The scale bars represent 100 µm. Statistical analysis was conducted using one-way ANOVA (Dunnett's test) where $p<0.05$ was designated as statistically significant. Results are the mean ± Standard deviation. Abbreviations: AP - *Athrixia phylicoides*; ANOVA - analysis of variance; micro - microvesicular; medio - mediovesicular; macro - macrovesicular.

Chapter 4

4. Discussion

4.1. *In vitro* effect of *A. phylicoides*

4.1.1. Effect of *A. phylicoides* on cell viability

Insulin resistance is a risk factor for type 2 diabetes and it has been largely driven by over-nutrition (Gupta *et al*., 2012). The sites of insulin manifestation include the muscle, liver and adipose tissue. Therefore, murine skeletal muscle cells (C2C12), human liver cells (C3A) and rat adipocytes (3T3-L1) were chosen as models of insulin resistance. *Athrixia phylicoides* has been used as a refreshment drink for decades and its anti-oxidant properties have been established due to its high content of phenolic and polyphenolic compounds (McGaw *et al*., 2007). Chellan *et al* (2012) further demonstrated their potential as an anti-diabetic treatment. The three cell lines resembling the target tissues of insulin resistance were used to test for the cytotoxicity of the aqueous extract of *A. phylicoides*. The extract showed no evident effect on cell viability even at the highest concentration (2 mg/ml) in C2C12 (Figure 3.1) and C3A cell lines (Figure 3.6). A decrease in cell viability was only observed in the 3T3-L1 cells. These changes could be due to prolonged exposure of the 3T3-L1 cells to the extract (Figure 3.8). Treating 3T3-L1 cell with the working concentrations (10 and 100 µg/ml) for 24 hrs in the presence of palmitic acid showed no effect on cell viability.

4.1.2. Effect of palmitic acid on glucose uptake in skeletal muscle, liver and fat cells

Many studies have demonstrated the effect of excess free fatty acid in the development of insulin resistance and its progression to T2D (Chen *et al*., 2016; Joshi-Barve *et al*., 2007; Kennedy *et al*., 2009; Konstantynowicz-Nowicka *et al*., 2015; Kwak *et al*., 2016; Sawada *et al*., 2012). Long chain fatty acids such as palmitic acid have been used to induce insulin resistance at a concentration of 750 µM *in vitro* (Davis *et al*., 2009; Han *et al*., 2011; Hirabara *et al*., 2010; Joshi-Barve *et al*., 2007; Konstantynowicz-Nowicka *et al*., 2015; Kwak *et al*., 2016; Mazibuko *et al*., 2013).

In order to induce insulin resistance, cells (C2C12, C3A and 3T3-L1) were incubated in the presence of palmitic acid for 16 hrs. In C2C12 cells, insulin resistance was achieved (Figure 3.2). This was demonstrated by a decrease in glucose uptake in palmitate treated cells.

Human liver cells (C3A) remained sensitive towards insulin even after treatment with palmitic acid. Insulin increased glucose uptake, regardless of the presence of palmitic

acid, indicating that insulin resistance was not achieved (Figure 3.7). Concentrations of palmitic acids as low as 0.2 and 0.4 mM have been shown to induce insulin resistance in hepatocytes after prolonged exposure (24 hrs) (Zhao *et al*., 2015). Therefore, incubating C3A cells in palmitic acid for longer could have produced insulin resistance. In future, different concentrations and durations for palmitic acid treatment need to be established.

Adipocytes (3T3-L1) were also responsive towards insulin stimulation even after prolonged exposure to palmitic acid (Figure 3.10 A). This was demonstrated by the overall increase in insulin stimulated glucose uptake. The concentration of palmitic acid used also proved to be insufficient to induce insulin resistance in this cell line. Adipocytes treated with a combination of long chain saturated fatty acids have been shown to present hypertrophy and impaired insulin stimulated glucose uptake (Kim *et al*., 2015; Nguyen *et al*., 2005). Therefore, using a cocktail of long-chain saturated fatty acids could successfully induce insulin resistance.

4.1.3. Effect of *A. phylicoides* and metformin on glucose uptake

In a previous study, the aqueous extract of *A. phylicoides* demonstrated enhanced basal glucose uptake and utilization in C2C12 and Chang cells following a 3 hrs of exposure (Chellan *et al*., 2012). In this study, the extract did not increase basal glucose uptake in both chosen concentrations (Figure 3.2). However, *A. phylicoides* improved insulin stimulated glucose uptake in insulin-resistant cells. This means that the extract improved glucose uptake by restoring insulin sensitivity at the 100 µg/ml treatment. This property could be attributed to bioactive phenolic compounds such as chlorogenic acid, present in *A phylicoides*, which have been identified as insulin sensitizers capable of reducing insulin resistance in a similar manner as the anti-diabetic drug metformin (Dai *et al*., 2013; Deng *et al*., 2012; Meng *et al*., 2013). Metformin increases glucose uptake through the upregulation of AMPK (Hawley *et al*., 2002; Musi and Goodyear, 2003; Ong *et al*., 2012). In this study, metformin also restored insulin sensitivity although it did not increase basal, i.e. non-insulin stimulated, glucose uptake (Figure 3.2). The concentration used in this study could have been insufficient, however, 1 µM treatment is commonly used (Chellan *et al*., 2012; Mazibuko *et al*., 2013).

Both the extract and metformin showed no effect on glucose uptake in the C3A cell line (Figure 3.7). In the 3T3-L1 cells, further studies are necessary to optimize experimental conditions.

4.1.4. Effect of insulin, palmitic acid and *A. phylicoides* on lipid accumulation

The adipose tissue accounts for about 10 % of insulin-mediated glucose uptake in the body (Wilcox, 2005). On the other hand, it plays an important role in fatty acid uptake (Wilcox, 2005). Adipose tissue dysfunction is largely associated with insulin resistance, which is mostly due to an over-supply of fatty acids (Holland *et al*., 2007; Phillips *et al*., 1996; Roden *et al*., 1996). Therefore, it was of interest to investigate the effect of *A. phylicoides* on lipid accumulation in 3T3-L1 adipocytes. No effect on lipid accumulation was shown by the lowest concentration (10 µg/ml) of the extract or by metformin. However, in the control and the extract treated cells at 100 µg/ml, lipid accumulation decreased due to palmitic acid treatment (Figure 3.10B). Lipid over-load in adipocytes is expected to increase intracellular lipid accumulation (Karpe *et al*., 2011; Kim *et al*., 2015). Metformin has been shown to inhibit intracellular fat accumulation in 3T3-L1 cells and also inhibited visceral fat accumulation in mice fed a high fat diet (Alexandre *et al*., 2008; Kim *et al*., 2010). In our experiments, it could be speculated that the rate of oxidation was equal to the rate at which the fatty acids entered the cells (Lee and Kim, 2010; Ruderman *et al*., 2003; Shirwany and Zou, 2014). However, further investigations need to be conducted in order to confirm these findings.

4.1.5. The effect of *A. phylicoides* on protein expression and phosphorylation of proteins associated with glucose metabolism

Since there were no significant differences in glucose uptake observed in 3T3-L1 adipocytes and C3A liver cells, the skeletal muscle cell line was used to further investigate the expression and phosphorylation of glucose metabolism associated proteins (AMPK, AKT and GLUT 4) using the highest concentration of the extract. The extract increased the phosphorylation to total AMPK ratio regardless of palmitic acid and insulin treatment (Figure 3.3B). The protein AMPK acts as an insulin independent master cellular energy regulator in a biological system. Once AMPK is activated, it facilitates signaling pathways that restores cellular ATP while inhibiting anabolic reactions (Chopra *et al*., 2012; Musi and Goodyear, 2003). The protein is highly

expressed during cellular stress and it can also be activated by pharmacological agents such as metformin, phenformin, and the AMP mimetic 5-aminoimidazole-4-carboxamide-1-β-d-ribofuranoside (AICAR) (Woollhead *et al*., 2007). Apart from these agents, natural products such as polyphenols and phenolic acids have been implicated in the upregulation and activation of AMPK (Bahadoran *et al*., 2013; Edirisinghe and Burton-Freeman, 2016; Zang *et al*., 2006). Phenolic compounds such as chlorogenic acid are known as insulin sensitizers that stimulate glucose metabolism through the activation of AMPK in skeletal muscle palmitate-induced insulin resistance (Ong *et al*., 2012, 2013). Para-coumaric acid, another phenolic acid found in *A. phylicoides*, has also been shown to improve glucose uptake together with lipid metabolism through the activation of AMPK in L6 skeletal muscle cells (Yoon *et al*., 2013). Therefore, it is likely that the observed upregulation of AMPK phosphorylation is due to the presence of these compounds in the extract of *A. phylicoides*.

The effect of *A. phylicoides* was investigated on the phosphorylation of AKT in order to assess the mechanism in which the extract induce glucose uptake. Insulin increased the phosphorylation to total AKT ratio regardless of the presence of palmitic acid or the extract. Increasing evidence suggests that chronic elevation of fatty acids, particularly palmitic acid, induces the accumulation of intramyocellular triglycerides and the generation of lipid intermediates such as diacylglycerol (DAG) and ceramides, which have been identified as the key players in the development of insulin resistance (Chavez and Summers, 2003; Chavez *et al*., 2003; Holland *et al*., 2007; Kraegen *et al*., 2001; Olson *et al*., 2012; Powell *et al*., 2004; Stannard and Johnson, 2004). As a model, chronic exposure of C2C12 cells to palmitic acid increases the generation of ceramide and DAG, thereby decreasing insulin signaling by inhibiting the phosphorylation of AKT and subsequent translocation of GLUT 4 to the plasma membrane (Powell *et al*., 2004; Schmitz-Peiffer *et al*., 1999; Teruel *et al*., 2001; Mahfouz *et al*., 2014). The results indicate that phosphorylation of AKT was not affected by the extract or palmitic acid in this study (Figure 3.4), possibly due to high variability of the data.

Since an increase in insulin stimulates glucose uptake, which was observed with the highest concentration of the extract, the expression of GLUT 4 was investigated. Results showed no changes in the expression of GLUT 4 (Figure 3.5). The translocation of GLUT 4 to the membrane is not only regulated by AKT but also through

the activation of AMPK, that could account for the observed increased glucose uptake (Huang and Czech, 2007; Ikemoto *et al*., 1995; Wood and Trayhurn, 2003). Quantifying membrane GLUT 4 should be used in future. Taking these observations into consideration, it seems likely the extract of *A. phylicoides* improved glucose transport in insulin-resistant C2C12 cells mainly through AMPK dependent pathways.

4.2. Inhibitory effect *of A. phylicoides* on PTP1B enzyme

In enzyme kinetics, it is assumed that a compound with a potent inhibitory effect has an IC_{50} that is ≤ 10 µM or ≤ 20 µg/ml (Dierks *et al*., 2001; Kong *et al*., 2011; Zou *et al*., 2002). In this study, the extract was able to inhibit the activity of PTP1B at a concentration < 20 µg/ml (Figure 3.11), suggesting that *A. phylicoides* may be potent inhibitor of this anti-diabetic drug target enzyme (PTP1B). The concentration in which the extract inhibited the activity of the enzyme was not tested in cells, therefore, further studies to validate this inhibitory effect of PTP1B in the target tissues of insulin resistance are required.

4.3. *In Vivo* effect of the aqueous extract of *A. phylicoides*

4.3.1. Effect of *A. phylicoides* on body weight gain, food and water intake

The effect of *A. phylicoides* on the development of diabetes was investigated using diabetic *db/db* mice, where metformin, vildagliptin and SB1 were used as controls. *Db/db* mice are a spontaneous diabetic model, which contain a mutation on chromosome 4 of the leptin receptor (Belke and Severson, 2012; King, 2012; Wang *et al*., 2014). The model represents a phenotype similar to that observed in patients who are type 2 diabetic (Ernst *et al*., 2013). At about 6 week of age, *db/db* mice present with a significant increase in body weight in comparison to the lean mice (Kanasaki and Koya, 2011; Kobayashi *et al*., 2000; Koranyi *et al*., 1990).

Leptin controls energy balance by regulating satiety and increasing energy expenditure (Patton and DeGolier, 2010). Therefore a deficiency in leptin or the leptin signaling leads to increased energy intake and a decrease in energy expenditure, such is common in *db/db* mice (Friedman and Halaas, 1998; Patton and DeGolier, 2010). The extract of *A. phylicoides* was unable to suppress body weight gain (Figure 3.12C), however, it did not stimulate appetite as reflected by the food intake. Food consumption of the untreated obese control group was comparable to the *A.*

phylicoides treated group (Figure 3.12B). The results obtained from this study are in agreement with previous findings, where *A. phylicoides* treated Wistar rats showed no effect on body weight and food intake after 3 months of treatment (Chellan *et al*., 2008). Vildagliptin is known as a weight neutral drug (Foley and Jordan, 2010), hence no changes in body weight gain were observed after mice were treated with vildagliptin (Figure 2.12C). There were also no changes observed in body weight gain or food intake observed in the other treatment groups (metformin, vildagliptin and SB1). In a study conducted by Patton and DeGolier (2010), *db/db* mice showed a significant increase in water consumption. A similar observation was also made in the current study (Figure 3.12A). This clearly demonstrated the diabetic state of the model.

4.3.2. Effect of *A. phylicoides* on glycemic control in *db/db* mice

Diabetic *db/db* mice present hyperglycemia at 4-8 weeks of age (King, 2012). The glucose lowering effect of metformin and vildagliptin are well established (Cho *et al*., 2015; Kikuchi *et al*., 2009; Kristensen *et al*., 2014; Mathieu and Degrande, 2008; Viollet *et al*., 2012; Wiernsperger and Bailey, 1999). The results obtained from this study do not correspond to previous findings, which could be due to high variability observed in the data (Figure 3.13). A food trial was conducted at the beginning of the study and actual treatment was only started on week 7. At week 8, *db/db* mice are considered as severely diabetic (King, 2012), therefore, starting treatment earlier could have produced different results.

4.3.3. Effect of *A. phylicoides* on insulin concentration and sensitivity in *db/db* mice

Hyperinsulinemia is a common condition observed in type 2 diabetes where there is an increase in the levels of circulating insulin relative to the levels of glucose in the blood (Kanasaki and Koya, 2011). In the diabetic *db/db* mouse model, hyperinsulinemia can be observed as early as 2 weeks after birth (Kanasaki and Koya, 2011; King, 2012). In the current study, no statistically significant changes in insulin concentrations were observed in all treatment groups after 4 weeks. However, a marked decrease was observed in the vildagliptin, metformin and SB1 group (Figure 3.16A). These findings are in correlation with the HOMA-IR index calculated after the end of this study using serum insulin concentrations (Figure 3.16B). The extract of *A. phylicoides* did not improve insulin resistance over the four weeks.

4.3.4. Effect of *A. phylicoides* on serum lipid profile and hepatic steatosis

Diabetes dyslipidemia is characterized by elevated levels of triglycerides, low high density lipoproteins-cholesterol (HDL-cholesterol) levels and low density lipoprotein (LDL) particles. The use of metformin has been shown to increase HDL concentration and also reduce plasma triglyceride concentrations. In this study, *db/db* mice were treated for 4 weeks and the lipid profile was assessed in blood plasma after termination. Results obtained demonstrated no effect on serum cholesterol levels (Figure 3.17A). However, an increase in serum HDL-cholesterol concentration in the metformin treated group was observed (Figure 3.17B). The results are in agreement with previous human studies where metformin was shown to increase HDL-cholesterol levels (Ghatak *et al*., 2011; Zhang *et al*., 2015a). Even though metformin was able to increase the level of HDL-cholesterol, it had no effect on triglyceride concentrations (Figure 3.17C).

Studies have associated DPP-4 inhibitors with decreased levels of triglycerides, cholesterol and HDL-cholesterol (Horton *et al*., 2010; Pavithra and Chaitanya, 2015). In the current study vildagliptin showed no cholesterol and HDL-cholesterol lowering effects (Figure 3.17A; Figure 3.17B). However, a marked decrease in triglyceride concentration was observed after mice were treated with the lowest concentration of the extract (Figure 3.17C). Due to the marked effect observed in serum triglyceride concentrations, it was of interest to investigate the effect of *A. phylicoides* on hepatic steatosis using liver sections harvested from *db/db* mice. Histological evaluation of the Haematoxylin and eosin stained liver section showed that *A. phylicoides* markedly reduced the occurrence of macrovesicular and mediovesicular changes at the highest dose, suggesting that the severity of steatosis may have been ameliorated (Figure 3.18). The observed marked beneficial effect of *A. phylicoides* on hypertriglyceridemia and steatosis warrants further investigations, such as a quantification of liver triglycerides. Should the latter provide significant results, the effects of the extract on lipogenesis regulators, such as sterol regulatory binding protein 1c (SREBP-1c), carbohydrate-responsive element-binding protein (ChREBP), fatty acid synthase (FASN), and CCAAT-enhancer-binding protein beta (C/EBPβ) in the livers of these *db/db* mice should be investigated.

Chapter 5

5. Conclusion

5.1. Conclusion

In this study, we have investigated the effect of *A. phylicoides* on differentiated insulin-resistant cells that represent the skeletal muscle, liver and adipose tissue. We have demonstrated that *A. phylicoides* improves insulin sensitivity in skeletal muscle cells and through an AMPK dependent pathway. However, similar effects were not observed in the other cell lines (C3A, 3T3-L1). The potential of *A. phylicoides* as a potent inhibitor of the enzyme PTP1B was also demonstrated. Although the extract did not improve insulin sensitivity or decrease fasting plasma glucose concentration in *db/db* mice *in vivo*, *A. phylicoides* may have beneficial effects on liver steatosis and modulate hypertriglyceridemia.

5.2. Future work

Based on the knowledge obtained from this study, future experiments should investigate the expression of the PTP1B enzyme in cell lysates as well as the effects of the extract on lipogenesis regulators in the livers of *db/db* mice. Future experiments should be conducted in order to establish the anti-diabetic effects of the major phenolic and polyphenolic compounds identified (6-hydroxyluteolin-7-O-β-glucoside, chlorogenic acid and protocatechuic acid) from the extract and to also identify the main active constituents.

6. Bibliography

Abdul-Ghani, M.A., and DeFronzo, R.A. (2010). Pathogenesis of insulin resistance in skeletal muscle. BioMed Res. Int. *2010*. 476279

ADA (American Diabetes Association). (2010). Diagnosis and Classification of Diabetes Mellitus. Diabetes Care *33*, S62–S69.

Adeva-Andany, M.M., González-Lucán, M., Donapetry-García, C., Fernández-Fernández, C., and Ameneiros-Rodríguez, E. (2016). Glycogen metabolism in humans. BBA Clin. *5*, 85–100.

Adlercreutz, H., and Mazur, W. (1997). Phyto-oestrogens and Western diseases. Ann. Med. *29*, 95–120.

Aguirre, V., Werner, E.D., Giraud, J., Lee, Y.H., Shoelson, S.E., and White, M.F. (2002). Phosphorylation of Ser307 in Insulin Receptor Substrate-1 Blocks Interactions with the Insulin Receptor and Inhibits Insulin Action. J. Biol. Chem. *277*, 1531–1537.

Aherne, S.A., and O'Brien, N.M. (2002). Dietary flavonols: chemistry, food content, and metabolism. Nutrition *18*, 75–81.

Ahmadipour, F., Vakili, T., Absalan, A., Mohiti-Ardakani, J., Hadinedoushan, H., Khalili, M., and Pourrajab, F. (2012). C2C12 Cell Line is a Good Model to Explore the Effects of Herbal Extracts on GLUT4 Expression and Translocation. Iran. J. Diabetes Obes. *4*, 143–151.

Alexandre, K.B., Smit, A.M., Gray, I.P., and Crowther, N.J. (2008). Metformin inhibits intracellular lipid accumulation in the murine pre-adipocyte cell line, 3T3-L1. ResearchGate *10*, 688–690.

Arias, N., Macarulla, M.T., Aguirre, L., Martinez-Castano, M.G., and Portillo, M.P. (2014). Quercetin can reduce insulin resistance without decreasing adipose tissue and skeletal muscle fat accumulation. Genes Nutr. *9*, 361.

Arsenijevic, T., Grégoire, F., Delforge, V., Delporte, C., and Perret, J. (2012). Murine 3T3-L1 Adipocyte Cell Differentiation Model: Validated Reference Genes for qPCR Gene Expression Analysis. PLOS ONE *7*, e37517.

Babu, P.V.A., Liu, D., and Gilbert, E.R. (2013). Recent advances in understanding the anti-diabetic actions of dietary flavonoids. J. Nutr. Biochem. *24*, 1777–1789.

Bahadoran, Z., Mirmiran, P., and Azizi, F. (2013). Dietary polyphenols as potential nutraceuticals in management of diabetes: a review. J. Diabetes Metab. Disord. *12*, 43.

Bailey, K.L., Goraya, J., and Rennard S.L. (2011). The Role of Systemic Infl ammation in COPD, Nici, L., and ZuWallack, R (Eds), *Chronic Obstructive*

Pulmonary Disease: Co-Morbidities and Systemic Consequences (pp 15-30). Humana Press, New York.

Beckman, C.H. (2000). Phenolic-storing cells: keys to programmed cell death and periderm formation in wilt disease resistance and in general defence responses in plants? Physiol. Mol. Plant Pathol. *57*, 101–110.

Belke, D.D., and Severson, D.L. (2012). Diabetes in mice with monogenic obesity: the *db/db* mouse and its use in the study of cardiac consequences. Methods Mol. Biol. Clifton NJ *933*, 47–57.

Bhattacharya, S., Dey, D., and Roy, S.S. (2007). Molecular mechanism of insulin resistance. J. Biosci. *32*, 405–413.

Bikman, B.T., and Summers, S.A. (2011). Ceramides as modulators of cellular and whole-body metabolism. J. Clin. Invest. *121*, 4222–4230.

Blüher, M. (2013). Importance of estrogen receptors in adipose tissue function. Mol. Metab. *2*, 130–132.

Boden, G. (2009). Endoplasmic Reticulum Stress: Another Link Between Obesity and Insulin Resistance/Inflammation? Diabetes *58*, 518–519.

Bogdanov, P., Corraliza, L., Villena, J.A., Carvalho, A.R., Garcia-Arumí, J., Ramos, D., Ruberte, J., Simó, R., and Hernández, C. (2014). The db/db Mouse: A Useful Model for the Study of Diabetic Retinal Neurodegeneration. PLOS ONE *9*, e97302.

Bollheimer, L.C., Skelly, R.H., Chester, M.W., McGarry, J.D., and Rhodes, C.J. (1998). Chronic exposure to free fatty acid reduces pancreatic beta cell insulin content by increasing basal insulin secretion that is not compensated for by a corresponding increase in proinsulin biosynthesis translation. J. Clin. Invest. *101*, 1094–1101.

Boura-Halfon, S., and Zick, Y. (2009). Phosphorylation of IRS proteins, insulin action, and insulin resistance. Am. J. Physiol. - Endocrinol. Metab. *296*, E581–E591.

Bradford, M.M. (1976). A rapid and sensitive method for the quantitation of microgram quantities of protein utilizing the principle of protein-dye binding. Anal. Biochem. *72*, 248–254.

Bravo, R., Parra, V., Gatica, D., Rodriguez, A.E., Torrealba, N., Paredes, F., Wang, Z.V., Zorzano, A., Hill, J.A., Jaimovich, E., et al. (2013). Endoplasmic Reticulum and the Unfolded Protein Response: Dynamics and Metabolic Integration. Int. Rev. Cell Mol. Biol. *301*, 215–290.

Bugianesi, E., McCullough, A.J., and Marchesini, G. (2005). Insulin resistance: A metabolic pathway to chronic liver disease. Hepatology *42*, 987–1000.

Bulló-Bonet, M., García-Lorda, P., López-Soriano, F. j., Argilés, J. m., and Salas-Salvadó, J. (1999). Tumour necrosis factor, a key role in obesity? FEBS Lett. *451*, 215–219.

Bunner, A.E., Chandrasekera, P.C., and Barnard, N.D. (2014). Knockout mouse models of insulin signaling: Relevance past and future. World J. Diabetes *5*, 146–159.

Campos, M. da G.R., and Matos, M.P. (2010). Bioactivity of Isoflavones: Assessment through a Theoretical Model as a Way to Obtain a “Theoretical Efficacy Related to Estradiol (TERE).” Int. J. Mol. Sci. *11*, 480–491.

Cerf, M.E. (2013). Beta Cell Dysfunction and Insulin Resistance. Front. Endocrinol. *4*, 37.

Chang, L., Chiang, S.-H., and Saltiel, A.R. (2004). Insulin signaling and the regulation of glucose transport. Mol. Med. Camb. Mass *10*, 65–71.

Chavez, J.A., and Summers, S.A. (2003). Characterizing the effects of saturated fatty acids on insulin signaling and ceramide and diacylglycerol accumulation in 3T3-L1 adipocytes and C2C12 myotubes. Arch. Biochem. Biophys. *419*, 101–109.

Chavez, J.A., and Summers, S.A. (2012). A Ceramide-Centric View of Insulin Resistance. Cell Metab. *15*, 585–594.

Cheatham, B., and Kahn, C.R. (1995). Insulin Action and the Insulin Signaling Network*. Endocr. Rev. *16*, 117–142.

Chellan, N., De Beer, D., Muller, C., Joubert, E., and Louw, J. (2008). A toxicological assessment of *Athrixia phylicoides* aqueous extract following sub-chronic ingestion in a rat model. Hum. Exp. Toxicol. *27*, 819–825.

Chellan, N., Muller, C.J.F., de Beer, D., Joubert, E., Page, B.J., and Louw, J. (2012). An *in vitro* assessment of the effect of *Athrixia phylicoides* DC. aqueous extract on glucose metabolism. Phytomedicine *19*, 730–736.

Chen, X., Xu, S., Wei, S., Deng, Y., Li, Y., Yang, F., and Liu, P. (2016). Comparative Proteomic Study of Fatty Acid-treated Myoblasts Reveals Role of Cox-2 in Palmitate-induced Insulin Resistance. Sci. Rep. *6*, 21454.

Cho, K., Chung, J.Y., Cho, S.K., Shin, H.-W., Jang, I.-J., Park, J.-W., Yu, K.-S., and Cho, J.-Y. (2015). Antihyperglycemic mechanism of metformin occurs via the AMPK/LXRα/POMC pathway. Sci. Rep. *5*, 8145.

Chopra, I., Li, H.F., Wang, H., and Webster, K.A. (2012). Phosphorylation of the insulin receptor by AMP-activated protein kinase (AMPK) promotes ligand-independent activation of the insulin signalling pathway in rodent muscle. Diabetologia *55*, 783–794.

Cohen, P. (1999). The Croonian Lecture 1998. Identification of a protein kinase cascade of major importance in insulin signal transduction. Philos. Trans. R. Soc. B Biol. Sci. *354*, 485–495.

Cohen, M., Kitsberg, D., Tsytkin, S., Shulman, M., Aroeti, B., and Nahmias, Y. (2014). Live imaging of GLUT2 glucose-dependent trafficking and its inhibition in polarized epithelial cysts. Open Biol. *4*, 140091.

Coll, T., Palomer, X., Blanco-Vaca, F., Escolà-Gil, J.C., Sánchez, R.M., Laguna, J.C., and Vázquez-Carrera, M. (2010). Cyclooxygenase 2 Inhibition Exacerbates Palmitate-Induced Inflammation and Insulin Resistance in Skeletal Muscle Cells. Endocrinology *151*, 537–548.

Consitt, L.A., Bell, J.A., and Houmard, J.A. (2009). Intramuscular Lipid Metabolism, Insulin Action and Obesity. IUBMB Life *61*, 47–55.

Cooper, R., Morré, D.J., and Morré, D.M. (2005). Medicinal benefits of green tea: Part I. Review of noncancer health benefits. J. Altern. Complement. Med. *11*, 521–528.

Cross, D.A.E., Alessi, D.R., Cohen, P., Andjelkovich, M., and Hemmings, B.A. (1995). Inhibition of glycogen synthase kinase-3 by insulin mediated by protein kinase B. Nature *378*, 785–789.

Cross, D.A.E., Watt, P.W., Shaw, M., van der Kaay, J., Downes, C.P., Holder, J.C., and Cohen, P. (1997). Insulin activates protein kinase B, inhibits glycogen synthase kinase-3 and activates glycogen synthase by rapamycin-insensitive pathways in skeletal muscle and adipose tissue. FEBS Lett. *406*, 211–215.

Dai, X., Ding, Y., Zhang, Z., Cai, X., Bao, L., and Li, Y. (2013). Quercetin but not quercitrin ameliorates tumor necrosis factor-alpha-induced insulin resistance in C2C12 skeletal muscle cells. Biol. Pharm. Bull. *36*, 788–795.

Dandona, P., Aljada, A., and Bandyopadhyay, A. (2004). Inflammation: the link between insulin resistance, obesity and diabetes. Update *25*, 4.

D'Archivio, M., Filesi, C., Varì, R., Scazzocchio, B., and Masella, R. (2010). Bioavailability of the Polyphenols: Status and Controversies. Int. J. Mol. Sci. *11*, 1321–1342.

Dasuri, K., Ebenezer, P., Fernandez-Kim, S.O., Zhang, L., Gao, Z., Bruce-Keller, A.J., Freeman, L.R., and Keller, J.N. (2013). Role of Physiological Levels of 4-Hydroxynonenal on Adipocyte Biology: Implications for Obesity and Metabolic Syndrome. Free Radic. Res. *47*, 8–19.

Davis, J.E., Gabler, N.K., Walker-Daniels, J., and Spurlock, M.E. (2009). The c-Jun N-terminal kinase mediates the induction of oxidative stress and insulin resistance by palmitate and toll-like receptor 2 and 4 ligands in 3T3-L1 adipocytes. Horm. Metab. Res. *41*, 523–530.

De Beer, D., Joubert, E., Malherbe, C.J., and Brand, D.J. (2011). Use of countercurrent chromatography during isolation of 6-hydroxyluteolin-7-O-β-glucoside, a major antioxidant of *Athrixia phylicoides*. J. Chromatogr. A *1218*, 6179–6186.

DeFronzo, R.A., and Ferrannini, E. (1991). Insulin resistance. A multifaceted syndrome responsible for NIDDM, obesity, hypertension, dyslipidemia, and atherosclerotic cardiovascular disease. Diabetes Care *14*, 173–194.

Demozay, D., Mas, J.-C., Rocchi, S., and Van Obberghen, E. (2008). FALDH reverses the deleterious action of oxidative stress induced by lipid peroxidation product 4-hydroxynonenal on insulin signaling in 3T3-L1 adipocytes. Diabetes *57*, 1216–1226.

Deng, Y.-T., Chang, T.-W., Lee, M.-S., and Lin, J.-K. (2012). Suppression of Free Fatty Acid-Induced Insulin Resistance by Phytopolyphenols in C2C12 Mouse Skeletal Muscle Cells. J. Agric. Food Chem. *60*, 1059–1066.

Dierks, E.A., Stams, K.R., Lim, H.-K., Cornelius, G., Zhang, H., and Ball, S.E. (2001). A Method for the Simultaneous Evaluation of the Activities of Seven Major Human Drug-Metabolizing Cytochrome P450s Using an *in Vitro* Cocktail of Probe Substrates and Fast Gradient Liquid Chromatography Tandem Mass Spectrometry. Drug Metab. Dispos. *29*, 23–29.

Dimitriadis, G., Mitrou, P., Lambadiari, V., Maratou, E., and Raptis, S.A. (2011). Insulin effects in muscle and adipose tissue. Diabetes Res. Clin. Pract. *93 Suppl 1*, S52-59.

Donath, M.Y., Ehses, J.A., Maedler, K., Schumann, D.M., Ellingsgaard, H., Eppler, E., and Reinecke, M. (2005). Mechanisms of β-Cell Death in Type 2 Diabetes. Diabetes *54*, S108–S113.

Dong, Y., Gao, G., Fan, H., Li, S., Li, X., and Liu, W. (2015). Activation of the Liver X Receptor by Agonist TO901317 Improves Hepatic Insulin Resistance via Suppressing Reactive Oxygen Species and JNK Pathway. PLOS ONE *10*, e0124778.

Drel, V.R., Mashtalir, N., Ilnytska, O., Shin, J., Li, F., Lyzogubov, V.V., and Obrosova, I.G. (2006). The leptin-deficient (*ob/ob)* mouse: a new animal model of peripheral neuropathy of type 2 diabetes and obesity. Diabetes *55*, 3335–3343.

Drury, D.R. (1940). The Rôle of Insulin in Carbohydrate Metabolism. Am. J. Physiol. -- Leg. Content *131*, 536–543.

Duncan, R.E., Ahmadian, M., Jaworski, K., Sarkadi-Nagy, E., and Sul, H.S. (2007). Regulation of Lipolysis in Adipocytes. Annu. Rev. Nutr. *27*, 79–101.

Edirisinghe, I., and Burton-Freeman, B. (2016). Anti-diabetic actions of Berry polyphenols – Review on proposed mechanisms of action. J. Berry Res. *6*, 237–250.

Eid, H.M., Martineau, L.C., Saleem, A., Muhammad, A., Vallerand, D., Benhaddou-Andaloussi, A., Nistor, L., Afshar, A., Arnason, J.T., and Haddad, P.S. (2010). Stimulation of AMP-activated protein kinase and enhancement of basal glucose uptake in muscle cells by quercetin and quercetin glycosides, active principles of the antidiabetic medicinal plant Vaccinium vitis-idaea. Mol. Nutr. Food Res. *54*, 991–1003.

Eid, H.M., Nachar, A., Thong, F., Sweeney, G., and Haddad, P.S. (2015). The molecular basis of the antidiabetic action of quercetin in cultured skeletal muscle cells and hepatocytes. Pharmacogn. Mag. *11*, 74–81.

Ernst, A., Sharma, A.N., Elased, K.M., Guest, P.C., Rahmoune, H., and Bahn, S. (2013). Diabetic *db/db* mice exhibit central nervous system and peripheral molecular alterations as seen in neurological disorders. Transl. Psychiatry *3*, e263.

Esposito, K., and Giugliano, D. (2004). The metabolic syndrome and inflammation: association or causation? Nutr. Metab. Cardiovasc. Dis. NMCD *14*, 228–232.

Esser, N., Legrand-Poels, S., Piette, J., Scheen, A.J., and Paquot, N. (2014). Inflammation as a link between obesity, metabolic syndrome and type 2 diabetes. Diabetes Res. Clin. Pract. *105*, 141–150.

Farah, A., Monteiro, M., Donangelo, C.M., and Lafay, S. (2008). Chlorogenic Acids from Green Coffee Extract are Highly Bioavailable in Humans. J. Nutr. *138*, 2309–2315.

de Ferranti, S., and Mozaffarian, D. (2008). The Perfect Storm: Obesity, Adipocyte Dysfunction, and Metabolic Consequences. Clin. Chem. *54*, 945–955.

Fladeby, C., Skar, R., and Serck-Hanssen, G. (2003). Distinct regulation of glucose transport and GLUT1/GLUT3 transporters by glucose deprivation and IGF-I in chromaffin cells. Biochim. Biophys. Acta BBA - Mol. Cell Res. *1593*, 201–208.

Foley, J.E., and Jordan, J. (2010). Weight neutrality with the DPP-4 inhibitor, vildagliptin: Mechanistic basis and clinical experience. Vasc. Health Risk Manag. *6*, 541–548.

Fonseca, V.A. (2009). Defining and Characterizing the Progression of Type 2 Diabetes. Diabetes Care *32*, S151–S156.

Foster, D.W. (2012). Malonyl-CoA: the regulator of fatty acid synthesis and oxidation. J. Clin. Invest. *122*, 1958–1959.

Francés, D.E., Motiño, O., Agrá, N., González-Rodríguez, Á., Fernández-Álvarez, A., Cucarella, C., Mayoral, R., Castro-Sánchez, L., García-Casarrubios, E., Boscá, L., et al. (2015). Hepatic cyclooxygenase-2 expression protects against diet-induced steatosis, obesity, and insulin resistance. Diabetes *64*, 1522–1531.

Friedman, J.M., and Halaas, J.L. (1998). Leptin and the regulation of body weight in mammals. Nature *395*, 763–770.

Galbo, T., Perry, R.J., Nishimura, E., Samuel, V.T., Quistorff, B., and Shulman, G.I. (2013). PP2A inhibition results in hepatic insulin resistance despite Akt2 activation. Aging *5*, 770–781.

Garrett, R., & Grisham, C. M. (2008). Metabolism and its regulation. *Biochemistry 6th edition* (pp 583-957), Cengage Learning. *Boston*.

Ghatak, S.B., Dhamecha, P.S., Bhadada, S.V., and Panchal, S.J. (2011). Investigation of the potential effects of metformin on atherothrombotic risk factors in hyperlipidemic rats. Eur. J. Pharmacol. *659*, 213–223.

Greenberg, A.S., Kraemer, F.B., Soni, K.G., Jedrychowski, M.P., Yan, Q.-W., Graham, C.E., Bowman, T.A., and Mansur, A. (2011). Lipid droplet meets a mitochondrial protein to regulate adipocyte lipolysis. EMBO J. *30*, 4337–4339.

Gual, P., Le Marchand-Brustel, Y., and Tanti, J.-F. (2005). Positive and negative regulation of insulin signaling through IRS-1 phosphorylation. Biochimie *87*, 99–109.

Guilherme, A., Virbasius, J.V., Puri, V., and Czech, M.P. (2008). Adipocyte dysfunctions linking obesity to insulin resistance and type 2 diabetes. Nat. Rev. Mol. Cell Biol. *9*, 367–377.

Guillam, M.-T., Hümmler, E., Schaerer, E., Wu, J.-Y., Birnbaum, M.J., Beermann, F., Schmidt, A., Dériaz, N., and Thorens, B. (1997). Early diabetes and abnormal postnatal pancreatic islet development in mice lacking Glut-2. Nat. Genet. *17*, 327–330.

Gülçin, İ. (2006). Antioxidant activity of caffeic acid (3,4-dihydroxycinnamic acid). Toxicology *217*, 213–220.

Guo, S. (2014). Insulin signaling, resistance, and metabolic syndrome: insights from mouse models into disease mechanisms. J. Endocrinol. *220*, T1–T23.

Guo, X., Geng, M., and Du, G. (2005). Glucose transporter 1, distribution in the brain and in neural disorders: its relationship with transport of neuroactive drugs through the blood-brain barrier. Biochem. Genet. *43*, 175–187.

Gupta, D., Krueger, C.B., and Lastra, G. (2012). Over-nutrition, obesity and insulin resistance in the development of β-cell dysfunction. Curr. Diabetes Rev. *8*, 76–83.

Hage Hassan, R., Bourron, O., and Hajduch, E. (2014). Defect of insulin signal in peripheral tissues: Important role of ceramide. World J. Diabetes *5*, 244–257.

Haghani, K., Pashaei, S., Vakili, S., Taheripak, G., and Bakhtiyari, S. (2015). TNF-α knockdown alleviates palmitate-induced insulin resistance in C2C12 skeletal muscle cells. Biochem. Biophys. Res. Commun. *460*, 977–982.

Han, M.S., Lim, Y.-M., Quan, W., Kim, J.R., Chung, K.W., Kang, M., Kim, S., Park, S.Y., Han, J.-S., Park, S.-Y., et al. (2011). Lysophosphatidylcholine as an effector of fatty acid-induced insulin resistance. J. Lipid Res. *52*, 1234–1246.

Hardie, D.G., and Pan, D.A. (2002). Regulation of fatty acid synthesis and oxidation by the AMP-activated protein kinase. Biochem. Soc. Trans. *30*, 1064–1070.

Hardie, D.G., Ross, F.A., and Hawley, S.A. (2012). AMPK: a nutrient and energy sensor that maintains energy homeostasis. Nat. Rev. Mol. Cell Biol. *13*, 251.

Hasnain, S.Z., Lourie, R., Das, I., Chen, A.C.-H., and McGuckin, M.A. (2012). The interplay between endoplasmic reticulum stress and inflammation. Immunol. Cell Biol. *90*, 260–270.

Hawley, S.A., Gadalla, A.E., Olsen, G.S., and Hardie, D.G. (2002). The Antidiabetic Drug Metformin Activates the AMP-Activated Protein Kinase Cascade via an Adenine Nucleotide-Independent Mechanism. Diabetes *51*, 2420–2425.

Hawley, S.A., Ross, F.A., Gowans, G.J., Tibarewal, P., Leslie, N.R., and Hardie, D.G. (2014). Phosphorylation by Akt within the ST loop of AMPK-α1 down-regulates its activation in tumour cells. Biochem. J. *459*, 275–287.

Hirabara, S.M., Curi, R., and Maechler, P. (2010). Saturated Fatty Acid-Induced Insulin Resistance Is Associated With Mitochondrial Dysfunction in Skeletal Muscle Cells. J. Cell. Physiol. *222*, 187.

Hoene, M., and Weigert, C. (2008). The role of interleukin-6 in insulin resistance, body fat distribution and energy balance. Obes. Rev. *9*, 20–29.

Holland, W.L., Knotts, T.A., Chavez, J.A., Wang, L.-P., Hoehn, K.L., and Summers, S.A. (2007). Lipid Mediators of Insulin Resistance. Nutr. Rev. *65*, S39–46.

Honardoost, M., Arefian, E., Soleimani, M., Soudi, S., and Sarookhani, M.R. (2016). Development of Insulin Resistance through Induction of miRNA-135 in C2C12 Cells. Cell J. Yakhteh *18*, 353–361.

Hopkins, T.A., Dyck, J.R.B., and Lopaschuk, G.D. (2003). AMP-activated protein kinase regulation of fatty acid oxidation in the ischaemic heart. Biochem. Soc. Trans. *31*, 207–212.

Horton, E.S., Silberman, C., Davis, K.L., and Berria, R. (2010). Weight Loss, Glycemic Control, and Changes in Cardiovascular Biomarkers in Patients With Type 2 Diabetes Receiving Incretin Therapies or Insulin in a Large Cohort Database. ResearchGate *33*, 1759–1765.

Hotamisligil, G.S. (2010). Endoplasmic Reticulum Stress and the Inflammatory Basis of Metabolic Disease. Cell *140*, 900–917.

Hotamisligil, G.S., Arner, P., Caro, J.F., Atkinson, R.L., and Spiegelman, B.M. (1995). Increased adipose tissue expression of tumor necrosis factor-alpha in human obesity and insulin resistance. J. Clin. Invest. *95*, 2409–2415.

Hotamisligil, G.S., Peraldi, P., Budavari, A., Ellis, R., White, M.F., and Spiegelman, B.M. (1996). IRS-1-Mediated Inhibition of Insulin Receptor Tyrosine Kinase Activity in TNF-α- and Obesity-Induced Insulin Resistance. Science *271*, 665–670.

Huang, S., and Czech, M.P. (2007). The GLUT4 Glucose Transporter. Cell Metab. *5*, 237–252.

Huang, C., Thirone, A.C.P., Huang, X., and Klip, A. (2005). Differential contribution of insulin receptor substrates 1 versus 2 to insulin signaling and glucose uptake in l6 myotubes. J. Biol. Chem. *280*, 19426–19435.

Hundal, R.S., Krssak, M., Dufour, S., Laurent, D., Lebon, V., Chandramouli, V., Inzucchi, S.E., Schumann, W.C., Petersen, K.F., Landau, B.R., et al. (2000).

Mechanism by which metformin reduces glucose production in type 2 diabetes. Diabetes *49*, 2063–2069.

Hutchings, A., Scott, A.H., Lewis, G., and Cunningham, A. Zulu Medicinal Plants, An Inventory, 1996. ISBN 0 *86980*, 7.

IDF (International Federation of Diabetes). (2014). IDF DiabetesIABETES AtlasTLAS. *Sixth edition*.*edition*. http://www.diabetesatlas.org

Ikeda, H. (1994). KK mouse. Diabetes Res. Clin. Pract. *24 Suppl*, S313-316.

Ikemoto, S., Thompson, K.S., Itakura, H., Lane, M.D., and Ezaki, O. (1995). Expression of an Insulin-Responsive Glucose Transporter (GLUT4) Minigene in Transgenic Mice: Effect of Exercise and Role in Glucose Homeostasis. Proc. Natl. Acad. Sci. *92,* 865–869.

Inzucchi, S.E., Bergenstal, R.M., Buse, J.B., Diamant, M., Ferrannini, E., Nauck, M., Peters, A.L., Tsapas, A., Wender, R., and Matthews, D.R. (2012). Management of Hyperglycemia in Type 2 Diabetes: A Patient-Centered Approach. Diabetes Care *35*, 1364–1379.

Iwakami, S., Misu, H., Takeda, T., Sugimori, M., Matsugo, S., Kaneko, S., and Takamura, T. (2011). Concentration-dependent Dual Effects of Hydrogen Peroxide on Insulin Signal Transduction in H4IIEC Hepatocytes. PLoS ONE *6*, e27401.

Jagtap, S., Meganathan, K., Wagh, V., Winkler, J., Hescheler, J., and Sachinidis, A. (2009). Chemoprotective Mechanism of the Natural Compounds, Epigallocatechin-3-O-Gallate, Quercetin and Curcumin Against Cancer and Cardiovascular Diseases. Curr. Med. Chem. *16*, 1451–1462.

Jeon, S.-M. (2016). Regulation and function of AMPK in physiology and diseases. Exp. Mol. Med. *48*, e245.

Jiamsripong, P., Mookadam, M., Honda, T., Khandheria, B.K., and Mookadam, F. (2008). The Metabolic Syndrome and Cardiovascular Disease: Part I. Prev. Cardiol. *11*, 155–161.

Jiang, D., Li, D., and Wu, W. (2013). Inhibitory Effects and Mechanisms of Luteolin on Proliferation and Migration of Vascular Smooth Muscle Cells. Nutrients *5*, 1648–1659.

Jiao, P., Chen, Q., Shah, S., Du, J., Tao, B., Tzameli, I., Yan, W., and Xu, H. (2009). Obesity-Related Upregulation of Monocyte Chemotactic Factors in Adipocytes. Diabetes *58*, 104–115.

Jiao, P., Ma, J., Feng, B., Zhang, H., Alan-Diehl, J., Eugene-Chin, Y., Yan, W., and Xu, H. (2011). FFA-Induced Adipocyte Inflammation and Insulin Resistance: Involvement of ER Stress and IKKβ Pathways. Obesity *19*, 483–491.

Jornayvaz, F.R., and Shulman, G.I. (2012). Diacylglycerol Activation of Protein Kinase Cε and Hepatic Insulin Resistance. Cell Metab. *15*, 574–584.

Jornayvaz, F.R., Birkenfeld, A.L., Jurczak, M.J., Kanda, S., Guigni, B.A., Jiang, D.C., Zhang, D., Lee, H.-Y., Samuel, V.T., and Shulman, G.I. (2011). Hepatic insulin resistance in mice with hepatic overexpression of diacylglycerol acyltransferase 2. Proc. Natl. Acad. Sci. U. S. A. *108*, 5748–5752.

Joshi-Barve, S., Barve, S.S., Amancherla, K., Gobejishvili, L., Hill, D., Cave, M., Hote, P., and McClain, C.J. (2007). Palmitic acid induces production of proinflammatory cytokine interleukin-8 from hepatocytes. Hepatology *46*, 823–830.

Joubert, E., Gelderblom, W.C.A., Louw, A., and de Beer, D. (2008). South African herbal teas: *Aspalathus linearis*, *Cyclopia spp*. and *Athrixia phylicoides*—A review. J. Ethnopharmacol. *119*, 376–412.

Jové, M., Planavila, A., Sánchez, R.M., Merlos, M., Laguna, J.C., and Vázquez-Carrera, M. (2006). Palmitate induces tumor necrosis factor-alpha expression in C2C12 skeletal muscle cells by a mechanism involving protein kinase C and nuclear factor-kappaB activation. Endocrinology *147*, 552–561.

Kahn, B.B. (1992). Facilitative glucose transporters: regulatory mechanisms and dysregulation in diabetes. J. Clin. Invest. *89*, 1367–1374.

Kahn, S.E. (2003). The relative contributions of insulin resistance and beta-cell dysfunction to the pathophysiology of Type 2 diabetes. Diabetologia *46*, 3–19.

Kahn, B.B., Alquier, T., Carling, D., and Hardie, D.G. (2005). AMP-activated protein kinase: ancient energy gauge provides clues to modern understanding of metabolism. Cell Metab. *1*, 15–25.

Kahn, S.E., Larson, V.G., Beard, J.C., Cain, K.C., Fellingham, G.W., Schwartz, R.S., Veith, R.C., Stratton, J.R., Cerqueira, M.D., and Abrass, I.B. (1990). Effect of exercise on insulin action, glucose tolerance, and insulin secretion in aging. Am. J. Physiol.-Endocrinol. Metab. *258*, E937–E943.

Kahn, S.E., Hull, R.L., and Utzschneider, K.M. (2006). Mechanisms linking obesity to insulin resistance and type 2 diabetes. Diabetes Metab Syndr Obes, *7*, 587-591

Kanasaki, K., and Koya, D. (2011). Biology of Obesity: Lessons from Animal Models of Obesity. BioMed Res. Int. *2011*, e197636.

Kaneto, H., Nakatani, Y., Kawamori, D., Miyatsuka, T., Matsuoka, T., Matsuhisa, M., and Yamasaki, Y. (2006). Role of oxidative stress, endoplasmic reticulum stress, and c-Jun N-terminal kinase in pancreatic β-cell dysfunction and insulin resistance. Int. J. Biochem. Cell Biol. *38*, 782–793.

Kaneto, H., Katakami, N., Kawamori, D., Miyatsuka, T., Sakamoto, K. 'ya, Matsuoka, T.-A., Matsuhisa, M., and Yamasaki, Y. (2007). Involvement of Oxidative Stress in the Pathogenesis of Diabetes. Antioxid. Redox Signal. *9*, 355–366.

Karpe, F., Dickmann, J.R., and Frayn, K.N. (2011). Fatty Acids, Obesity, and Insulin Resistance: Time for a Reevaluation. Diabetes *60*, 2441–2449.

9.

Kava, R., Greenwood, M.R.C., and Johnson, P.R. (1990). Zucker (fa/fa) Rat. ILAR J. *32*, 4–8.

Kawanaka, K., Han, D.-H., Gao, J., Nolte, L.A., and Holloszy, J.O. (2001). Development of Glucose-induced Insulin Resistance in Muscle Requires Protein Synthesis. J. Biol. Chem. *276*, 20101–20107.

Kawasaki, N., Asada, R., Saito, A., Kanemoto, S., and Imaizumi, K. (2012). Obesity-induced endoplasmic reticulum stress causes chronic inflammation in adipose tissue. Sci. Rep. *2*, 799.

Kawser Hossain, M., Abdal Dayem, A., Han, J., Yin, Y., Kim, K., Kumar Saha, S., Yang, G.-M., Choi, H.Y., and Cho, S.-G. (2016). Molecular mechanisms of the anti-obesity and anti-diabetic properties of flavonoids. Int. J. Mol. Sci. *17*, 569.

Kelly, J.H. (1994). Permanent human hepatocyte cell line and its use in a liver assist device (LAD). *U.S. Patent No. 5,290,684*. Washington, DC: U.S. Patent and Trademark Office.

Kennedy, A., Martinez, K., Chuang, C.-C., LaPoint, K., and McIntosh, M. (2009). Saturated Fatty Acid-Mediated Inflammation and Insulin Resistance in Adipose Tissue: Mechanisms of Action and Implications. J. Nutr. *139*, 1–4.

Kershaw, E.E., and Flier, J.S. (2004). Adipose tissue as an endocrine organ. J. Clin. Endocrinol. Metab. *89*, 2548–2556.

Khan, A.H., and Pessin, J.E. (2002). Insulin regulation of glucose uptake: a complex interplay of intracellular signalling pathways. Diabetologia *45*, 1475–1483.

Kikuchi, M., Abe, N., Kato, M., Terao, S., Mimori, N., and Tachibana, H. (2009). Vildagliptin dose-dependently improves glycemic control in Japanese patients with type 2 diabetes mellitus. Diabetes Res. Clin. Pract. *83*, 233–240.

Kim, J.I., Huh, J.Y., Sohn, J.H., Choe, S.S., Lee, Y.S., Lim, C.Y., Jo, A., Park, S.B., Han, W., and Kim, J.B. (2015). Lipid-Overloaded Enlarged Adipocytes Provoke Insulin Resistance Independent of Inflammation. Mol. Cell. Biol. *35*, 1686–1699.

Kim, Y.-H., Lee, Y.J., Jeong, Y.-Y., Kim, Y.-W., Park, S.-Y., Doh, K.-O., and Kim, J.-Y. (2010). The effect of metformin on liver lipid accumulation in mice fed a high-fat diet. J. Korean Soc. Appl. Biol. Chem. *53*, 198–205.

King, A.J. (2012). The use of animal models in diabetes research. Br. J. Pharmacol. *166*, 877–894.

Kobayashi, K., Forte, T.M., Taniguchi, S., Ishida, B.Y., Oka, K., and Chan, L. (2000). The *db/db* mouse, a model for diabetic dyslipidemia: Molecular characterization and effects of western diet feeding. Metabolism *49*, 22–31.

Kong, W.M., Chik, Z., Ramachandra, M., Subramaniam, U., Aziddin, R.E.R., and Mohamed, Z. (2011). Evaluation of the effects of *Mitragyna speciosa* alkaloid extract on cytochrome P450 enzymes using a high throughput assay. Mol. Basel Switz. *16*, 7344–7356.

Konstantynowicz-Nowicka, K., Harasim, E., Baranowski, M., and Chabowski, A. (2015). New Evidence for the Role of Ceramide in the Development of Hepatic Insulin Resistance. PLoS ONE *10,* e0116858.

Koranyi, L., James, D., Mueckler, M., and Permutt, M.A. (1990). Glucose transporter levels in spontaneously obese (*db/db*) insulin-resistant mice. J. Clin. Invest. *85*, 962–967.

Kraegen, E.W., Cooney, G.J., Ye, J., and Thompson, A.L. (2001). Triglycerides, fatty acids and insulin resistance--hyperinsulinemia. Exp. Clin. Endocrinol. Diabetes Off. J. Ger. Soc. Endocrinol. Ger. Diabetes Assoc. *109*, S516-526.

Kristensen, J.M., Treebak, J.T., Schjerling, P., Goodyear, L., and Wojtaszewski, J.F.P. (2014). Two weeks of metformin treatment induces AMPK-dependent enhancement of insulin-stimulated glucose uptake in mouse soleus muscle. Am. J. Physiol. - Endocrinol. Metab. *306*, E1099–E1109.

Kwak, H.J., Choi, H.-E., Jang, J., Park, S.K., Bae, Y.-A., and Cheon, H.G. (2016). Bortezomib attenuates palmitic acid-induced ER stress, inflammation and insulin resistance in myotubes via AMPK dependent mechanism. Cell. Signal. *28*, 788–797.

Lang, C.H., Dobrescu, C., and Bagby, G.J. (1992). Tumor necrosis factor impairs insulin action on peripheral glucose disposal and hepatic glucose output. Endocrinology *130*, 43–52.

Lebovitz, H.E. (1999). Type 2 Diabetes: An Overview. Clin. Chem. *45*, 1339–1345.

Lee, W.H., and Kim, S.G. (2010). AMPK-Dependent Metabolic Regulation by PPAR Agonists. PPAR Res. *2010*, e549101.

Lerotholi, L., Chaudhary, S.K., Combrinck, S., and Viljoen, A. (2017). Bush tea (*Athrixia phylicoides*): A review of the traditional uses, bioactivity and phytochemistry. South Afr. J. Bot. *110*, 4-17.

Leturque, A., Brot-Laroche, E., Le Gall, M., Stolarczyk, E., and Tobin, V. (2005). The role of GLUT2 in dietary sugar handling. J. Physiol. Biochem. *61*, 529–537.

Li, C., and Zhang, B.B. (2000). Insulin signaling and action: glucose, lipids, protein. De Groot, L.J., Chrousos, G., Dungan, K., Feingold K.R., Grossman, A., Hershman, J.M., Koch, C., Korbonits, M., McLachlan, R., New, M., Purnell, J, Rebar, R, Singer F, Vinik, A (Eds), *Endotext [Internet]. MDText.com, Inc.* South Dartmouth.

Li, H.B., Yang, Y.R.Y., Mo, Z.J., Ding, Y., Jiang, W.J., Li, H.B., Yang, Y.R.Y., Mo, Z.J., Ding, Y., and Jiang, W.J. (2015). Silibinin improves palmitate-induced insulin resistance in C2C12 myotubes by attenuating IRS-1/PI3K/Akt pathway inhibition. Braz. J. Med. Biol. Res. *48*, 440–446.

Lin, C.-L., and Lin, J.-K. (2008). Epigallocatechin gallate (EGCG) attenuates high glucose-induced insulin signaling blockade in human hepG2 hepatoma cells. Mol. Nutr. Food Res. *52*, 930–939.

Liu, Z., Fu, C., Wang, W., and Xu, B. (2010). Prevalence of chronic complications of type 2 diabetes mellitus in outpatients - a cross-sectional hospital based survey in urban China. Health Qual. Life Outcomes *8*, 62.

López-Lázaro, M. (2009). Distribution and Biological Activities of the Flavonoid Luteolin. Mini-Rev. Med. Chem. *9*, 31–59.

Lorenzo, J.M., and Munekata, P.E.S. (2016). Phenolic compounds of green tea: Health benefits and technological application in food. Asian Pac. J. Trop. Biomed. *6*, 709–719.

Lowell, B.B., and Shulman, G.I. (2004). Mitochondrial Dysfunction and Type 2 Diabetes. Biochem J *378*, 105.

de Luca, C., and Olefsky, J.M. (2008). Inflammation and Insulin Resistance. FEBS Lett. *582*, 97–105.

Mahfouz, R., Khoury, R., Blachnio-Zabielska, A., Turban, S., Loiseau, N., Lipina, C., Stretton, C., Bourron, O., Ferré, P., Foufelle, F., et al. (2014). Characterising the Inhibitory Actions of Ceramide upon Insulin Signaling in Different Skeletal Muscle Cell Models: A Mechanistic Insight. PLOS ONE *9*, e101865.

Majo, D.D., Giammanco, M., Guardia, M.L., Tripoli, E., Giammanco, S., and Finotti, E. (2005). Flavanones in Citrus fruit: Structure–antioxidant activity relationships. Food Res. Int. *38*, 1161–1166.

Makki, K., Froguel, P., and Wolowczuk, I. (2013). Adipose Tissue in Obesity-Related Inflammation and Insulin Resistance: Cells, Cytokines, and Chemokines. Int. Sch. Res. Not. *2013*, e139239.

Manach, C., Scalbert, A., Morand, C., Rémésy, C., and Jiménez, L. (2004). Polyphenols: food sources and bioavailability. Am. J. Clin. Nutr. *79*, 727–747.

Mao, H.Z., Roussos, E.T., and Péterfy, M. (2006). Genetic analysis of the diabetes-prone C57BLKS/J mouse strain reveals genetic contribution from multiple strains. Biochim. Biophys. Acta *1762*, 440–446.

Marshall, S., Bacote, V., and Traxinger, R.R. (1991). Discovery of a metabolic pathway mediating glucose-induced desensitization of the glucose transport system. Role of hexosamine biosynthesis in the induction of insulin resistance. J. Biol. Chem. *266*, 4706–4712.

Mashibye, M.J., Madau, F.N., Soundy, P., and Van, R. (2006). A new flavonol from *Athrixia phylicoides* (Bush Tea). S. Afr. J. Chem. *59*, 1-2.

Mathieu, C., and Degrande, E. (2008). Vildagliptin: a new oral treatment for type 2 diabetes mellitus. Vasc. Health Risk Manag. *4*, 1349–1360.

Mavri-Damelin, D., Damelin, L.H., Eaton, S., Rees, M., Selden, C., and Hodgson, H.J.F. (2008). Cells for bioartificial liver devices: The human hepatoma-derived cell line C3A produces urea but does not detoxify ammonia. Biotechnol. Bioeng. *99*, 644–651.

Mazibuko (2014). *In vitro* and *in vivo* effect of *Aspalathus linearis* and its major polyphenols on carbohydrate and lipid metabolism in insulin resistant models. Thesis for the degree of Doctor of Philosophy, University of Zululand.

Mazibuko, S.E., Muller, C.J.F., Joubert, E., de Beer, D., Johnson, R., Opoku, A.R., and Louw, J. (2013). Amelioration of palmitate-induced insulin resistance in C_2C_{12} muscle cells by rooibos (*Aspalathus linearis)*. Phytomedicine Int. J. Phytother. Phytopharm. *20*, 813–819.

Mazibuko, S.E., Joubert, E., Johnson, R., Louw, J., Opoku, A.R., and Muller, C.J. (2015). Aspalathin improves glucose and lipid metabolism in 3T3-L1 adipocytes exposed to palmitate. Mol. Nutr. Food Res. *59*, 2199–2208.

McGaw, L.J., Steenkamp, V., and Eloff, J.N. (2007). Evaluation of *Athrixia* bush tea for cytotoxicity, antioxidant activity, caffeine content and presence of pyrrolizidine alkaloids. J. Ethnopharmacol. *110*, 16–22.

McMahon, D.K., Anderson, P.A., Nassar, R., Bunting, J.B., Saba, Z., Oakeley, A.E., and Malouf, N.N. (1994). C2C12 cells: biophysical, biochemical, and immunocytochemical properties. Am. J. Physiol. *266*, C1795-1802.

Meijssen, S., Cabezas, M.C., Ballieux, C.G.M., Derksen, R.J., Bilecen, S., and Erkelens, D.W. (2001). Insulin Mediated Inhibition of Hormone Sensitive Lipase Activity *in Vivo* in Relation to Endogenous Catecholamines in Healthy Subjects. J. Clin. Endocrinol. Metab. *86*, 4193–4197.

Meng, S., Cao, J., Feng, Q., Peng, J., and Hu, Y. (2013). Roles of Chlorogenic Acid on Regulating Glucose and Lipids Metabolism: A Review. Evid. Based Complement. Alternat. Med. *2013*, e801457.

Messina, M.J. (1999). Legumes and soybeans: overview of their nutritional profiles and health effects. Am. J. Clin. Nutr. *70*, 439s–450s.

Mihaylova, M.M., and Shaw, R.J. (2011). The AMP-activated protein kinase (AMPK) signaling pathway coordinates cell growth, autophagy, & metabolism. Nat. Cell Biol. *13*, 1016–1023.

Misu, H., Takamura, T., Takayama, H., Hayashi, H., Matsuzawa-Nagata, N., Kurita, S., Ishikura, K., Ando, H., Takeshita, Y., Ota, T., et al. (2010). A liver-derived secretory protein, selenoprotein P, causes insulin resistance. Cell Metab. *12*, 483–495.

Monteiro, R., and Azevedo, I. (2010). Chronic Inflammation in Obesity and the Metabolic Syndrome. Mediators Inflamm. *2010*, 289645.

Mosmann, T. (1983). Rapid colorimetric assay for cellular growth and survival: application to proliferation and cytotoxicity assays. J. Immunol. Methods *65,* 55-63.

Mubarak, A., Hodgson, J.M., Considine, M.J., Croft, K.D., and Matthews, V.B. (2013). Supplementation of a high-fat diet with chlorogenic acid is associated with insulin resistance and hepatic lipid accumulation in mice. J. Agric. Food Chem. *61*, 4371–4378.

Mueckler, M. (1994). Facilitative glucose transporters. Eur. J. Biochem. *219*, 713–725.

Munday, M.R. (2002). Regulation of mammalian acetyl-CoA carboxylase. Biochem. Soc. Trans. *30*, 1059–1064.

Muoio, D.M., and Newgard, C.B. (2008). Molecular and metabolic mechanisms of insulin resistance and β-cell failure in type 2 diabetes. Nat. Rev. Mol. Cell Biol. *9*, 193.

Musi, N., and Goodyear, L.J. (2003). AMP-activated protein kinase and muscle glucose uptake. Acta Physiol. Scand. *178*, 337–345.

Nakae, J., Oki, M., and Cao, Y. (2008). The FoxO transcription factors and metabolic regulation. FEBS Lett. *582*, 54–67.

Nandi, A., Kitamura, Y., Kahn, C.R., and Accili, D. (2004). Mouse Models of Insulin Resistance. Physiol. Rev. *84*, 623–647.

Nedachi, T., and Kanzaki, M. (2006). Regulation of glucose transporters by insulin and. Am J Physiol Endocrinol Metab *291*, E817–E828.

Nelson, B.A., Robinson, K.A., and Buse, M.G. (2000). High glucose and glucosamine induce insulin resistance via different mechanisms in 3T3-L1 adipocytes. Diabetes *49*, 981–991.

Nguyen, M.A., Satoh, H., Favelyukis, S., Babendure, J.L., Imamura, T., Sbodio, J.I., Zalevsky, J., Dahiyat, B.I., Chi, N.-W., and Olefsky, J.M. (2005). JNK and tumor necrosis factor-α mediate free fatty acid-induced insulin resistance in 3T3-L1 adipocytes. J. Biol. Chem. *280*, 35361–35371.

Nguyen, M.T.A., Chen, A., Lu, W.J., Fan, W., Li, P.-P., Oh, D.Y., and Patsouris, D. (2012). Regulation of Chemokine and Chemokine Receptor Expression by PPARγ in Adipocytes and Macrophages. PLOS ONE *7*, e34976.

Oh, K.-J., Han, H.-S., Kim, M.-J., and Koo, S.-H. (2013). CREB and FoxO1: two transcription factors for the regulation of hepatic gluconeogenesis. BMB Rep. *46*, 567–574.

Olson, A.L. (2012). Regulation of GLUT4 and Insulin-Dependent Glucose Flux. Int. Sch. Res. Not. *2012*, e856987.

Olson, K., Hendricks, B., and Murdock, D.K. (2012). The Triglyceride to HDL Ratio and Its Relationship to Insulin Resistance in Pre- and Postpubertal Children: Observation from the Wausau SCHOOL Project. Cholesterol *2012*, e794252.

Ong, K.W., Hsu, A., and Tan, B.K.H. (2012). Chlorogenic Acid Stimulates Glucose Transport in Skeletal Muscle via AMPK Activation: A Contributor to the Beneficial Effects of Coffee on Diabetes. PLoS ONE *7,* e32718.

Ong, K.W., Hsu, A., and Tan, B.K.H. (2013). Anti-diabetic and anti-lipidemic effects of chlorogenic acid are mediated by ampk activation. Biochem. Pharmacol. *85*, 1341–1351.

Padayachee, K. (2011). The phytochemistry and biological activities of *Athrixia Phylicoides*. Thesis for the degree of Master of Science, University of Witwatersrand.

Pandey, K.B., and Rizvi, S.I. (2009). Plant polyphenols as dietary antioxidants in human health and disease. Oxid. Med. Cell. Longev. *2*, 270–278.

Park, K., Li, Q., Rask-Madsen, C., Mima, A., Mizutani, K., Winnay, J., Maeda, Y., D'Aquino, K., White, M.F., Feener, E.P., et al. (2013). Serine Phosphorylation Sites on IRS2 Activated by Angiotensin II and Protein Kinase C To Induce Selective Insulin Resistance in Endothelial Cells. Mol. Cell. Biol. *33*, 3227–3241.

Park, S.Y., Ryu, J., and Lee, W. (2005). O-GlcNAc modification on IRS-1 and Akt2 by PUGNAc inhibits their phosphorylation and induces insulin resistance in rat primary adipocytes. Exp. Mol. Med. *37*, 220–229.

Patton, J., and DeGolier, T. (2010). Modeling leptin receptor insensitivity by comparing how leptin or leptin receptor mutations in mice affect body weight, basal metabolism, body temperature and feeding behaviors. Bios *81*, 76–83.

Pavithra, N., and Chaitanya, M. (2015). Lipid Lowering Effect of Anti Diabetic Agents-Recent Research. Inter. J. Pharma research & Rev. *4*, 73-80.

Peer, N., Steyn, K., Lombard, C., Lambert, E.V., Vythilingum, B., and Levitt, N.S. (2012). Rising Diabetes Prevalence among Urban-Dwelling Black South Africans. PLoS ONE *7*.

Perry, R.J., Samuel, V.T., Petersen, K.F., and Shulman, G.I. (2014). The role of hepatic lipids in hepatic insulin resistance and type 2 diabetes. Nature *510*, 84–91.

Pessin, J.E., and Saltiel, A.R. (2000). Signaling pathways in insulin action: molecular targets of insulin resistance. J. Clin. Invest. *106*, 165–169.

Petersen, K.F., and Shulman, G.I. (2002). Pathogenesis of skeletal muscle insulin resistance in type 2 diabetes mellitus. Am. J. Cardiol. *90*, 11–18.

Phillips, D.I.W., Caddy, S., Ilic, V., Fielding, B.A., Frayn, K.N., Borthwick, A.C., and Taylor, R. (1996). Intramuscular triglyceride and muscle insulin sensitivity: Evidence for a relationship in nondiabetic subjects. Metabolism *45*, 947–950.

Pietta, P.G. (2000). Flavonoids as antioxidants. J. Nat. Prod. *63*, 1035–1042.

Pietta, P., Minoggio, M., and Bramati, L. (2003). Plant Polyphenols: Structure, Occurrence and Bioactivity. In Studies in Natural Products Chemistry, A. Rahman, ed. (Elsevier), pp. 257–312.

Pooley, B. (1998). A field guide to wild flowers of KwaZulu-Natal and the eastern region. Durb. Natal Flora Publ. Trust 630p-Col Illus ISBN 062021502X En Icones Maps Geog *5*.

Poulos, S.P., Dodson, M.V., and Hausman, G.J. (2010). Cell line models for differentiation: preadipocytes and adipocytes. Exp. Biol. Med. *235*, 1185–1193.

Powell, D.J., Hajduch, E., Kular, G., and Hundal, H.S. (2003). Ceramide Disables 3-Phosphoinositide Binding to the Pleckstrin Homology Domain of Protein Kinase B (PKB)/Akt by a PKCζ-Dependent Mechanism. Mol. Cell. Biol. *23*, 7794–7808.

Powell, D.J., Turban, S., Alexander, G., Hajduch, E., and Hundal, H.S. (2004). Intracellular ceramide synthesis and protein kinase Cζ activation play an essential role in palmitate-induced insulin resistance in rat L6 skeletal muscle cells. Biochem. J. *382*, 619–629.

Puigserver, P., Rhee, J., Donovan, J., Walkey, C.J., Yoon, J.C., Oriente, F., Kitamura, Y., Altomonte, J., Dong, H., Accili, D., et al. (2003). Insulin-regulated hepatic gluconeogenesis through FOXO1-PGC-1alpha interaction. Nature *423*, 550–555.

Qu, S., Altomonte, J., Perdomo, G., He, J., Fan, Y., Kamagate, A., Meseck, M., and Dong, H.H. (2006). Aberrant Forkhead Box O1 Function Is Associated with Impaired Hepatic Metabolism. Endocrinology *147*, 5641–5652.

Radavelli-Bagatini, S., Blair, A.R., Proietto, J., Spritzer, P.M., and Andrikopoulos, S. (2011). The New Zealand obese mouse model of obesity insulin resistance and poor breeding performance: evaluation of ovarian structure and function. J. Endocrinol. *209*, 307–315.

Ragheb, R., Shanab, G.M.L., Medhat, A.M., Seoudi, D.M., Adeli, K., and Fantus, I.G. (2009). Free fatty acid-induced muscle insulin resistance and glucose uptake dysfunction: Evidence for PKC activation and oxidative stress-activated signaling pathways. Biochem. Biophys. Res. Commun. *389*, 211–216.

Rampedi, I.T., and Olivier, J. (2005). The use and potential commercial development of Athrixia phylicoides. ACTA Acad.-Univ. FREE STATE *37*, 165.

Rayasam, G.V., Tulasi, V.K., Sodhi, R., Davis, J.A., and Ray, A. (2009). Glycogen synthase kinase 3: more than a namesake. Br. J. Pharmacol. *156*, 885–898.

Reaven, G.M. (1988). Role of Insulin Resistance in Human Disease. Diabetes *37*, 1595–1607.

Robbins, R.J. (2003). Phenolic Acids in Foods: An Overview of Analytical Methodology. J Agric Food Chem *51*, 2866–2887.

Roden, M., Price, T.B., Perseghin, G., Petersen, K.F., Rothman, D.L., Cline, G.W., and Shulman, G.I. (1996). Mechanism of free fatty acid-induced insulin resistance in humans. J. Clin. Invest. *97*, 2859–2865.

Rotter, V., Nagaev, I., and Smith, U. (2003). Interleukin-6 (IL-6) Induces Insulin Resistance in 3T3-L1 Adipocytes and Is, Like IL-8 and Tumor Necrosis Factor-α, Overexpressed in Human Fat Cells from Insulin-resistant Subjects. J. Biol. Chem. *278*, 45777–45784.

Ruderman, N.B., Cacicedo, J.M., Itani, S., Yagihashi, N., Saha, A.K., Ye, J.M., Chen, K., Zou, M., Carling, D., Boden, G., et al. (2003). Malonyl-CoA and AMP-activated protein kinase (AMPK): possible links between insulin resistance in muscle and early endothelial cell damage in diabetes. Biochem. Soc. Trans. *31*, 202–206.

Rudich, A., Tirosh, A., Potashnik, R., Hemi, R., Kanety, H., and Bashan, N. (1998). Prolonged oxidative stress impairs insulin-induced GLUT4 translocation in 3T3-L1 adipocytes. Diabetes *47*, 1562–1569.

Rutkowski, J.M., Stern, J.H., and Scherer, P.E. (2015). The cell biology of fat expansion. J Cell Biol *208*, 501–512.

Saha, A.K., and Ruderman, N.B. (2003). Malonyl-CoA and AMP-activated protein kinase: an expanding partnership. Mol. Cell. Biochem. *253*, 65–70.

Saha, A.K., Schwarsin, A.J., Roduit, R., Massé, F., Kaushik, V., Tornheim, K., Prentki, M., and Ruderman, N.B. (2000). Activation of Malonyl-CoA Decarboxylase in Rat Skeletal Muscle by Contraction and the AMP-activated Protein Kinase Activator 5-Aminoimidazole-4-carboxamide-1-β-d-ribofuranoside. J. Biol. Chem. *275*, 24279–24283.

Sakamoto, K., and Holman, G.D. (2008). Emerging role for AS160/TBC1D4 and TBC1D1 in the regulation of GLUT4 traffic. Am. J. Physiol. Endocrinol. Metab. *295*, E29–E37.

Saltiel, A.R., and Kahn, C.R. (2001). Insulin signalling and the regulation of glucose and lipid metabolism. Nature *414*, 799–806.

Salvadó, L., Palomer, X., Barroso, E., and Vázquez-Carrera, M. (2015). Targeting endoplasmic reticulum stress in insulin resistance. Trends Endocrinol. Metab. *26*, 438–448.

Samuel, V.T., Liu, Z.-X., Qu, X., Elder, B.D., Bilz, S., Befroy, D., Romanelli, A.J., and Shulman, G.I. (2004). Mechanism of Hepatic Insulin Resistance in Non-alcoholic Fatty Liver Disease. J. Biol. Chem. *279*, 32345–32353.

Savage, D.B., Petersen, K.F., and Shulman, G.I. (2007). Disordered lipid metabolism and the pathogenesis of insulin resistance. Physiol. Rev. *87*, 507–520.

Sawada, K., Kawabata, K., Yamashita, T., Kawasaki, K., Yamamoto, N., and Ashida, H. (2012). Ameliorative effects of polyunsaturated fatty acids against palmitic acid-induced insulin resistance in L6 skeletal muscle cells. Lipids Health Dis. *11*, 1.

Scalbert, A., and Williamson, G. (2000). Dietary Intake and Bioavailability of Polyphenols. J. Nutr. *130*, 2073S–2085S.

Schmitz-Peiffer, C. (2010). Targeting Ceramide Synthesis to Reverse Insulin Resistance. Diabetes *59*, 2351–2353.

Schmitz-Peiffer, C. (2013). The tail wagging the dog – regulation of lipid metabolism by protein kinase C. FEBS J. *280*, 5371–5383.

Schmitz-Peiffer, C., Craig, D.L., and Biden, T.J. (1999). Ceramide generation is sufficient to account for the inhibition of the insulin-stimulated PKB pathway in C2C12 skeletal muscle cells pretreated with palmitate. J. Biol. Chem. *274*, 24202–24210.

Semaming, Y., Pannengpetch, P., Chattipakorn, S.C., and Chattipakorn, N. (2015). Pharmacological Properties of Protocatechuic Acid and Its Potential Roles as Complementary Medicine. Evid.-Based Complement. Altern. Med. *2015*, 593902.

Senn, J.J., Klover, P.J., Nowak, I.A., Zimmers, T.A., Koniaris, L.G., Furlanetto, R.W., and Mooney, R.A. (2003). Suppressor of cytokine signaling-3 (SOCS-3), a potential mediator of interleukin-6-dependent insulin resistance in hepatocytes. J. Biol. Chem. *278*, 13740–13746.

Setchell, K.D. (1998). Phytoestrogens: the biochemistry, physiology, and implications for human health of soy isoflavones. Am. J. Clin. Nutr. *68*, 1333S–1346S.

Seyer, P., Vallois, D., Poitry-Yamate, C., Schütz, F., Metref, S., Tarussio, D., Maechler, P., Staels, B., Lanz, B., Grueter, R., et al. (2013). Hepatic glucose sensing is required to preserve β cell glucose competence. J. Clin. Invest. *123*, 1662–1676.

Sharma, K., McCue, P., and Dunn, S.R. (2003). Diabetic kidney disease in the *db/db* mouse. Am. J. Physiol. - Ren. Physiol. *284*, F1138–F1144.

Shi, H., Kokoeva, M.V., Inouye, K., Tzameli, I., and others (2006). TLR4 links innate immunity and fatty acid-induced insulin resistance. J. Clin. Invest. *116*, 3015.

Shirwany, N.A., and Zou, M.-H. (2014). AMPK: a cellular metabolic and redox sensor. A minireview. Front. Biosci. Landmark Ed. *19*, 447–474.

Shulman, G.I. (2000). Cellular mechanisms of insulin resistance. J. Clin. Invest. *106*, 171–176.

Singh, A. (2011). Phytochemicals. *Herbalism, Phytochemistry and Ethnopharmacology* (pp 36-114). *Science Publishers, British Channel Islands*.

Snel, M., Jonker, J.T., Schoones, J., Lamb, H., de Roos, A., Pijl, H., Smit, J.W.A., Meinders, A.E., and Jazet, I.M. (2012). Ectopic Fat and Insulin Resistance: Pathophysiology and Effect of Diet and Lifestyle Interventions. Int. J. Endocrinol. *2012*, e983814.

Song, M.J., Kim, K.H., Yoon, J.M., and Kim, J.B. (2006). Activation of Toll-like receptor 4 is associated with insulin resistance in adipocytes. Biochem. Biophys. Res. Commun. *346*, 739–745.

Srinivasan, M., Sudheer, A.R., and Menon, V.P. (2007). Ferulic Acid: Therapeutic Potential Through Its Antioxidant Property. J. Clin. Biochem. Nutr. *40*, 92–100.

Srivastava, R.A.K., Pinkosky, S.L., Filippov, S., Hanselman, J.C., Cramer, C.T., and Newton, R.S. (2012). AMP-activated protein kinase: an emerging drug target to regulate imbalances in lipid and carbohydrate metabolism to treat cardio-metabolic diseases. J. Lipid Res. *53*, 2490–2514.

Stannard, S.R., and Johnson, N.A. (2004). Insulin resistance and elevated triglyceride in muscle: more important for survival than “thrifty” genes? J. Physiol. *554*, 595–607.

Stumvoll, M., Goldstein, B.J., and van Haeften, T.W. (2005). Type 2 diabetes: principles of pathogenesis and therapy. The Lancet *365*, 1333–1346.

Sudeep, H.V., Venkatakrishna, K., Patel, D., and Shyamprasad, K. (2016). Biomechanism of chlorogenic acid complex mediated plasma free fatty acid metabolism in rat liver. BMC Complement. Altern. Med. *16*, 274.

Suganami, T., Tanimoto-Koyama, K., Nishida, J., Itoh, M., Yuan, X., Mizuarai, S., Kotani, H., Yamaoka, S., Miyake, K., Aoe, S., et al. (2007). Role of the Toll-like Receptor 4/NF-κB Pathway in Saturated Fatty Acid–Induced Inflammatory Changes in the Interaction Between Adipocytes and Macrophages. Arterioscler. Thromb. Vasc. Biol. *27*, 84–91.

Sun, K., Tordjman, J., Clément, K., and Scherer, P.E. (2013). Fibrosis and Adipose Tissue Dysfunction. Cell Metab. *18*, 470–477.

Tal, M., Liang, Y., Najafi, H., Lodish, H.F., and Matschinsky, F.M. (1992). Expression and function of GLUT-1 and GLUT-2 glucose transporter isoforms in cells of cultured rat pancreatic islets. J. Biol. Chem. *267*, 17241–17247.

Teruel, T., Hernandez, R., and Lorenzo, M. (2001). Ceramide Mediates Insulin Resistance by Tumor Necrosis Factor-α in Brown Adipocytes by Maintaining Akt in an Inactive Dephosphorylated State. Diabetes *50*, 2563–2571.

Theoharides, T.C., Conti, P., and Economu, M. (2014). Brain inflammation, neuropsychiatric disorders, and immunoendocrine effects of luteolin. J. Clin. Psychopharmacol. *34*, 187–189.

Theoharides, T.C., Stewart, J.M., Hatziagelaki, E., and Kolaitis, G. (2015). Brain “fog,” inflammation and obesity: key aspects of neuropsychiatric disorders improved by luteolin. Front. Neurosci. *9*, 225.

Thomson, M.J., Williams, M.G., and Frost, S.C. (1997). Development of Insulin Resistance in 3T3-L1 Adipocytes. J. Biol. Chem. *272*, 7759–7764.

Thorens, B., and Mueckler, M. (2010). Glucose transporters in the 21st Century. Am. J. Physiol. - Endocrinol. Metab. *298*, E141–E145.

Tian, Y.-F., Hsia, T.-L., Hsieh, C.-H., Huang, D.-W., Chen, C.-H., and Hsieh, P.-S. (2011). importance of cyclooxygenase 2-mediated oxidative stress in obesity-induced muscular insulin resistance in high-fat-fed rats. Life Sci. *89*, 107-114.

Towler, M.C., and Hardie, D.G. (2007). AMP-activated protein kinase in metabolic control and insulin signaling. Circ. Res. *100*, 328–341.

Trak-Smayra, V., Paradis, V., Massart, J., Nasser, S., Jebara, V., and Fromenty, B. (2011). Pathology of the liver in obese and diabetic *ob/ob* and *db/db* mice fed a standard or high-calorie diet. Int. J. Exp. Pathol. *92*, 413–421.

Tsuchiya, Y., Hatakeyama, H., Emoto, N., Wagatsuma, F., Matsushita, S., and Kanzaki, M. (2010). Palmitate-induced Down-regulation of Sortilin and Impaired GLUT4 Trafficking in C2C12 Myotubes. J. Biol. Chem. *285*, 34371–34381.

Turban, S., and Hajduch, E. (2011). Protein kinase C isoforms: Mediators of reactive lipid metabolites in the development of insulin resistance. FEBS Lett. *585*, 269–274.

Valverde, A.M., Teruel, T., Navarro, P., Benito, M., and Lorenzo, M. (1998). Tumor necrosis factor-alpha causes insulin receptor substrate-2-mediated insulin resistance and inhibits insulin-induced adipogenesis in fetal brown adipocytes. Endocrinology *139*, 1229–1238.

Van der Poll, T., Romijn, J.A., Endert, E., Borm, J.J., Büller, H.R., and Sauerwein, H.P. (1991). Tumor necrosis factor mimics the metabolic response to acute infection in healthy humans. Am. J. Physiol. *261*, E457-465.

Van Wyk, B.-E., Gericke, N.(2000). Beverages. *People's plants: A guide to useful plants of Southern Africa* (pp 102-312). Briza Publications, Pretoria.

Viollet, B., Horman, S., Leclerc, J., Lantier, L., Foretz, M., Billaud, M., Giri, S., and Andreelli, F. (2010). AMPK inhibition in health and disease. Crit. Rev. Biochem. Mol. Biol. *45*, 276–295.

Viollet, B., Guigas, B., Sanz Garcia, N., Leclerc, J., Foretz, M., and Andreelli, F. (2012). Cellular and molecular mechanisms of metformin: an overview. Clin. Sci. Lond. Engl. 1979 *122*, 253–270.

Volate, S.R., Davenport, D.M., Muga, S.J., and Wargovich, M.J. (2005). Modulation of aberrant crypt foci and apoptosis by dietary herbal supplements (quercetin, curcumin, silymarin, ginseng and rutin). Carcinogenesis *26*, 1450–1456.

Wakil, S.J., and Abu-Elheiga, L.A. (2009). Fatty acid metabolism: target for metabolic syndrome. J. Lipid Res. *50*, S138–S143.

Wang, B., P., C.C., and Pippin, J.J. (2014). Leptin- and Leptin Receptor-Deficient Rodent Models: Relevance for Human Type 2 Diabetes. Curr. Diabetes Rev. *10*, 131–145.

Watt, J.M., Breyer-Brandwijk, M.G., and others (1932). The Medicinal and Poisonous Plants of Southern Africa. Ulster. Med. J. *2*, 112.

Weiss, M., Steiner, D.F., and Philipson, L.H. (2000). Insulin Biosynthesis, Secretion, Structure, and Structure-Activity Relationships. In Endotext, L.J. De Groot, G. Chrousos, K. Dungan, K.R. Feingold, A. Grossman, J.M. Hershman, C. Koch, M. Korbonits, R. McLachlan, M. New, et al., eds. (South Dartmouth (MA): MDText.com, Inc.), p.White, M.F. (2003). Insulin Signaling in Health and Disease. Science *302*, 1710–1711.

Whiteman, E.L., Cho, H., and Birnbaum, M.J. (2002). Role of Akt/protein kinase B in metabolism. Trends Endocrinol. Metab. TEM *13*, 444–451.

WHO (World Health Organisation). (2013). World health statistics 2013. www.who.int/gho/publications/world_health_statistics/EN_WHS2013

WHO (World Health Organisation). (2016). Global report on diabetes. http://www.who.int/diabetes/global-report/en/

Wiernsperger, N.F., and Bailey, C.J. (1999). The antihyperglycaemic effect of metformin: therapeutic and cellular mechanisms. Drugs *58 Suppl 1*, 31-39; discussion 75-82.

Wieser, V., Moschen, A.R., and Tilg, H. (2013). Inflammation, cytokines and insulin resistance: a clinical perspective. Arch. Immunol. Ther. Exp. (Warsz.) *61*, 119–125.

Wilcox, G. (2005). Insulin and Insulin Resistance. Clin. Biochem. Rev. *26*, 19–39.

Witters, L.A., and Kemp, B.E. (1992). Insulin activation of acetyl-CoA carboxylase accompanied by inhibition of the 5'-AMP-activated protein kinase. J. Biol. Chem. *267*, 2864–2867.

Wood, I.S., and Trayhurn, P. (2003). Glucose transporters (GLUT and SGLT): expanded families of sugar transport proteins. Br. J. Nutr. *89*, 3–9.

Woollhead, A.M., Sivagnanasundaram, J., Kalsi, K.K., Pucovsky, V., Pellatt, L.J., Scott, J.W., Mustard, K.J., Hardie, D.G., and Baines, D.L. (2007). Pharmacological activators of AMP-activated protein kinase have different effects on Na+ transport processes across human lung epithelial cells. Br. J. Pharmacol. *151*, 1204–1215.

Xu, M.-L., Liu, J., Zhu, C., Gao, Y., Zhao, S., Liu, W., and Zhang, Y. (2015). Interactions between soy isoflavones and other bioactive compounds: a review of their potentially beneficial health effects. Phytochem. Rev. *14*, 459–467.

Yaffe, D., and Saxel, O. (1977). Serial passaging and differentiation of myogenic cells isolated from dystrophic mouse muscle. Nature *270*, 725–727.

Yano, M., Hasegawa, G., Ishii, M., Yamasaki, M., Fukui, M., Nakamura, N., and Yoshikawa, T. (2004). Short-term exposure of high glucose concentration induces generation of reactive oxygen species in endothelial cells: implication for the oxidative stress associated with postprandial hyperglycemia. Redox Rep. Commun. Free Radic. Res. *9*, 111–116.

Yoo, D.Y., Choi, J.H., Kim, W., Nam, S.M., Jung, H.Y., Kim, J.H., Won, M.-H., Yoon, Y.S., and Hwang, I.K. (2013). Effects of luteolin on spatial memory, cell proliferation,

and neuroblast differentiation in the hippocampal dentate gyrus in a scopolamine-induced amnesia model. Neurol. Res. *35*, 813–820.

Yoon, S.-A., Kang, S.-I., Shin, H.-S., Kang, S.-W., Kim, J.-H., Ko, H.-C., and Kim, S.-J. (2013). p-Coumaric acid modulates glucose and lipid metabolism via AMP-activated protein kinase in L6 skeletal muscle cells. Biochem. Biophys. Res. Commun. *432*, 553–557.

Yu, Y., and Chai, J. (2015). The function of miRNAs and their potential as therapeutic targets in burn-induced insulin resistance (Review). Int. J. Mol. Med. *35*, 305–310.

Yu, C., Chen, Y., Cline, G.W., Zhang, D., Zong, H., Wang, Y., Bergeron, R., Kim, J.K., Cushman, S.W., Cooney, G.J., et al. (2002). Mechanism by which fatty acids inhibit insulin activation of insulin receptor substrate-1 (IRS-1)-associated phosphatidylinositol 3-kinase activity in muscle. J. Biol. Chem. *277*, 50230–50236.

Yu, T., Jhun, B.S., and Yoon, Y. (2011). High-glucose stimulation increases reactive oxygen species production through the calcium and mitogen-activated protein kinase-mediated activation of mitochondrial fission. Antioxid. Redox Signal. *14*, 425–437.

Zang, L.-Y., Cosma, G., Gardner, H., Shi, X., Castranova, V., and Vallyathan, V. (2000). Effect of antioxidant protection by p-coumaric acid on low-density lipoprotein cholesterol oxidation. Am. J. Physiol. - Cell Physiol. *279*, C954–C960.

Zang, L.-Y., Cosma, G., Gardner, H., Castranova, V., and Vallyathan, V. (2003). Effect of chlorogenic acid on hydroxyl radical. Mol. Cell. Biochem. *247*, 205–210.

Zang, M., Xu, S., Maitland-Toolan, K.A., Zuccollo, A., Hou, X., Jiang, B., Wierzbicki, M., Verbeuren, T.J., and Cohen, R.A. (2006). Polyphenols Stimulate AMP-Activated Protein Kinase, Lower Lipids, and Inhibit Accelerated Atherosclerosis in Diabetic LDL Receptor–Deficient Mice. Diabetes *55*, 2180–2191.

Zhang, K., and Kaufman, R.J. (2008). From endoplasmic-reticulum stress to the inflammatory response. Nature *454*, 455–462.

Zhang, C., Gao, F., Luo, H., Zhang, C.-T., and Zhang, R. (2015a). Differential response in levels of high-density lipoprotein cholesterol to one-year metformin treatment in prediabetic patients by race/ethnicity. Cardiovasc. Diabetol. *14*, 79.

Zhang, W.Y., Lee, J.-J., Kim, I.-S., Kim, Y., Park, J.-S., and Myung, C.-S. (2010). 7-O-methylaromadendrin stimulates glucose uptake and improves insulin resistance *in vitro*. Biol. Pharm. Bull. *33*, 1494–1499.

Zhang, X.-T., Yu, C.-J., Liu, J.-W., Zhang, Y.-P., Zhang, C., Song, C.-X., Xie, J.-S., Sai, J.-Y., Zheng, J.-T., and Wang, F. (2015b). Qizhi Jiangtang Jiaonang Improves Insulin Signaling and Reduces Inflammatory Cytokine Secretion and Reactive Oxygen Species Formation in Insulin Resistant HepG2 Cells. Evid.-Based Complement. Altern. Med. *2015*, 518639.

Zhao, L., Guo, X., Wang, O., Zhang, H., Wang, Y., Zhou, F., Liu, J., and Ji, B. (2016). Fructose and glucose combined with free fatty acids induce metabolic disorders in HepG2 cell: A new model to study the impacts of high-fructose/sucrose and high-fat diets *in vitro*. Mol. Nutr. Food Res. *60*, 909–921.

Zhao, Y., Tang, Z., Shen, A., Tao, T., Wan, C., Zhu, X., Huang, J., Zhang, W., Xia, N., Wang, S., et al. (2015). The Role of PTP1B O-GlcNAcylation in Hepatic Insulin Resistance. Int. J. Mol. Sci. *16,* 22856-22869.

Zhou, Y., Gu, P., Shi, W., Li, J., Hao, Q., Cao, X., Lu, Q., and Zeng, Y. (2016). MicroRNA-29a induces insulin resistance by targeting PPARδ in skeletal muscle cells. Int. J. Mol. Med. *37*, 931–938.

Zhu, Q.Y., Zhang, A., Tsang, D., Huang, Y., and Chen, Z.-Y. (1997). Stability of Green Tea Catechins. J. Agric. Food Chem. *45*, 4624–4628.

Zierath, J.R., Krook, A., and Wallberg-Henriksson, H. (2000). Insulin action and insulin resistance in human skeletal muscle. Diabetologia *43*, 821–835.

Zou, L., Harkey, M.R., and Henderson, G.L. (2002). Effects of herbal components on cDNA-expressed cytochrome P450 enzyme catalytic activity. Life Sci. *71*, 1579–1589.

ADDENDUM 1 ANOVA tables

Analysis of Variance Report

Dataset	P:\...\3H glucose uptake\stats file for NCSS incl WB.NCSS
Filter	treatment = "Ctrl"
Response	C2C12_Glucose_uptake

Expected Mean Squares Section

Source Term	DF	Term Fixed?	Denominator Term	Expected Mean Square
A: PA	1	Yes	S(AB)	S+bsA
B: Ins	1	Yes	S(AB)	S+asB
AB	1	Yes	S(AB)	S+sAB
S(AB)	30	No		S

Note: Expected Mean Squares are for the balanced cell-frequency case.

Analysis of Variance Table

Source Term	DF	Sum of Squares (Alpha=0.05)	Mean Square	F-Ratio	Prob Level	Power
A: PA	1	3803.933	3803.933	7.16	0.011984*	0.735182
B: Ins	1	3535.322	3535.322	6.65	0.015064*	0.703876
AB	1	3068.191	3068.191	5.77	0.022683*	0.642455
S	30	15948.54	531.618			
Total (Adjusted)	33	25990.1				
Total	34					

* Term significant at alpha = 0.05

Means and Standard Error Section

Term	Count	Mean	Standard Error
All	34	109.135	
A: PA			
(-) PA	16	119.7308	5.764211
(+) PA	18	98.53934	5.43455
B: Ins			
(-) Ins	17	98.9203	5.592106
(+) Ins	17	119.3498	5.592106
AB: PA,Ins			
(-) PA,(-) Ins	8	100	8.151825
(-) PA,(+) Ins	8	139.4615	8.151825
(+) PA,(-) Ins	9	97.8406	7.685615
(+) PA,(+) Ins	9	99.2381	7.685615

Analysis of Variance Report

Dataset	P:\...\3H glucose uptake\stats file for NCSS incl WB.NCSS
Filter	treatment = "Ctrl"
Response	C3A_Glucose_uptake

Expected Mean Squares Section

Source Term	DF	Term Fixed?	Denominator Term	Expected Mean Square
A: PA	1	Yes	S(AB)	S+bsA
B: Ins	1	Yes	S(AB)	S+asB
AB	1	Yes	S(AB)	S+sAB
S(AB)	27	No		S

Note: Expected Mean Squares are for the balanced cell-frequency case.

Analysis of Variance Table

Source Term	DF	Sum of Squares	Mean Square	F-Ratio	Prob Level	Power (Alpha=0.05)
A: PA	1	103.4143	103.4143	0.10	0.759757	0.060240
B: Ins	1	12193.68	12193.68	11.25	0.002370*	0.898484
AB	1	305.7747	305.7747	0.28	0.599631	0.080597
S	27	29259.49	1083.685			
Total (Adjusted)	30	41740.07				
Total	31					

* Term significant at alpha = 0.05

Means and Standard Error Section

Term	Count	Mean	Standard Error
All	31	124.9365	
A: PA			
(-) PA	15	123.1	8.499743
(+) PA	16	126.773	8.229841
B: Ins			
(-) Ins	17	104.9944	7.984119
(+) Ins	14	144.8786	8.798071
AB: PA,Ins			
(-) PA,(-) Ins	8	100	11.63875
(-) PA,(+) Ins	7	146.2	12.44235
(+) PA,(-) Ins	9	109.9889	10.97312
(+) PA,(+) Ins	7	143.5571	12.44235

Analysis of Variance Report

Dataset	P:\...\3H glucose uptake\stats file for NCSS incl WB.NCSS
Filter	treatment = "Ctrl"
Response	MTT_3T3

Expected Mean Squares Section

Source Term	DF	Term Fixed?	Denominator Term	Expected Mean Square
A: PA	1	Yes	S(AB)	S+bsA
B: Ins	1	Yes	S(AB)	S+asB
AB	1	Yes	S(AB)	S+sAB
S(AB)	20	No		S

Note: Expected Mean Squares are for the balanced cell-frequency case.

Analysis of Variance Table

Source Term	DF	Sum of Squares	Mean Square	F-Ratio	Prob Level	Power (Alpha=0.10)
A: PA	1	241.0468	241.0468	0.67	0.424020	0.203425
B: Ins	1	26557.45	26557.45	73.39	0.000000*	1.000000
AB	1	341.864	341.864	0.94	0.342674	0.245078
S	20	7237.277	361.8639			
Total (Adjusted)	23	34377.63				
Total	24					

* Term significant at alpha = 0.10

Means and Standard Error Section

Term	Count	Mean	Standard Error
All	24	140.21	
A: PA			
(-) PA	12	137.0408	5.491386
(+) PA	12	143.3792	5.491386
B: Ins			
(-) Ins	12	106.945	5.491386
(+) Ins	12	173.475	5.491386
AB: PA,Ins			
(-) PA,(-) Ins	6	100.0017	7.765993
(-) PA,(+) Ins	6	174.08	7.765993
(+) PA,(-) Ins	6	113.8883	7.765993
(+) PA,(+) Ins	6	172.87	7.765993

Analysis of Variance Report

Dataset	P:\...\3H glucose uptake\stats file for NCSS incl WB.NCSS
Filter	treatment = "Ctrl"
Response	3T3_Glucose_uptake

Expected Mean Squares Section

Source Term	DF	Term Fixed?	Denominator Term	Expected Mean Square
A: PA	1	Yes	S(AB)	S+bsA
B: Ins	1	Yes	S(AB)	S+asB
AB	1	Yes	S(AB)	S+sAB
S(AB)	38	No		S

Note: Expected Mean Squares are for the balanced cell-frequency case.

Analysis of Variance Table

Source Term	DF	Sum of Squares	Mean Square	F-Ratio	Prob Level	Power (Alpha=0.05)
A: PA	1	626.502	626.502	0.32	0.572722	0.085931
B: Ins	1	2722.024	2722.024	1.41	0.242994	0.211666
AB	1	336.1006	336.1006	0.17	0.679214	0.069117
S	38	73539.91	1935.261			
Total (Adjusted)	41	77325.3				
Total	42					

* Term significant at alpha = 0.05

Means and Standard Error Section

Term	Count	Mean	Standard Error
All	42	107.0436	
A: PA			
(-) PA	20	110.9205	9.836822
(+) PA	22	103.1668	9.379041
B: Ins			
(-) Ins	20	98.96273	9.836822
(+) Ins	22	115.1245	9.379041
AB: PA,Ins			
(-) PA,(-) Ins	9	100	14.66387
(-) PA,(+) Ins	11	121.8409	13.26397
(+) PA,(-) Ins	11	97.92545	13.26397
(+) PA,(+) Ins	11	108.4082	13.26397

Analysis of Variance Report

Dataset	P:\...\3H glucose uptake\stats file for NCSS incl WB.NCSS
Filter	treatment = "Ctrl"
Response	ORO_correct

Expected Mean Squares Section

Source Term	DF	Term Fixed?	Denominator Term	Expected Mean Square
A: PA	1	Yes	S(AB)	S+bsA
B: Ins	1	Yes	S(AB)	S+asB
AB	1	Yes	S(AB)	S+sAB
S(AB)	37	No		S

Note: Expected Mean Squares are for the balanced cell-frequency case.

Analysis of Variance Table

Source Term	DF	Sum of Squares	Mean Square	F-Ratio	Prob Level	Power (Alpha=0.10)
A: PA	1	1337.938	1337.938	4.49	0.040865*	0.668370
B: Ins	1	564.6248	564.6248	1.89	0.176924	0.385935
AB	1	231.5796	231.5796	0.78	0.383693	0.223914
S	37	11024.91	297.9706			
Total (Adjusted)	40	13110.69				
Total	41					

* Term significant at alpha = 0.10

Means and Standard Error Section

Term	Count	Mean	Standard Error
All	41	88.19086	
A: PA			
(-) PA	21	93.90823	3.766839
(+) PA	20	82.4735	3.859862
B: Ins			
(-) Ins	20	91.905	3.859862
(+) Ins	21	84.47673	3.766839
AB: PA,Ins			
(-) PA,(-) Ins	10	100.001	5.458669
(-) PA,(+) Ins	11	87.81545	5.204637
(+) PA,(-) Ins	10	83.809	5.458669
(+) PA,(+) Ins	10	81.138	5.458669

Analysis of Variance Report

Dataset	P:\...\3H glucose uptake\stats file for NCSS incl WB.NCSS
Filter	treatment = "Met"
Response	C2C12_ Glucose_uptake

Expected Mean Squares Section

Source Term	DF	Term Fixed?	Denominator Term	Expected Mean Square
A: PA	1	Yes	S(AB)	S+bsA
B: Ins	1	Yes	S(AB)	S+asB
AB	1	Yes	S(AB)	S+sAB
S(AB)	32	No		S

Note: Expected Mean Squares are for the balanced cell-frequency case.

Analysis of Variance Table

Source Term	DF	Sum of Squares	Mean Square	F-Ratio	Prob Level	Power (Alpha=0.05)
A: PA	1	18824.88	18824.88	30.68	0.000004*	0.999671
B: Ins	1	8260.54	8260.54	13.46	0.000879*	0.944847
AB	1	1062.402	1062.402	1.73	0.197597	0.247750
S	32	19636.91	613.6534			
Total (Adjusted)	35	47784.73				
Total	36					

* Term significant at alpha = 0.05

Means and Standard Error Section

Term	Count	Mean	Standard Error
All	36	108.673	
A: PA			
(-) PA	18	131.5403	5.838823
(+) PA	18	85.80571	5.838823
B: Ins			
(-) Ins	18	93.52509	5.838823
(+) Ins	18	123.8209	5.838823
AB: PA,Ins			
(-) PA,(-) Ins	9	110.96	8.257342
(-) PA,(+) Ins	9	152.1207	8.257342
(+) PA,(-) Ins	9	76.09021	8.257342
(+) PA,(+) Ins	9	95.52121	8.257342

Analysis of Variance Report

Dataset	P:\...\3H glucose uptake\stats file for NCSS incl WB.NCSS
Filter	treatment = "Met"
Response	C3A_ Glucose_uptake

Expected Mean Squares Section

Source Term	DF	Term Fixed?	Denominator Term	Expected Mean Square
A: PA	1	Yes	S(AB)	S+bsA
B: Ins	1	Yes	S(AB)	S+asB
AB	1	Yes	S(AB)	S+sAB
S(AB)	30	No		S

Note: Expected Mean Squares are for the balanced cell-frequency case.

Analysis of Variance Table

Source Term	DF	Sum of Squares	Mean Square	F-Ratio	Prob Level	Power (Alpha=0.05)
A: PA	1	396.0693	396.0693	0.58	0.450772	0.114686
B: Ins	1	6669.492	6669.492	9.83	0.003821*	0.858541
AB	1	7.492593	7.492593	0.01	0.917000	0.051187
S	30	20350.94	678.3647			
Total (Adjusted)	33	27666.99				
Total	34					

* Term significant at alpha = 0.05

Means and Standard Error Section

Term	Count	Mean	Standard Error
All	34	102.1722	
A: PA			
(-) PA	16	98.73889	6.511359
(+) PA	18	105.6056	6.138968
B: Ins			
(-) Ins	18	88.08334	6.138968
(+) Ins	16	116.2611	6.511359
AB: PA,Ins			
(-) PA,(-) Ins	9	84.17778	8.681811
(-) PA,(+) Ins	7	113.3	9.844249
(+) PA,(-) Ins	9	91.98889	8.681811
(+) PA,(+) Ins	9	119.2222	8.681811

Analysis of Variance Report

Dataset	P:\...\3H glucose uptake\stats file for NCSS incl WB.NCSS
Filter	treatment = "Met"
Response	MTT_3T3

Expected Mean Squares Section

Source Term	DF	Term Fixed?	Denominator Term	Expected Mean Square
A: PA	1	Yes	S(AB)	S+bsA
B: Ins	1	Yes	S(AB)	S+asB
AB	1	Yes	S(AB)	S+sAB
S(AB)	20	No		S

Note: Expected Mean Squares are for the balanced cell-frequency case.

Analysis of Variance Table

Source Term	DF	Sum of Squares	Mean Square	F-Ratio	Prob Level	Power (Alpha=0.10)
A: PA	1	439.9841	439.9841	0.49	0.492346	0.176430
B: Ins	1	30138.18	30138.18	33.51	0.000012*	0.999959
AB	1	1800.241	1800.241	2.00	0.172520	0.391778
S	20	17988.46	899.4232			
Total (Adjusted)	23	50366.87				
Total	24					

* Term significant at alpha = 0.10

Means and Standard Error Section

Term	Count	Mean	Standard Error
All	24	141.5558	
A: PA			
(-) PA	12	137.2742	8.657478
(+) PA	12	145.8375	8.657478
B: Ins			
(-) Ins	12	106.1192	8.657478
(+) Ins	12	176.9925	8.657478
AB: PA,Ins			
(-) PA,(-) Ins	6	93.17667	12.24352
(-) PA,(+) Ins	6	181.3717	12.24352
(+) PA,(-) Ins	6	119.0617	12.24352
(+) PA,(+) Ins	6	172.6133	12.24352

Analysis of Variance Report

Dataset	P:\...\3H glucose uptake\stats file for NCSS incl WB.NCSS
Filter	treatment = "Met"
Response	3T3_ Glucose_uptake

Expected Mean Squares Section

Source Term	DF	Term Fixed?	Denominator Term	Expected Mean Square
A: PA	1	Yes	S(AB)	S+bsA
B: Ins	1	Yes	S(AB)	S+asB
AB	1	Yes	S(AB)	S+sAB
S(AB)	37	No		S

Note: Expected Mean Squares are for the balanced cell-frequency case.

Analysis of Variance Table

Source Term	DF	Sum of Squares	Mean Square	F-Ratio	Prob Level	Power (Alpha=0.05)
A: PA	1	23.01793	23.01793	0.03	0.872582	0.052841
B: Ins	1	20944.65	20944.65	23.73	0.000021*	0.997296
AB	1	6232.068	6232.068	7.06	0.011560*	0.734949
S	37	32654.95	882.5662			
Total (Adjusted)	40	59516.6				
Total	41					

* Term significant at alpha = 0.05

Means and Standard Error Section

Term	Count	Mean	Standard Error
All	41	97.94558	
A: PA			
(-) PA	20	98.69743	6.642914
(+) PA	21	97.19373	6.482821
B: Ins			
(-) Ins	20	75.26606	6.642914
(+) Ins	21	120.6251	6.482821
AB: PA,Ins			
(-) PA,(-) Ins	9	63.64667	9.902672
(-) PA,(+) Ins	11	133.7482	8.957304
(+) PA,(-) Ins	11	86.88545	8.957304
(+) PA,(+) Ins	10	107.502	9.3945

Analysis of Variance Report

Dataset	P:\...\3H glucose uptake\stats file for NCSS incl WB.NCSS
Filter	treatment = "Met"
Response	ORO_correct

Expected Mean Squares Section

Source Term	DF	Term Fixed?	Denominator Term	Expected Mean Square
A: PA	1	Yes	S(AB)	S+bsA
B: Ins	1	Yes	S(AB)	S+asB
AB	1	Yes	S(AB)	S+sAB
S(AB)	37	No		S

Note: Expected Mean Squares are for the balanced cell-frequency case.

Analysis of Variance Table

Source Term	DF	Sum of Squares	Mean Square	F-Ratio	Prob Level	Power (Alpha=0.10)
A: PA	1	793.5066	793.5066	1.13	0.294214	0.277740
B: Ins	1	103.1447	103.1447	0.15	0.703457	0.123974
AB	1	336.5618	336.5618	0.48	0.492662	0.177421
S	37	25932.9	700.8892			
Total (Adjusted)	40	27169.59				
Total	41					

* Term significant at alpha = 0.10

Means and Standard Error Section

Term	Count	Mean	Standard Error
All	41	86.80505	
A: PA			
(-) PA	21	91.20809	5.777168
(+) PA	20	82.402	5.919836
B: Ins			
(-) Ins	20	88.3925	5.919836
(+) Ins	21	85.21759	5.777168
AB: PA,Ins			
(-) PA,(-) Ins	10	89.928	8.371912
(-) PA,(+) Ins	11	92.48818	7.982305
(+) PA,(-) Ins	10	86.857	8.371912
(+) PA,(+) Ins	10	77.947	8.371912

Analysis of Variance Report

Dataset	P:\...\3H glucose uptake\stats file for NCSS incl WB.NCSS
Filter	treatment = "AP10"
Response	C2C12_Glucose_uptake

Expected Mean Squares Section

Source Term	DF	Term Fixed?	Denominator Term	Expected Mean Square
A: PA	1	Yes	S(AB)	S+bsA
B: Ins	1	Yes	S(AB)	S+asB
AB	1	Yes	S(AB)	S+sAB
S(AB)	30	No		S

Note: Expected Mean Squares are for the balanced cell-frequency case.

Analysis of Variance Table

Source Term	DF	Sum of Squares	Mean Square	F-Ratio	Prob Level	Power (Alpha=0.05)
A: PA	1	1484.615	1484.615	3.65	0.065835	0.455516
B: Ins	1	8054.752	8054.752	19.78	0.000110*	0.990380
AB	1	3804.84	3804.84	9.34	0.004673*	0.840711
S	30	12218.19	407.2731			
Total (Adjusted)	33	26003.77				
Total	34					

* Term significant at alpha = 0.05

Means and Standard Error Section

Term	Count	Mean	Standard Error
All	34	101.2079	
A: PA			
(-) PA	17	107.8273	4.894613
(+) PA	17	94.58846	4.894613
B: Ins			
(-) Ins	17	85.78948	4.894613
(+) Ins	17	116.6263	4.894613
AB: PA,Ins			
(-) PA,(-) Ins	8	81.81194	7.135064
(-) PA,(+) Ins	9	133.8427	6.727003
(+) PA,(-) Ins	9	89.76702	6.727003
(+) PA,(+) Ins	8	99.4099	7.135064

Analysis of Variance Report

Dataset	P:\...\3H glucose uptake\stats file for NCSS incl WB.NCSS
Filter	treatment = "AP10"
Response	C3A_Glucose_uptake

Expected Mean Squares Section

Source Term	DF	Term Fixed?	Denominator Term	Expected Mean Square
A: PA	1	Yes	S(AB)	S+bsA
B: Ins	1	Yes	S(AB)	S+asB
AB	1	Yes	S(AB)	S+sAB
S(AB)	32	No		S

Note: Expected Mean Squares are for the balanced cell-frequency case.

Analysis of Variance Table

Source Term	DF	Sum of Squares	Mean Square	F-Ratio	Prob Level	Power (Alpha=0.05)
A: PA	1	50.88445	50.88445	0.04	0.833755	0.054844
B: Ins	1	7344.49	7344.49	6.46	0.016054*	0.693371
AB	1	129.2011	129.2011	0.11	0.738177	0.062351
S	32	36364.07	1136.377			
Total (Adjusted)	35	43888.65				
Total	36					

* Term significant at alpha = 0.05

Means and Standard Error Section

Term	Count	Mean	Standard Error
All	36	122.1444	
A: PA			
(-) PA	18	123.3333	7.94557
(+) PA	18	120.9556	7.94557
B: Ins			
(-) Ins	18	107.8611	7.94557
(+) Ins	18	136.4278	7.94557
AB: PA,Ins			
(-) PA,(-) Ins	9	107.1556	11.23673
(-) PA,(+) Ins	9	139.5111	11.23673
(+) PA,(-) Ins	9	108.5667	11.23673
(+) PA,(+) Ins	9	133.3445	11.23673

Analysis of Variance Report

Dataset	P:\...\3H glucose uptake\stats file for NCSS incl WB.NCSS
Filter	treatment = "AP10"
Response	MTT_3T3

Expected Mean Squares Section

Source Term	DF	Term Fixed?	Denominator Term	Expected Mean Square
A: PA	1	Yes	S(AB)	S+bsA
B: Ins	1	Yes	S(AB)	S+asB
AB	1	Yes	S(AB)	S+sAB
S(AB)	20	No		S

Note: Expected Mean Squares are for the balanced cell-frequency case.

Analysis of Variance Table

Source Term	DF	Sum of Squares	Mean Square	F-Ratio	Prob Level	Power (Alpha=0.10)
A: PA	1	68.1077	68.1077	0.10	0.755340	0.115775
B: Ins	1	14502.69	14502.69	21.25	0.000169*	0.997462
AB	1	806.3163	806.3163	1.18	0.289969	0.279579
S	20	13648.51	682.4255			
Total (Adjusted)	23	29025.63				
Total	24					

* Term significant at alpha = 0.10

Means and Standard Error Section

Term	Count	Mean	Standard Error
All	24	128.6237	
A: PA			
(-) PA	12	130.3083	7.54114
(+) PA	12	126.9392	7.54114
B: Ins			
(-) Ins	12	104.0417	7.54114
(+) Ins	12	153.2058	7.54114
AB: PA,Ins			
(-) PA,(-) Ins	6	99.93	10.66478
(-) PA,(+) Ins	6	160.6867	10.66478
(+) PA,(-) Ins	6	108.1533	10.66478
(+) PA,(+) Ins	6	145.725	10.66478

Analysis of Variance Report

Dataset	P:\...\3H glucose uptake\stats file for NCSS incl WB.NCSS
Filter	treatment = "AP10"
Response	3T3_Glucose_uptake

Expected Mean Squares Section

Source Term	DF	Term Fixed?	Denominator Term	Expected Mean Square
A: PA	1	Yes	S(AB)	S+bsA
B: Ins	1	Yes	S(AB)	S+asB
AB	1	Yes	S(AB)	S+sAB
S(AB)	38	No		S

Note: Expected Mean Squares are for the balanced cell-frequency case.

Analysis of Variance Table

Source Term	DF	Sum of Squares	Mean Square	F-Ratio	Prob Level	Power (Alpha=0.05)
A: PA	1	3327.52	3327.52	4.52	0.040059*	0.544673
B: Ins	1	221.6762	221.6762	0.30	0.586397	0.083381
AB	1	197.3253	197.3253	0.27	0.607655	0.079662
S	38	27975.4	736.1948			
Total (Adjusted)	41	31702.91				
Total	42					

* Term significant at alpha = 0.05

Means and Standard Error Section

Term	Count	Mean	Standard Error
All	42	86.71195	
A: PA			
(-) PA	22	77.80091	5.784756
(+) PA	20	95.623	6.067103
B: Ins			
(-) Ins	21	84.41196	5.920887
(+) Ins	21	89.01196	5.920887
AB: PA,Ins			
(-) PA,(-) Ins	11	77.67091	8.180881
(-) PA,(+) Ins	11	77.93091	8.180881
(+) PA,(-) Ins	10	91.153	8.580179
(+) PA,(+) Ins	10	100.093	8.580179

Analysis of Variance Report

Dataset	P:\...\3H glucose uptake\stats file for NCSS incl WB.NCSS
Filter	treatment = "AP10"
Response	ORO_correct

Expected Mean Squares Section

Source Term	DF	Term Fixed?	Denominator Term	Expected Mean Square
A: PA	1	Yes	S(AB)	S+bsA
B: Ins	1	Yes	S(AB)	S+asB
AB	1	Yes	S(AB)	S+sAB
S(AB)	38	No		S

Note: Expected Mean Squares are for the balanced cell-frequency case.

Analysis of Variance Table

Source Term	DF	Sum of Squares	Mean Square	F-Ratio	Prob Level	Power (Alpha=0.10)
A: PA	1	310.9978	310.9978	1.21	0.278081	0.289573
B: Ins	1	269.4488	269.4488	1.05	0.312190	0.265485
AB	1	613.7123	613.7123	2.39	0.130441	0.450393
S	38	9759.813	256.8372			
Total (Adjusted)	41	10982.92				
Total	42					

* Term significant at alpha = 0.10

Means and Standard Error Section

Term	Count	Mean	Standard Error
All	42	89.28057	
A: PA			
(-) PA	21	92.00482	3.497191
(+) PA	21	86.55632	3.497191
B: Ins			
(-) Ins	21	86.74482	3.497191
(+) Ins	21	91.81631	3.497191
AB: PA,Ins			
(-) PA,(-) Ins	10	93.296	5.067911
(-) PA,(+) Ins	11	90.71364	4.832063
(+) PA,(-) Ins	11	80.19363	4.832063
(+) PA,(+) Ins	10	92.919	5.067911

Analysis of Variance Report

Dataset P:\...\3H glucose uptake\stats file for NCSS incl WB.NCSS
Filter treatment = "AP100"
Response C2C12_Glucose_uptake

Expected Mean Squares Section

Source Term	DF	Term Fixed?	Denominator Term	Expected Mean Square
A: PA	1	Yes	S(AB)	S+bsA
B: Ins	1	Yes	S(AB)	S+asB
AB	1	Yes	S(AB)	S+sAB
S(AB)	31	No		S

Note: Expected Mean Squares are for the balanced cell-frequency case.

Analysis of Variance Table

Source Term	DF	Sum of Squares	Mean Square	F-Ratio	Prob Level	Power (Alpha=0.05)
A: PA	1	5.909669	5.909669	0.02	0.899883	0.051734
B: Ins	1	6748.814	6748.814	18.37	0.000164*	0.985750
AB	1	1.610341	1.610341	0.00	0.947633	0.050472
S	31	11386.46	367.305			
Total (Adjusted)	34	18160.66				
Total	35					

* Term significant at alpha = 0.05

Means and Standard Error Section

Term	Count	Mean	Standard Error
All	35	94.11781	
A: PA			
(-) PA	17	93.70636	4.648244
(+) PA	18	94.52925	4.517282
B: Ins			
(-) Ins	18	80.21365	4.517282
(+) Ins	17	108.022	4.648244
AB: PA,Ins			
(-) PA,(-) Ins	9	79.58743	6.388401
(-) PA,(+) Ins	8	107.8253	6.775922
(+) PA,(-) Ins	9	80.83987	6.388401
(+) PA,(+) Ins	9	108.2186	6.388401

Analysis of Variance Report

Dataset	P:\...\3H glucose uptake\stats file for NCSS incl WB.NCSS
Filter	treatment = "AP100"
Response	C3A_Glucose_uptake

Expected Mean Squares Section

Source Term	DF	Term Fixed?	Denominator Term	Expected Mean Square
A: PA	1	Yes	S(AB)	S+bsA
B: Ins	1	Yes	S(AB)	S+asB
AB	1	Yes	S(AB)	S+sAB
S(AB)	30	No		S

Note: Expected Mean Squares are for the balanced cell-frequency case.

Analysis of Variance Table

Source Term	DF	Sum of Squares	Mean Square	F-Ratio	Prob Level	Power (Alpha=0.05)
A: PA	1	1059.127	1059.127	1.50	0.230396	0.220085
B: Ins	1	11104.46	11104.46	15.71	0.000422*	0.969551
AB	1	1578.582	1578.582	2.23	0.145469	0.304273
S	30	21200.64	706.6879			
Total (Adjusted)	33	35389.9				
Total	34					

* Term significant at alpha = 0.05

Means and Standard Error Section

Term	Count	Mean	Standard Error
All	34	112.7868	
A: PA			
(-) PA	17	107.1958	6.447471
(+) PA	17	118.3778	6.447471
B: Ins			
(-) Ins	17	94.68333	6.447471
(+) Ins	17	130.8903	6.447471
AB: PA,Ins			
(-) PA,(-) Ins	9	82.26667	8.8612
(-) PA,(+) Ins	8	132.125	9.398723
(+) PA,(-) Ins	8	107.1	9.398723
(+) PA,(+) Ins	9	129.6555	8.8612

Analysis of Variance Report

Dataset	P:\...\3H glucose uptake\stats file for NCSS incl WB.NCSS
Filter	treatment = "AP100"
Response	MTT_3T3

Expected Mean Squares Section

Source Term	DF	Term Fixed?	Denominator Term	Expected Mean Square
A: PA	1	Yes	S(AB)	S+bsA
B: Ins	1	Yes	S(AB)	S+asB
AB	1	Yes	S(AB)	S+sAB
S(AB)	20	No		S

Note: Expected Mean Squares are for the balanced cell-frequency case.

Analysis of Variance Table

Source Term	DF	Sum of Squares	Mean Square	F-Ratio	Prob Level	Power (Alpha=0.10)
A: PA	1	2214.913	2214.913	3.78	0.066215*	0.591907
B: Ins	1	17313.96	17313.96	29.51	0.000026*	0.999837
AB	1	257.1531	257.1531	0.44	0.515476	0.168604
S	20	11732.72	586.6362			
Total (Adjusted)	23	31518.75				
Total	24					

* Term significant at alpha = 0.10

Means and Standard Error Section

Term	Count	Mean	Standard Error
All	24	140.0408	
A: PA			
(-) PA	12	130.4342	6.991878
(+) PA	12	149.6475	6.991878
B: Ins			
(-) Ins	12	113.1817	6.991878
(+) Ins	12	166.9	6.991878
AB: PA,Ins			
(-) PA,(-) Ins	6	100.3017	9.888008
(-) PA,(+) Ins	6	160.5667	9.888008
(+) PA,(-) Ins	6	126.0617	9.888008
(+) PA,(+) Ins	6	173.2333	9.888008

Analysis of Variance Report

Dataset	P:\...\3H glucose uptake\stats file for NCSS incl WB.NCSS
Filter	treatment = "AP100"
Response	3T3_Glucose_uptake

Expected Mean Squares Section

Source Term	DF	Term Fixed?	Denominator Term	Expected Mean Square
A: PA	1	Yes	S(AB)	S+bsA
B: Ins	1	Yes	S(AB)	S+asB
AB	1	Yes	S(AB)	S+sAB
S(AB)	35	No		S

Note: Expected Mean Squares are for the balanced cell-frequency case.

Analysis of Variance Table

Source Term	DF	Sum of Squares	Mean Square	F-Ratio	Prob Level	Power (Alpha=0.05)
A: PA	1	1234.644	1234.644	1.79	0.189081	0.256077
B: Ins	1	627.3383	627.3383	0.91	0.346260	0.153147
AB	1	88.60522	88.60522	0.13	0.721895	0.064072
S	35	24088.2	688.2344			
Total (Adjusted)	38	25965.32				
Total	39					

* Term significant at alpha = 0.05

Means and Standard Error Section

Term	Count	Mean	Standard Error
All	39	92.21164	
A: PA			
(-) PA	19	86.57928	6.018543
(+) PA	20	97.844	5.86615
B: Ins			
(-) Ins	19	88.19678	6.018543
(+) Ins	20	96.2265	5.86615
AB: PA,Ins			
(-) PA,(-) Ins	9	81.05556	8.74474
(-) PA,(+) Ins	10	92.103	8.295989
(+) PA,(-) Ins	10	95.338	8.295989
(+) PA,(+) Ins	10	100.35	8.295989

Analysis of Variance Report

Dataset	P:\...\3H glucose uptake\stats file for NCSS incl WB.NCSS
Filter	treatment = "AP100"
Response	ORO_correct

Expected Mean Squares Section

Source Term	DF	Term Fixed?	Denominator Term	Expected Mean Square
A: PA	1	Yes	S(AB)	S+bsA
B: Ins	1	Yes	S(AB)	S+asB
AB	1	Yes	S(AB)	S+sAB
S(AB)	36	No		S

Note: Expected Mean Squares are for the balanced cell-frequency case.

Analysis of Variance Table

Source Term	DF	Sum of Squares	Mean Square	F-Ratio	Prob Level	Power (Alpha=0.10)
A: PA	1	2342.068	2342.068	4.78	0.035466*	0.691173
B: Ins	1	197.1945	197.1945	0.40	0.530046	0.164927
AB	1	39.80462	39.80462	0.08	0.777373	0.113230
S	36	17657.46	490.4851			
Total (Adjusted)	39	20287.02				
Total	40					

* Term significant at alpha = 0.10

Means and Standard Error Section

Term	Count	Mean	Standard Error
All	40	83.18021	
A: PA			
(-) PA	20	90.85142	4.952197
(+) PA	20	75.509	4.952197
B: Ins			
(-) Ins	19	80.95428	5.080847
(+) Ins	21	85.40614	4.83285
AB: PA,Ins			
(-) PA,(-) Ins	9	89.62556	7.382299
(-) PA,(+) Ins	11	92.07727	6.677541
(+) PA,(-) Ins	10	72.283	7.003464
(+) PA,(+) Ins	10	78.735	7.003464

Analysis of Variance Report

Dataset P:\...\3H glucose uptake\stats file for NCSS incl WB.NCSS
Response FpAMPK

Expected Mean Squares Section

Source Term	DF	Term Fixed?	Denominator Term	Expected Mean Square
A: PA	1	Yes	S(ABC)	S+bcsA
B: Ins	1	Yes	S(ABC)	S+acsB
AB	1	Yes	S(ABC)	S+csAB
C: treatment	1	Yes	S(ABC)	S+absC
AC	1	Yes	S(ABC)	S+bsAC
BC	1	Yes	S(ABC)	S+asBC
ABC	1	Yes	S(ABC)	S+sABC
S(ABC)	16	No		S

Note: Expected Mean Squares are for the balanced cell-frequency case.

Analysis of Variance Table

Source Term	DF	Sum of Squares	Mean Square	F-Ratio	Prob Level	Power (Alpha=0.10)
A: PA	1	0.1536	0.1536	0.94	0.347441	0.241551
B: Ins	1	0.1014	0.1014	0.62	0.443059	0.194593
AB	1	0.0002666667	0.0002666667	0.00	0.968326	0.100253
C: treatment	1	0.2166	0.2166	1.32	0.267234	0.296279
AC	1	0.06826667	0.06826667	0.42	0.527850	0.164120
BC	1	6.666667E-05	6.666667E-05	0.00	0.984159	0.100063
ABC	1	0.06826667	0.06826667	0.42	0.527850	0.164120
S	16	2.622667	0.1639167			
Total (Adjusted)	23	3.231133				
Total	24					

* Term significant at alpha = 0.10

Means and Standard Error Section

Term	Count	Mean	Standard Error
All	24	1.138333	
A: PA			
(-) PA	12	1.058333	0.1168748
(+) PA	12	1.218333	0.1168748
B: Ins			
(-) Ins	12	1.073333	0.1168748
(+) Ins	12	1.203333	0.1168748
C: treatment			
AP100	12	1.233333	0.1168748
Ctrl	12	1.043333	0.1168748
AB: PA,Ins			
(-) PA,(-) Ins	6	0.99	0.1652859
(-) PA,(+) Ins	6	1.126667	0.1652859
(+) PA,(-) Ins	6	1.156667	0.1652859
(+) PA,(+) Ins	6	1.28	0.1652859
AC: PA,treatment			
(-) PA,AP100	6	1.1	0.1652859
(-) PA,Ctrl	6	1.016667	0.1652859
(+) PA,AP100	6	1.366667	0.1652859
(+) PA,Ctrl	6	1.07	0.1652859
BC: Ins,treatment			
(-) Ins,AP100	6	1.17	0.1652859

(-) Ins,Ctrl	6	0.9766667	0.1652859
(+) Ins,AP100	6	1.296667	0.1652859

Analysis of Variance Report

Dataset P:\...\3H glucose uptake\stats file for NCSS incl WB.NCSS
Response FpAMPK

Means and Standard Error Section

Term	Count	Mean	Standard Error
BC: Ins,treatment			
(+) Ins,Ctrl	6	1.11	0.1652859
ABC: PA,Ins,treatment			
(-) PA,(-) Ins,AP100	3	0.98	0.2337496
(-) PA,(-) Ins,Ctrl	3	1	0.2337496
(-) PA,(+) Ins,AP100	3	1.22	0.2337496
(-) PA,(+) Ins,Ctrl	3	1.033333	0.2337496
(+) PA,(-) Ins,AP100	3	1.36	0.2337496
(+) PA,(-) Ins,Ctrl	3	0.9533333	0.2337496
(+) PA,(+) Ins,AP100	3	1.373333	0.2337496
(+) PA,(+) Ins,Ctrl	3	1.186667	0.2337496

Analysis of Variance Report

Dataset P:\...\3H glucose uptake\stats file for NCSS incl WB.NCSS
Response FtAMPK

Expected Mean Squares Section

Source Term	DF	Term Fixed?	Denominator Term	Expected Mean Square
A: PA	1	Yes	S(ABC)	S+bcsA
B: Ins	1	Yes	S(ABC)	S+acsB
AB	1	Yes	S(ABC)	S+csAB
C: treatment	1	Yes	S(ABC)	S+absC
AC	1	Yes	S(ABC)	S+bsAC
BC	1	Yes	S(ABC)	S+asBC
ABC	1	Yes	S(ABC)	S+sABC
S(ABC)	8	No		S

Note: Expected Mean Squares are for the balanced cell-frequency case.

Analysis of Variance Table

Source Term	DF	Sum of Squares	Mean Square	F-Ratio	Prob Level	Power (Alpha=0.10)
A: PA	1	0.03216039	0.03216039	0.42	0.536982	0.158737
B: Ins	1	0.08477511	0.08477511	1.10	0.325610	0.251134
AB	1	0.01174878	0.01174878	0.15	0.706823	0.121620
C: treatment	1	0.001436819	0.001436819	0.02	0.894927	0.102653
AC	1	0.01761957	0.01761957	0.23	0.645837	0.132357
BC	1	0.01068626	0.01068626	0.14	0.719696	0.119672
ABC	1	0.004259235	0.004259235	0.06	0.820316	0.107857
S	8	0.6184341	0.07730426			
Total (Adjusted)	15	0.7811202				
Total	16					

* Term significant at alpha = 0.10

Means and Standard Error Section

Term	Count	Mean	Standard Error
All	16	1.01931	
A: PA			
(-) PA	8	1.064143	0.09830073
(+) PA	8	0.9744768	0.09830073
B: Ins			
(-) Ins	8	0.9465197	0.09830073
(+) Ins	8	1.092101	0.09830073
C: treatment			
AP100	8	1.028786	0.09830073
Ctrl	8	1.009834	0.09830073
AB: PA,Ins			
(-) PA,(-) Ins	4	1.018451	0.1390182
(-) PA,(+) Ins	4	1.109836	0.1390182
(+) PA,(-) Ins	4	0.8745885	0.1390182
(+) PA,(+) Ins	4	1.074365	0.1390182
AC: PA,treatment			
(-) PA,AP100	4	1.040435	0.1390182
(-) PA,Ctrl	4	1.087852	0.1390182
(+) PA,AP100	4	1.017138	0.1390182
(+) PA,Ctrl	4	0.9318158	0.1390182
BC: Ins,treatment			
(-) Ins,AP100	4	0.9818397	0.1390182

(-) Ins,Ctrl	4	0.9111997	0.1390182
(+) Ins,AP100	4	1.075733	0.1390182

Analysis of Variance Report

Dataset P:\...\3H glucose uptake\stats file for NCSS incl WB.NCSS
Response FtAMPK

Means and Standard Error Section

Term	Count	Mean	Standard Error
BC: Ins,treatment			
(+) Ins,Ctrl	4	1.108468	0.1390182
ABC: PA,Ins,treatment			
(-) PA,(-) Ins,AP100	2	1.036902	0.1966015
(-) PA,(-) Ins,Ctrl	2	1	0.1966015
(-) PA,(+) Ins,AP100	2	1.043968	0.1966015
(-) PA,(+) Ins,Ctrl	2	1.175704	0.1966015
(+) PA,(-) Ins,AP100	2	0.9267774	0.1966015
(+) PA,(-) Ins,Ctrl	2	0.8223996	0.1966015
(+) PA,(+) Ins,AP100	2	1.107498	0.1966015
(+) PA,(+) Ins,Ctrl	2	1.041232	0.1966015

Analysis of Variance Report

Dataset P:\...\3H glucose uptake\stats file for NCSS incl WB.NCSS
Response FAMPKratio

Expected Mean Squares Section

Source Term	DF	Term Fixed?	Denominator Term	Expected Mean Square
A: PA	1	Yes	S(ABC)	S+bcsA
B: Ins	1	Yes	S(ABC)	S+acsB
AB	1	Yes	S(ABC)	S+csAB
C: treatment	1	Yes	S(ABC)	S+absC
AC	1	Yes	S(ABC)	S+bsAC
BC	1	Yes	S(ABC)	S+asBC
ABC	1	Yes	S(ABC)	S+sABC
S(ABC)	8	No		S

Note: Expected Mean Squares are for the balanced cell-frequency case.

Analysis of Variance Table

Source Term	DF	Sum of Squares	Mean Square	F-Ratio	Prob Level	Power (Alpha=0.10)
A: PA	1	0.0729	0.0729	1.73	0.224725	0.332058
B: Ins	1	0.065025	0.065025	1.54	0.249198	0.308779
AB	1	0.01	0.01	0.24	0.639119	0.133701
C: treatment	1	0.225625	0.225625	5.36	0.049329*	0.680307
AC	1	0.0625	0.0625	1.48	0.257837	0.301211
BC	1	0.024025	0.024025	0.57	0.471712	0.180151
ABC	1	0.0016	0.0016	0.04	0.850315	0.105420
S	8	0.3369	0.0421125			
Total (Adjusted)	15	0.798575				
Total	16					

* Term significant at alpha = 0.10

Means and Standard Error Section

Term	Count	Mean	Standard Error
All	16	1.16125	
A: PA			
(-) PA	8	1.09375	0.07255386
(+) PA	8	1.22875	0.07255386
B: Ins			
(-) Ins	8	1.225	0.07255386
(+) Ins	8	1.0975	0.07255386
C: treatment			
AP100	8	1.28	0.07255386
Ctrl	8	1.0425	0.07255386
AB: PA,Ins			
(-) PA,(-) Ins	4	1.1325	0.1026067
(-) PA,(+) Ins	4	1.055	0.1026067
(+) PA,(-) Ins	4	1.3175	0.1026067
(+) PA,(+) Ins	4	1.14	0.1026067
AC: PA,treatment			
(-) PA,AP100	4	1.275	0.1026067
(-) PA,Ctrl	4	0.9125	0.1026067
(+) PA,AP100	4	1.285	0.1026067
(+) PA,Ctrl	4	1.1725	0.1026067
BC: Ins,treatment			
(-) Ins,AP100	4	1.305	0.1026067

(-) Ins,Ctrl	4	1.145	0.1026067
(+) Ins,AP100	4	1.255	0.1026067

Analysis of Variance Report

Dataset P:\...\3H glucose uptake\stats file for NCSS incl WB.NCSS
Response FAMPKratio

Means and Standard Error Section

Term	Count	Mean	Standard Error
BC: Ins,treatment			
(+) Ins,Ctrl	4	0.94	0.1026067
ABC: PA,Ins,treatment			
(-) PA,(-) Ins,AP100	2	1.265	0.1451077
(-) PA,(-) Ins,Ctrl	2	1	0.1451077
(-) PA,(+) Ins,AP100	2	1.285	0.1451077
(-) PA,(+) Ins,Ctrl	2	0.825	0.1451077
(+) PA,(-) Ins,AP100	2	1.345	0.1451077
(+) PA,(-) Ins,Ctrl	2	1.29	0.1451077
(+) PA,(+) Ins,AP100	2	1.225	0.1451077
(+) PA,(+) Ins,Ctrl	2	1.055	0.1451077

Analysis of Variance Report

Dataset P:\...\3H glucose uptake\stats file for NCSS incl WB.NCSS
Response FpAkt

Expected Mean Squares Section

Source Term	DF	Term Fixed?	Denominator Term	Expected Mean Square
A: PA	1	Yes	S(ABC)	S+bcsA
B: Ins	1	Yes	S(ABC)	S+acsB
AB	1	Yes	S(ABC)	S+csAB
C: treatment	1	Yes	S(ABC)	S+absC
AC	1	Yes	S(ABC)	S+bsAC
BC	1	Yes	S(ABC)	S+asBC
ABC	1	Yes	S(ABC)	S+sABC
S(ABC)	16	No		S

Note: Expected Mean Squares are for the balanced cell-frequency case.

Analysis of Variance Table

Source Term	DF	Sum of Squares	Mean Square	F-Ratio	Prob Level	Power (Alpha=0.10)
A: PA	1	2.024204	2.024204	8.12	0.011575*	0.860322
B: Ins	1	63.86344	63.86344	256.31	0.000000*	1.000000
AB	1	0.3577042	0.3577042	1.44	0.248296	0.312098
C: treatment	1	1.302004	1.302004	5.23	0.036232*	0.706430
AC	1	0.7385042	0.7385042	2.96	0.104413	0.501854
BC	1	0.1053375	0.1053375	0.42	0.524787	0.165076
ABC	1	0.03300417	0.03300417	0.13	0.720659	0.120563
S	16	3.9866	0.2491625			
Total (Adjusted)	23	72.4108				
Total	24					

* Term significant at alpha = 0.10

Means and Standard Error Section

Term	Count	Mean	Standard Error
All	24	2.157917	
A: PA			
(-) PA	12	2.448333	0.1440956
(+) PA	12	1.8675	0.1440956
B: Ins			
(-) Ins	12	0.5266666	0.1440956
(+) Ins	12	3.789167	0.1440956
C: treatment			
AP100	12	1.925	0.1440956
Ctrl	12	2.390833	0.1440956
AB: PA,Ins			
(-) PA,(-) Ins	6	0.695	0.2037819
(-) PA,(+) Ins	6	4.201667	0.2037819
(+) PA,(-) Ins	6	0.3583333	0.2037819
(+) PA,(+) Ins	6	3.376667	0.2037819
AC: PA,treatment			
(-) PA,AP100	6	2.04	0.2037819
(-) PA,Ctrl	6	2.856667	0.2037819
(+) PA,AP100	6	1.81	0.2037819
(+) PA,Ctrl	6	1.925	0.2037819
BC: Ins,treatment			
(-) Ins,AP100	6	0.36	0.2037819

(-) Ins,Ctrl	6	0.6933333	0.2037819
(+) Ins,AP100	6	3.49	0.2037819

Analysis of Variance Report

Dataset P:\...\3H glucose uptake\stats file for NCSS incl WB.NCSS
Response FpAkt

Means and Standard Error Section

Term	Count	Mean	Standard Error
BC: Ins,treatment			
(+) Ins,Ctrl	6	4.088333	0.2037819
ABC: PA,Ins,treatment			
(-) PA,(-) Ins,AP100	3	0.39	0.2881912
(-) PA,(-) Ins,Ctrl	3	1	0.2881912
(-) PA,(+) Ins,AP100	3	3.69	0.2881912
(-) PA,(+) Ins,Ctrl	3	4.713333	0.2881912
(+) PA,(-) Ins,AP100	3	0.33	0.2881912
(+) PA,(-) Ins,Ctrl	3	0.3866667	0.2881912
(+) PA,(+) Ins,AP100	3	3.29	0.2881912
(+) PA,(+) Ins,Ctrl	3	3.463333	0.2881912

Analysis of Variance Report

Dataset P:\...\3H glucose uptake\stats file for NCSS incl WB.NCSS
Response FtAkt

Expected Mean Squares Section

Source Term	DF	Term Fixed?	Denominator Term	Expected Mean Square
A: PA	1	Yes	S(ABC)	S+bcsA
B: Ins	1	Yes	S(ABC)	S+acsB
AB	1	Yes	S(ABC)	S+csAB
C: treatment	1	Yes	S(ABC)	S+absC
AC	1	Yes	S(ABC)	S+bsAC
BC	1	Yes	S(ABC)	S+asBC
ABC	1	Yes	S(ABC)	S+sABC
S(ABC)	8	No		S

Note: Expected Mean Squares are for the balanced cell-frequency case.

Analysis of Variance Table

Source Term	DF	Sum of Squares	Mean Square	F-Ratio	Prob Level	Power (Alpha=0.10)
A: PA	1	0.1540563	0.1540563	1.94	0.200697	0.357999
B: Ins	1	0.03150625	0.03150625	0.40	0.545894	0.156174
AB	1	0.00015625	0.00015625	0.00	0.965668	0.100282
C: treatment	1	0.06375625	0.06375625	0.80	0.395888	0.212140
AC	1	0.00050625	0.00050625	0.01	0.938253	0.100912
BC	1	0.01625625	0.01625625	0.21	0.662608	0.129145
ABC	1	0.00275625	0.00275625	0.03	0.856685	0.104963
S	8	0.63385	0.07923125			
Total (Adjusted)	15	0.9028438				
Total	16					

* Term significant at alpha = 0.10

Means and Standard Error Section

Term	Count	Mean	Standard Error
All	16	0.841875	
A: PA			
(-) PA	8	0.94	0.09951837
(+) PA	8	0.74375	0.09951837
B: Ins			
(-) Ins	8	0.88625	0.09951837
(+) Ins	8	0.7975	0.09951837
C: treatment			
AP100	8	0.77875	0.09951837
Ctrl	8	0.905	0.09951837
AB: PA,Ins			
(-) PA,(-) Ins	4	0.9875	0.1407402
(-) PA,(+) Ins	4	0.8925	0.1407402
(+) PA,(-) Ins	4	0.785	0.1407402
(+) PA,(+) Ins	4	0.7025	0.1407402
AC: PA,treatment			
(-) PA,AP100	4	0.8825	0.1407402
(-) PA,Ctrl	4	0.9975	0.1407402
(+) PA,AP100	4	0.675	0.1407402
(+) PA,Ctrl	4	0.8125	0.1407402
BC: Ins,treatment			
(-) Ins,AP100	4	0.855	0.1407402

(-) Ins,Ctrl	4	0.9175	0.1407402
(+) Ins,AP100	4	0.7025	0.1407402

Analysis of Variance Report

Dataset P:\...\3H glucose uptake\stats file for NCSS incl WB.NCSS
Response FtAkt

Means and Standard Error Section

Term	Count	Mean	Standard Error
BC: Ins,treatment			
(+) Ins,Ctrl	4	0.8925	0.1407402
ABC: PA,Ins,treatment			
(-) PA,(-) Ins,AP100	2	0.975	0.1990367
(-) PA,(-) Ins,Ctrl	2	1	0.1990367
(-) PA,(+) Ins,AP100	2	0.79	0.1990367
(-) PA,(+) Ins,Ctrl	2	0.995	0.1990367
(+) PA,(-) Ins,AP100	2	0.735	0.1990367
(+) PA,(-) Ins,Ctrl	2	0.835	0.1990367
(+) PA,(+) Ins,AP100	2	0.615	0.1990367
(+) PA,(+) Ins,Ctrl	2	0.79	0.1990367

Analysis of Variance Report

Dataset P:\...\3H glucose uptake\stats file for NCSS incl WB.NCSS
Response FAktratio

Expected Mean Squares Section

Source Term	DF	Term Fixed?	Denominator Term	Expected Mean Square
A: PA	1	Yes	S(ABC)	S+bcsA
B: Ins	1	Yes	S(ABC)	S+acsB
AB	1	Yes	S(ABC)	S+csAB
C: treatment	1	Yes	S(ABC)	S+absC
AC	1	Yes	S(ABC)	S+bsAC
BC	1	Yes	S(ABC)	S+asBC
ABC	1	Yes	S(ABC)	S+sABC
S(ABC)	8	No		S

Note: Expected Mean Squares are for the balanced cell-frequency case.

Analysis of Variance Table

Source Term	DF	Sum of Squares	Mean Square	F-Ratio	Prob Level	Power (Alpha=0.10)
A: PA	1	0.01500625	0.01500625	0.02	0.902396	0.102287
B: Ins	1	85.60876	85.60876	91.41	0.000012*	1.000000
AB	1	0.2997563	0.2997563	0.32	0.587086	0.145317
C: treatment	1	0.02805625	0.02805625	0.03	0.866888	0.104275
AC	1	0.5076563	0.5076563	0.54	0.482616	0.176224
BC	1	0.5076563	0.5076563	0.54	0.482616	0.176224
ABC	1	0.01890625	0.01890625	0.02	0.890530	0.102881
S	8	7.49255	0.9365687			
Total (Adjusted)	15	94.47834				
Total	16					

* Term significant at alpha = 0.10

Means and Standard Error Section

Term	Count	Mean	Standard Error
All	16	2.926875	
A: PA			
(-) PA	8	2.89625	0.3421565
(+) PA	8	2.9575	0.3421565
B: Ins			
(-) Ins	8	0.61375	0.3421565
(+) Ins	8	5.24	0.3421565
C: treatment			
AP100	8	2.96875	0.3421565
Ctrl	8	2.885	0.3421565
AB: PA,Ins			
(-) PA,(-) Ins	4	0.72	0.4838824
(-) PA,(+) Ins	4	5.0725	0.4838824
(+) PA,(-) Ins	4	0.5075	0.4838824
(+) PA,(+) Ins	4	5.4075	0.4838824
AC: PA,treatment			
(-) PA,AP100	4	2.76	0.4838824
(-) PA,Ctrl	4	3.0325	0.4838824
(+) PA,AP100	4	3.1775	0.4838824
(+) PA,Ctrl	4	2.7375	0.4838824
BC: Ins,treatment			
(-) Ins,AP100	4	0.4775	0.4838824

(-) Ins,Ctrl	4	0.75	0.4838824
(+) Ins,AP100	4	5.46	0.4838824

Analysis of Variance Report

Dataset P:\...\3H glucose uptake\stats file for NCSS incl WB.NCSS
Response FAktratio

Means and Standard Error Section

Term	Count	Mean	Standard Error
BC: Ins,treatment			
(+) Ins,Ctrl	4	5.02	0.4838824
ABC: PA,Ins,treatment			
(-) PA,(-) Ins,AP100	2	0.44	0.6843131
(-) PA,(-) Ins,Ctrl	2	1	0.6843131
(-) PA,(+) Ins,AP100	2	5.08	0.6843131
(-) PA,(+) Ins,Ctrl	2	5.065	0.6843131
(+) PA,(-) Ins,AP100	2	0.515	0.6843131
(+) PA,(-) Ins,Ctrl	2	0.5	0.6843131
(+) PA,(+) Ins,AP100	2	5.84	0.6843131
(+) PA,(+) Ins,Ctrl	2	4.975	0.6843131

Analysis of Variance Report

Dataset P:\...\3H glucose uptake\stats file for NCSS incl WB.NCSS
Response FGlut4

Expected Mean Squares Section

Source Term	DF	Term Fixed?	Denominator Term	Expected Mean Square
A: PA	1	Yes	S(ABC)	S+bcsA
B: Ins	1	Yes	S(ABC)	S+acsB
AB	1	Yes	S(ABC)	S+csAB
C: treatment	1	Yes	S(ABC)	S+absC
AC	1	Yes	S(ABC)	S+bsAC
BC	1	Yes	S(ABC)	S+asBC
ABC	1	Yes	S(ABC)	S+sABC
S(ABC)	8	No		S

Note: Expected Mean Squares are for the balanced cell-frequency case.

Analysis of Variance Table

Source Term	DF	Sum of Squares	Mean Square	F-Ratio	Prob Level	Power (Alpha=0.10)
A: PA	1	0.133225	0.133225	2.82	0.131812	0.456998
B: Ins	1	0.0001	0.0001	0.00	0.964453	0.100302
AB	1	0.042025	0.042025	0.89	0.373480	0.223436
C: treatment	1	0.0324	0.0324	0.68	0.431868	0.195865
AC	1	0.112225	0.112225	2.37	0.162046	0.408047
BC	1	0	0	0.00	1.000000	0.100000
ABC	1	0.042025	0.042025	0.89	0.373480	0.223436
S	8	0.3784	0.0473			
Total (Adjusted)	15	0.7404				
Total	16					

* Term significant at alpha = 0.10

Means and Standard Error Section

Term	Count	Mean	Standard Error
All	16	0.68	
A: PA			
(-) PA	8	0.77125	0.07689279
(+) PA	8	0.58875	0.07689279
B: Ins			
(-) Ins	8	0.6775	0.07689279
(+) Ins	8	0.6825	0.07689279
C: treatment			
AP100	8	0.635	0.07689279
Ctrl	8	0.725	0.07689279
AB: PA,Ins			
(-) PA,(-) Ins	4	0.82	0.1087428
(-) PA,(+) Ins	4	0.7225	0.1087428
(+) PA,(-) Ins	4	0.535	0.1087428
(+) PA,(+) Ins	4	0.6425	0.1087428
AC: PA,treatment			
(-) PA,AP100	4	0.6425	0.1087428
(-) PA,Ctrl	4	0.9	0.1087428
(+) PA,AP100	4	0.6275	0.1087428
(+) PA,Ctrl	4	0.55	0.1087428
BC: Ins,treatment			
(-) Ins,AP100	4	0.6325	0.1087428
(-) Ins,Ctrl	4	0.7225	0.1087428

(+) Ins,AP100	4	0.6375	0.1087428

Analysis of Variance Report

Dataset P:\...\3H glucose uptake\stats file for NCSS incl WB.NCSS
Response FGlut4

Means and Standard Error Section

Term	Count	Mean	Standard Error
BC: Ins,treatment			
(+) Ins,Ctrl	4	0.7275	0.1087428
ABC: PA,Ins,treatment			
(-) PA,(-) Ins,AP100	2	0.64	0.1537856
(-) PA,(-) Ins,Ctrl	2	1	0.1537856
(-) PA,(+) Ins,AP100	2	0.645	0.1537856
(-) PA,(+) Ins,Ctrl	2	0.8	0.1537856
(+) PA,(-) Ins,AP100	2	0.625	0.1537856
(+) PA,(-) Ins,Ctrl	2	0.445	0.1537856
(+) PA,(+) Ins,AP100	2	0.63	0.1537856
(+) PA,(+) Ins,Ctrl	2	0.655	0.1537856

ADDENDUM 2 Ethical clearance SAMRC

SOUTH AFRICAN MEDICAL RESEARCH COUNCIL

ETHICS COMMITTEE FOR RESEARCH ON ANIMALS (ECRA)

PO Box 19001, Tygerberg, 7505, Cape Town, South Africa;
off Hindle Road, Brentwood Park, Driftsands
Tel: +27 (0)21 955 1900, Fax: +27 (0)21 955 1330
E-mail: gieliana.fourie@mrc.ac.za
http://www.sahealthinfo.org/Modules/ethics.htm

15 September 2015

Dr N Chellan
Diabetes Discovery Platform
MEDICAL RESEARCH COUNCIL

Dear Dr Chellan,

YOUR APPLICATION TO THE ECRA : REF 03/15 "The metabolic activity of *Athrixia phylicoides* extract in diabetic *db/db* mice".

Thank you for your corrected application to the ECRA. The Committee reviewed it and it was approved. Please find attached your Certificate of Approval.

Note that you will be responsible for the submission of 6 monthly reports as requested by the ECRA Committee. If you encounter any difficulties during your approved period, please inform the ECRA thereof. If you need an extension for the study timeline, please request such an extension by a written letter to the Committee.

Kind regards.

PROF D DU TOIT
Chairperson : ECRA Committee

ADDENDUM 3 Ethical clearance University of Zululand

UNIVERSITY OF ZULULAND
RESEARCH ETHICS COMMITTEE
(Reg No: UZREC 171110-030)

RESEARCH & INNOVATION
Website: http://www.unizulu.ac.za
Private Bag X1001
KwaDlangezwa 3886
Tel: 035 902 6887
Fax: 035 902 6222
Email: MamqeleS@unizulu.ac.za

ETHICAL CLEARANCE CERTIFICATE

Certificate Number	**UZREC 171110-030 PGM 2015/193**							
Project Title	**Metabolic activity of *Athrixia* phylicoides**							
Principal Researcher/ Investigator	CM Masilela							
Supervisor and Co-supervisor	Dr. AP Kappo			Dr. C Muller				
Department	Biochemistry & Microbiology							
Nature of Project	Honours/4th Year		Master's	x	Doctoral		Departmental	

The University of Zululand's Research Ethics Committee (UZREC) hereby gives ethical approval in respect of the undertakings contained in the above-mentioned project proposal and the documents listed on page 2 of this Certificate.

Special conditions: (1) The Principal Researcher must report to the UZREC in the prescribed format, where applicable, annually and at the end of the project, in respect of ethical compliance.
(2) Documents marked "To be submitted" (see page 2) must be presented for ethical clearance before any data collection can commence.

The Researcher may therefore commence with the research as from the date of this Certificate, using the reference number indicated above, but may not conduct any data collection using research instruments that are yet to be approved.

Please note that the UZREC must be informed immediately of

- Any material change in the conditions or undertakings mentioned in the documents that were presented to the UZREC
- Any material breaches of ethical undertakings or events that impact upon the ethical conduct of the research

Classification:

Data collection	Animals	Human Health	Children	Vulnerable pp.	Other
X	X				

Low Risk	Medium Risk	High Risk
	X	

The table below indicates which documents the UZREC considered in granting this Certificate and which documents, if any, still require ethical clearance. (Please note that this is not a closed list and should new instruments be developed, these would require approval.)

Documents	Considered	To be submitted	Not required
Faculty Research Ethics Committee recommendation	X		
Animal Research Ethics Committee recommendation	X		
Health Research Ethics Committee recommendation			X
Ethical clearance application form	X		
Project registration proposal	X		
Informed consent from participants			X
Informed consent from parent/guardian			X
Permission for access to sites/information/participants			X
Permission to use documents/copyright clearance			X
Data collection/survey instrument/questionnaire			X
Data collection instrument in appropriate language		Only if necessary	
Other data collection instruments		Only if used	

The UZREC retains the right to

- Withdraw or amend this Certificate if
  - Any unethical principles or practices are revealed or suspected
  - Relevant information has been withheld or misrepresented
  - Regulatory changes of whatsoever nature so require
  - The conditions contained in this Certificate have not been adhered to
- Request access to any information or data at any time during the course or after completion of the project

The UZREC wishes the researcher well in conducting the research.

Professor Nokuthula Kunene
Chairperson: University Research Ethics Committee
12 November 2015

CHAIRPERSON
UNIVERSITY OF ZULULAND RESEARCH ETHICS COMMITTEE (UZREC)
REG NO: UZREC 171110-30
12 -11- 2015
RESEARCH & INNOVATION OFFICE

CM Masilela - PGM 2015/193

ADDENDUM 4 Research Outputs

Poster presentations:

Masilela CM, Muller CJF, Louw J, Ngema N, Chellan N, Kappo AMP, Riedel S. Metabolic and anti-diabetic effects of *Athrixia phylicoides*. SEMDSA Congress ,14-17 April 2016

Masilela CM, Muller CJF, Louw J, Ngema N, Chellan N, Kappo AMP, Riedel S. Metabolic and anti-diabetic effects of *Athrixia phylicoides.* MRC 10th Annual Early Career Scientist Conference, Cape Town 19-20 October 2016.

ADDENDUM 5 Turnitin report

Full report available on request

MSc Biochemistry Thesis

by Charity Masilela

FILE	CHARITY_MSC_BIOCHEMISTRY_THESIS.DOC (1.71M)		
TIME SUBMITTED	09-DEC-2016 05:55PM	WORD COUNT	25640
SUBMISSION ID	750583665	CHARACTER COUNT	156823

MSc Biochemistry Thesis

ORIGINALITY REPORT

%22	%13	%18	%5
SIMILARITY INDEX	INTERNET SOURCES	PUBLICATIONS	STUDENT PAPERS

PRIMARY SOURCES

1	www.dovepress.com Internet Source	%1
2	Mazibuko, S.E., C.J.F. Muller, E. Joubert, D. de Beer, R. Johnson, A.R. Opoku, and J. Louw. "Amelioration of palmitate-induced insulin resistance in C2C12 muscle cells by rooibos (Aspalathus linearis)", Phytomedicine, 2013. Publication	%1
3	"Abstract Book 2008", Diabetologia, 09/2007 Publication	%1
4	"Abstracts", Diabetologia, 08/2005 Publication	%1
5	"PanVascular Medicine", Springer Nature, 2015 Publication	%1
6	www.science.gov Internet Source	%1
7	"Abstracts 2007", Diabetologia, 08/20/2007 Publication	<%1

Subramoniam, Appian. "Anti-Diabetes Mellitus

ADDENDUM 6 Proofreading certificate

GRANTS INNOVATION &
PRODUCT DEVELOPMENT
BIOMEDICAL RESEARCH &
INNOVATION PLATFORM

12th December 2016

The Post-graduate Examination Committee
University of Zululand

MSc thesis Proofreading report Ms Charity Masilela

I have proofread the above thesis for English language correctness and readability and hereby certify that the thesis titled "Metabolic bioactivity of *Athrixia phylicoides*" is acceptable in its current form for examination and publication.

I hope you find this in order.

Yours sincerely,

CSChapman

Mrs. C.S. Chapman

Laboratory Manager
Biomedical Research and Innovation Platform